

Cytotoxic Granule Endocytosis in Primary Mouse Cytotoxic T Lymphocytes

Dissertation

**zur Erlangung des akademischen Grades des Doktors der
Naturwissenschaften (Dr. rer. nat.)
der Medizinischen Fakultät, Centrum für Integrative
Physiologie und Molekulare Medizin (CIPMM),
der Universität des Saarlandes**

vorgelegt von Hsin-Fang Chang

**Dezember 2016
Homburg/Saar**

Tag des
Promotionskolloquiums:

Dekan:

Vorsitzender:

Berichtersteller:

Dedicated to my beloved family

致我最親愛的家人

Acknowledgements

I would like to give my sincere thanks to all people who were involved in my work or being accompanied with me during these years of my PhD. First and foremost, I would like to give my deepest gratitude to my supervisor, Prof. Dr. Jens Rettig for encouragement, support and guidance over years. It would not be possible to complete my PhD without his supervision. He is by far more than a mentor in my scientific carrier but also being a friend with a very positive and optimistic personality in life.

I would like to extent my thanks to my colleagues, especially to Dr. Varsha Pattu, who guided and assisted me in initiating my thesis work. I would further like to give many thanks to Dr. Claudia Schirra for doing an outstanding job in electron microscopy experiments. I appreciate the help of Dr. Elmar Krause for microscopy and FACS, as well as Dr. Ute Becherer for TIRF microscopy and Dr. David Stevens for a lot of input in my projects. My essential thanks go to the technicians for excellent technical support, Anja Ludes, Tamara Paul, Margarete Klose, Manuela, Schneider, Anne Weinland, Jacqueline Vogel, Nina Blumberg, Katrin Sandmeier. Further thanks to Dr. Mahantappa Halimani and Yan Zhou for daily simple scientific help and being companion during certain periods of time. I enjoyed the companies with Hawraa Bzeih, Praneeth Chitirala, Marwa Sleiman and Olga Ratai for nice discussions in the lab about science and life. I also deeply appreciate the GK1326 graduate school for funding and an outstanding program during three years. I would like to thank my project collaborators in the Pharmacology department, especially Prof. Dr. Veit Flockerzi for nice discussions and suggestions, also technical help from Dr. Stefanie Mannebach-Götz, Dr. Andreas Beck, Dr. Claudia Fecher-Trost and Dr. Ulrich Wissenbach.

I also thank my Taiwanese friends in Saarbrücken, especially to Dr. Wei-Chen Chiu and Dr. Po-Hsien Lee for encouragement.

The most special and irreplaceable thanks go to my beloved family. I thank my parents for always being at my side and fully supporting me at any cost.

Contents

1. Abstract.....	1
2. Zusammenfassung.....	2
3. Introduction	4
3.1. Cytotoxic T lymphocytes effector function	4
3.2. Calcium signaling in T cell effector function.....	6
3.3. Calcium regulation in granule endocytosis.....	6
3.4. SNARE mediated granule exocytosis	7
3.5. Aim of the study	9
4. Material and Methods.....	10
4.1. Materials.....	10
4.1.1. Used commercial kits	10
4.1.2. Chemicals and reagents.....	10
4.1.3. Commercial antibodies	10
4.1.4. Media and solutions.....	11
4.1.5. Plasmids.....	13
4.2. Methods	13
4.2.1. Primary CD8 ⁺ lymphocyte isolation	13
4.2.2. Activation of naïve to effector cells (CTLs).....	13
4.2.3. Electroporation	14
4.2.4. Anti-RFP antibody labeling with Alexa fluorophore	14
4.2.5. Target cell culture	14
4.2.6. Live cell confocal imaging.....	14
4.2.6.1. Endocytosis.....	14
4.2.6.2. Acquisition settings	15
4.2.6.3. Analysis.....	15
4.2.7. Structured illumination microscopy.....	15
4.2.7.1. Structured illumination microscopy setup.....	15
4.2.7.2. Dynamin2 mutant experiment	15
4.2.7.3. Co-localization analysis.....	16
4.2.7.4. Dynasore experiments for IS formation and CD3 recycling	16
4.2.8. Population calcein killing assay	16
4.2.9. Western blot	17
4.2.9.1. Lysate preparation	17
4.2.9.2. Blotting	17
4.2.9.3. Immunocytochemistry	17
4.2.10. Degranulation assay.....	18
4.2.11. Total internal reflection fluorescence microscopy.....	18
4.2.12. Flower topology experiment	18
5. Results	20
5.1. Cytotoxic granule endocytosis in CTLs.....	20
5.1.1. LAMP1 endocytosis in CTLs	20
5.1.2. Specificity of the anti-RFP antibody.....	22
5.1.3. Cytotoxic granules endocytose at the IS in CTLs.....	23
5.2. Cytotoxic granules undergo Clathrin- and Dynamin-mediated endocytosis	25
5.2.1. Cytotoxic granule endocytosis is Dynamin-dependent.....	25
5.2.2. Clathrin and CALM mediate cytotoxic granule endocytosis	28
5.3. Endocytosed cytotoxic granules are re-filled with Granzyme B in CTLs	30
5.4. Endocytosis of CGs is required for CTL effector function	32
5.5. Calcium dependence of cytotoxic granule endocytosis	35

5.6.	Flower is expressed in mouse CTLs	36
5.7.	Topology of Flower protein.....	37
5.8.	Localization of Flower	39
5.9.	Exocytosis is unchanged in Flower-deficient CTLs	40
5.10.	Cellular calcium is unchanged in Flower-deficient CTLs.....	41
5.11.	Flower-deficiency leads to a block of CG endocytosis	42
5.12.	CG endocytosis is blocked in a very early stage in Flower-deficient CTLs.....	45
5.13.	High extracellular calcium can rescue the endocytosis defect in Flower-deficient CTLs.....	47
5.14.	Flower vesicles polarize early to the IS and localize in close proximity to fusogenic and endocytic cytotoxic granules	48
5.15.	Flower mutant can not rescue the endocytosis defect	50
6.	Discussion	52
6.1.	Cytotoxic granule endocytosis.....	52
6.2.	Calcium dependency of cytotoxic granule endocytosis	54
7.	Summary	64
8.	Outlook.....	65
9.	References	66

Abbreviations

CTL	cytotoxic T lymphocyte
NK	natural killer
CG	cytotoxic granule
APC	antigen-presenting cell
SMAC	supramolecular activation cluster
MTOC	microtubule-organizing center
IS	immunological synapse
PLC	phosphoinositide-specific phospholipase C
IP3	inositol-1,4,5-trisphosphate
DAG	diacylglycerol
ER	endoplasmic reticulum
STIM	stromal interaction molecule
SNARE	soluble N-ethylmaleimide-sensitive factor attachment protein (SNAP) receptor
Syb2	Synaptobrevin2
Sybki	Synaptobrevin2-mRFP knock-in
CLEM	correlative fluorescence light and electron microscopy
LAMP1	lysosomal-associated membrane protein 1
CCCP	carbonyl cyanide 3-chlorophenylhydrazone
DMSO	dimethyl sulfoxide
SIM	structured illumination microscopy
TIRF	total internal reflection fluorescence microscopy
TEM	transmission electron microscopy

List of Figures

Figure 1.	The immunological synapse.....	4
Figure 2.	Flower protein sequence alignment.....	7
Figure 3.	Synaptobrevin2 is a specific marker for fusogenic cytotoxic granules.....	8
Figure 4.	Serial killing by CTL.....	9
Figure 5.	Experimental strategy of investigating the topology of Flower protein.....	19
Figure 6.	Scheme of LAMP1 endocytosis.....	20
Figure 7.	Cytotoxic granule endocytosis in CTLs.	22
Figure 8.	LAMP1 endocytosis occurs only upon target cell contact in CTLs.....	21
Figure 9.	Scheme of cytotoxic granule endocytosis.....	23
Figure 10.	CG endocytosis occurs upon specific antigen recognition.	24
Figure 11.	CG endocytosis occurs only upon target cell contact in CTLs.....	24
Figure 12.	Endocytosed cytotoxic granules are polarized to the sequential immunological synapse.	25
Figure 13.	Endocytosis of CG membrane proteins at the IS is Dynamin-dependent.....	27
Figure 14.	Clathrin and CALM mediate CG endocytosis.....	29
Figure 15.	Endocytosed CGs are re-filled with Granzyme B within 60 min.....	31
Figure 16.	Endocytosed Synaptobrevin2 gradually co-localized with endocytosed LAMP1.....	32
Figure 17.	Endocytosis of CGs is required for fulfilling CTL effector function.	33
Figure 18.	Receptor signaling and IS formation is unchanged upon Dynasore pre-treatment.....	35
Figure 19.	Flower protein is expressed in primary CTLs from mouse.	36
Figure 20.	Flower protein contains four transmembrane segments.....	38
Figure 21.	Flower is localized on intracellular vesicles, but not on cytotoxic granules or on endosomal compartments.	39
Figure 22.	Exocytosis is unchanged in Flower-deficient CTLs.....	40
Figure 23.	Cellular calcium is unchanged upon CD3 activation in Flower-deficient CTLs....	41
Figure 24.	LAMP1 endocytosis is affected in Flower-deficient CTLs.	42
Figure 25.	Cytotoxic granule endocytosis is impaired in Flower-deficient CTLs.....	44
Figure 26.	Flower-deficiency leads to a delay of granule transport.....	45
Figure 27.	CG endocytosis is blocked in the early stage in Flower-deficient CTLs.....	46
Figure 28.	High extracellular calcium can rescue the endocytosis defect in Flower-deficient CTLs.	48
Figure 29.	Flower vesicles are polarized to the IS and localized around exocytic and endocytic cytotoxic granules.	50
Figure 30.	Flower mutant cannot rescue the endocytosis defect.....	51
Figure 31.	Proposed model.....	57
Figure 32.	Granule membrane is reserved after exocytosis and internalizes distinct from the plasma membrane.....	60

1. Abstract

Cytotoxic T lymphocytes (CTLs) fight against infection by eliminating virus-infected and malignant cells from the body. CTLs recognize its target upon specific T cell receptor engagement and consequently triggers cytotoxic granules (CGs) release to the cell-cell contact site, termed immunological synapse (IS) to induce target cell death. CTLs are efficient killers as multiple routes of fast lethal deliveries suggest, however whether the sustained cytotoxic supply from retrieved granules after fusion contributes to multiple target cell killing remains unknown. By using primary CTLs isolated from Synaptobrevin2-mRFP knock-in mice, we demonstrate endocytosis of the specific CG membrane protein Syb2 at the IS upon target cell contact by confocal live cell imaging. CG endocytosis is Clathrin- and Dynamin-dependent, and later on endocytosed CGs became re-filled with toxic substances like Granzyme B to again enable cytotoxicity. These endocytic granules polarized to respective synapses upon sequential target cell contacts. Importantly, blocking CG endocytosis reduces the serial killing efficiency by about 50%, indicating endocytic CGs contribute significantly to the overall cytotoxic capacity. These data demonstrate that continuous endocytosis of CG membrane proteins is a prerequisite for efficient serial killing of CTLs and identify key events in this process. We further investigate the involvement of the vesicular membrane protein Flower in the calcium-dependence of CG endocytosis. It was previously suggested to function as a calcium channel to regulate synaptic endocytosis in *drosophila*. Flower is proposed to transfer from vesicle to plasma membrane through vesicle fusion and thus regulates calcium influx. We showed that the Flower protein, which contains four transmembrane domains, is expressed in mouse CTLs. Flower-deficiency does not affect degranulation or CG exocytosis, however, it leads to a block of CG endocytosis at an early stage. This defect in endocytosis can be rescued by re-introducing Flower or by increasing extracellular calcium, suggesting that the phenotype is specifically due to a lack of Flower and that other calcium sources could compensate its function. Additionally, Flower vesicles polarize early to the IS and localize around exocytic and endocytic granules. Intriguingly, a Flower mutant with tyrosin motifs (YxxF) substituted to alanine shows a re-distribution from vesicles to the plasma membrane, but fails to rescue the endocytosis defect. This result implies that either Flower functions on vesicles rather than at the plasma membrane or that active Flower requires interaction with other molecules via its tyrosin motifs. Taken together, these data identify Flower as an essential molecule initiating granule endocytosis. However, further studies are required to answer the question whether Flower plays a role in calcium-dependence of endocytosis.

2. Zusammenfassung

Zytotoxische T Lymphozyten (CTLs) bekämpfen Infektionen, indem sie virusinfizierte oder entartete Zellen eliminieren. CTLs identifizieren ihre Zielzellen mit Hilfe spezifischer T-Zell Rezeptoren, was zur Ausbildung eines Zell-Zell-Kontaktes, der sogenannten Immunologischen Synapse, führt. An dieser IS erfolgt letztlich die Fusion zytotoxischer Granula (CGs), die den Zelltod der Zielzelle induzieren. CTLs sind effektive Tötungsmaschinen, da sie hintereinander Tausende an Zielzellen in kurzer Zeit eliminieren können. Allerdings ist unklar, inwieweit an dieser seriellen Zytotoxizität rezyklierte Granula beteiligt sind. Durch die Nutzung von CTLs, die aus Synaptobrevin2-mRFP Knock-in Mäusen gewonnen wurden, konnten wir mit Hilfe konfokaler Mikroskopie zeigen, dass Syb2 an der IS nach Zielzellkontakt endozytiert wird. Die Endozytose von CGs erfolgt über Clathrin- und Dynamin-abhängige Wege. Später werden endozytierte CGs mit toxischen Substanzen wie GranzymeB aufgefüllt, um die Zytotoxizität erneut herzustellen. Diese endozytotischen Granula polarisieren dann zu den jeweiligen Synapsen neuer Zielzellkontakte. Wichtiger Weise führt die Blockierung der Endozytose zu einer etwa um 50% reduzierten Tötungseffizienz, was ein Hinweis darauf ist, dass Endozytose zur zytotoxischen Gesamtkapazität signifikant beiträgt. Diese Daten zeigen, dass die Endozytose von CG Membranproteinen eine Voraussetzung für effizientes serielles Abtöten von Zielzellen durch CTLs ist und identifizieren Schlüsselereignisse dieses Prozesses. Weiterhin untersuchten wir ein Kandidatenmolekül für die Kalziumabhängigkeit der CG Endozytose. Dieses Flower genannte, vesikuläre Protein könnte in *Drosophila melanogaster* ein endozytoseregulierender Kalziumkanal sein. Es wird angenommen, dass Flower durch Fusion vom Vesikeln zur Plasmamembran transferiert wird und dort den Kalziumeinstrom reguliert. Wir konnten die Expression des Flower-Proteins, welches vier Transmembrandomänen enthält, in CTLs der Maus nachweisen. Das Fehlen des Flower-Proteins beeinflusste weder die Degranulation noch die Exozytose der CGs, führte aber zu einem vollständigen Block der CG Endozytose in einem frühen Stadium. Dieser Endozytose-Defekt konnte durch erneutes Hinzufügen von Flower oder durch eine Erhöhung der extrazellulären Kalziumkonzentration behoben werden. Es kann also angenommen werden, dass der Defekt spezifisch für das Fehlen von Flower war und andere Kalziumquellen das Fehlen von Flower kompensieren können. Hinzu kommt, dass Flower Vesikel früh zur IS polarisieren und in der Nähe exo- und endozytotischer Vesikel zu finden sind. Interessanter Weise zeigen Flower Mutanten, bei denen bestimmte Tyrosine zu Alanin ausgetauscht wurden, eine Neuverteilung von Flower von Vesikeln hin zur Plasmamembran, ohne jedoch den Endozytose-Defekt zu beheben. Diese Ergebnisse können in zweierlei Weise interpretiert werden: der Ort des Flower-Effekts ist eher das Vesikel als die Plasmamembran oder aktives Flower benötigt Interaktionen mit anderen Molekülen über seine Tyrosin Motive. Diese Daten legen nahe, dass Flower ein essentielles Molekül für die Auslösung der Endozytose ist. Allerdings sind für die Klärung der Frage, ob Flower eine Rolle in der

Kalziumabhängigkeit spielt, weitere Experimente in zukünftigen Untersuchungen notwendig.

3. Introduction

3.1. Cytotoxic T lymphocytes effector function

Cytotoxic lymphocytes consist of cytotoxic T lymphocytes (CTLs) and natural killer (NK) cells and play an essential role in immune surveillance. They destroy virus-infected or tumorigenic cells with remarkable specificity. CTLs recognize their targets through their T-cell receptor (TCR) and co-receptor CD8 which bind to peptide-major histocompatibility complex (MHC) class I expressed on the surface of antigen-presenting cells (APCs). Upon TCR engagement, receptors that are involved in target cell recognition are clustered to form the central supramolecular activation cluster (cSMAC) and induce the polarization of the centrosome (the microtubule-organizing center, MTOC) to the plasma membrane towards the target (Stinchcombe et al., 2001). This contact zone between CTL and target cell with specialized signaling domain is called immunological synapse (IS) (Grakoui et al., 1999; Monks et al., 1998) (Figure 1). These signaling events eventually trigger the polarization of cytotoxic granules (CGs) to the IS, followed by the release of cytotoxic contents such as Perforin and Granzymes into the synaptic cleft, leading to target cell death (Voskoboinik et al., 2010).

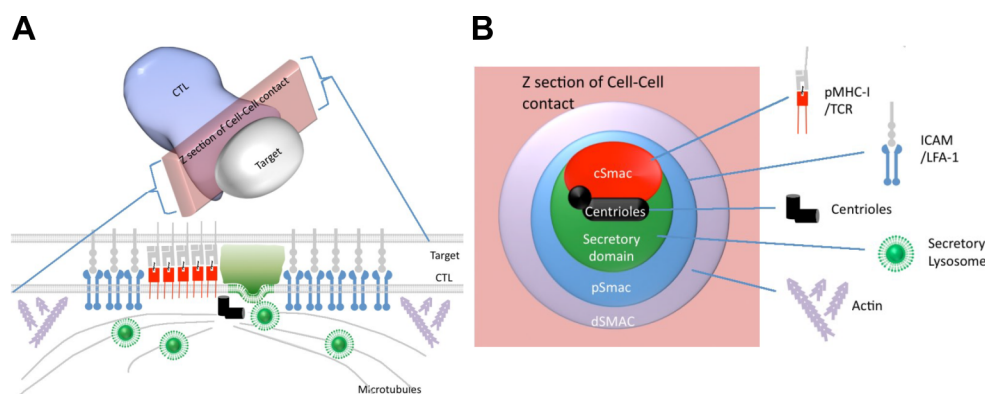


Figure 1. The immunological synapse.

(A) Scheme of the immunological synapse (IS) at the cross section between T cell and target cell contact. The IS formation leads to reorganization of actin, cytoskeleton and secretory lysosomes. (B) The relative positions of the cSMAC, pSMAC and dSMAC within the IS. Figure taken from (Griffiths et al., 2010).

CTLs hold an unique effector function to kill multiple targets by spatiotemporal coordination of IS and CG secretion which provides remarkable efficiency of lethal hit delivery (Weidinger et al., 2013). Several reports provide evidence for the efficient killing ability of CTLs. The serial killing was originally described by Isaaz et al. showing that multiple routes of lytic coordination contribute to efficient killing. TCR triggers CG degranulation, refilling of the granules and the newly synthesized lytic proteins secretion via a non-granule pathway. The newly synthesized lytic proteins can be stored in the cells and refill the granules. However, up to one third Granzyme

A and B can be secreted directly from the CTL via the constitutive secretory pathway where one third of the protein fails to acquire the granule targeting signal. Perforin is also secreted via the constitutive pathway from both the NK cell line YT and from CTL clones after TCR cross-linking. Blocking constitutive secretion does not affect the directional killing of recognized target cells, but abrogates bystander killing. This indicates that bystander killing arises from constitutive secretion via a non-granule pathway. The authors demonstrate that the perforin/granzyme-mediated lytic pathway can be maintained while CTLs kill multiple target cells, not only through refilling of lytic protein into the granules, but also via secretion from a non-granule-mediated pathway (Isaaz et al., 1995). More molecular details were reported later on TCR activation and cytotoxic responses. It has been suggested that IS formation plays a role in lytic granule polarization (Stinchcombe et al., 2001). However, several groups have shown that polarization of the lytic machinery can occur even in the absence of a mature IS (Faroudi et al., 2003; Purbhoo et al., 2004) or that the formation of the cSMAC is not required for cytolytic activity (O'Keefe and Gajewski, 2005). Purbhoo et al. demonstrated that CTLs are able to detect a single foreign antigen but require about ten pMHC complexes to generate a sizable calcium increase needed to form a mature synapse. However, only three pMHC complexes are required for killing. These data indicate that the fast killing process does not require stable synapse formation and complete signaling (Purbhoo et al., 2004). This finding agrees with the work done by Bertrand and his coworkers demonstrating that rapid lytic delivery occurs before MTOC polarization (Bertrand et al., 2013). It was widely assumed that the lethal hit delivery by CTLs is mechanistically linked to centrosome polarization to the IS, leading to directed release of lytic granules within a confined secretory domain. However, Bertrand et al. found that in many CTLs and target cell contacts, CG secretion precedes microtubule polarization, which can be detected during the first minute after cell-cell contact. Furthermore, inhibition of MTOC formation and centrosome polarization impairs neither granule release nor killing efficiency. Therefore, the authors suggest an extremely rapid step of lytic granule secretion for efficient lethal hit delivery (Bertrand et al., 2013). All these evidences including low-threshold cytotoxic responses and the rapid lytic granule secretion indicate that CTLs are highly efficient killers. However, the authors were unable to demonstrate the efficient multiple/serial killing, which requires a sustained supply of lethal hits to different targets. Isaaz et al. show the lytic protein refilling and secretion by an enzymatic assay and immunoblots (Isaaz et al., 1995), which is rather obscure since the overall protein level does not precisely describe the ongoing process in the cellular level. We therefore wanted to extend the concept of serial killing and hypothesized that after cytotoxic granule secretion, the granules are recycled and be reused in CTLs in order to have a sustained supply to complete efficient multiple killing. We addressed this hypothesis by performing live cell confocal imaging in combination with high-resolution SIM imaging to visualize granule retrieval in real-time and individual granule refilling at the cellular level.

3.2. Calcium signaling in T cell effector function

Killing is a multi-step process, which includes TCR recognition, cytoskeleton actin reorientation and finally cytotoxic granule release at the IS. Calcium is an important messenger involved in many steps of the signaling. Calcium signaling is involved in granule transport and release most likely through the regulation of calcium-responsive proteins such as myosin (Batters et al., 2016; Wada et al., 2016), synaptotagmin (Brose et al., 1992), Munc13 (Feldmann et al., 2003; Menager et al., 2007) and Calmodulin (Takayama and Sitkovsky, 1987; Trenn et al., 1989) to facilitate the rapid movement and fusion of granules with the plasma membrane. The end point of this cascade, target cell killing, also requires calcium influx (Esser et al., 1998; Lancki et al., 1987; MacLennan et al., 1980). The molecular mechanism of calcium entry in CTLs has been revealed in the past decade. First, the engagement of TCR leads to activation of phosphoinositide-specific phospholipase C (PLC) γ . PLC γ breaks down phosphatidylinositol-4,5-bisphosphate to generate inositol-1,4,5-trisphosphate (IP₃) and diacylglycerol (DAG). IP₃ activates the release of calcium from the endoplasmic reticulum (ER) into the cytoplasm by binding to IP₃ receptors (IP₃R) located on the ER membrane. The loss of calcium in the ER is sensed by Stromal interaction molecule (STIM) on the ER membrane surface. Upon ER store depletion, STIM clusters and relocates near the plasma membrane to interact with ORAI calcium channel to open the gates for calcium entry (Prakriya et al., 2006; Vig et al., 2006; Zweifach and Lewis, 1993). Calcium signaling also modulates T cell effector function. Live cell imaging in combination of using calcium indicator in CTLs correlates the cytosolic calcium increase before target cell death in a second to minute range time scale (Lopez et al., 2013; Lyubchenko et al., 2001). Lopez et al. demonstrate the sequential increase of cytosolic calcium in CTLs or NK cells in each single hit, which leads to target cell lysis (Lopez et al., 2013). Although calcium-dependent target cell lysis does not directly translate to calcium-dependent granule exocytosis, these imaging data correlating granule-mediated killing to target cell lysis indicate that granule exocytosis requires calcium influx.

3.3. Calcium regulation in granule endocytosis

Calcium triggers both exocytosis and endocytosis at many synapses. Exocytosis and endocytosis are tightly coupled processes. Endocytosis is thought to occur actively for replenishment of vesicle loading for efficient transmission or passively for maintenance of a homeostatic membrane balance. Following exocytosis, endocytosis is initiated to retrieve exocytosed vesicles within seconds to minutes. Calmodulin and its downstream molecule, the calcium-dependent phosphatase Calcineurin, are reported to play roles in calcium-dependent granule endocytosis (Marks and McMahon, 1998; Wu et al., 2009; Wu et al., 2014). However, calcium influx triggers vesicle exocytosis and also activates both proteins. Additionally, exocytosis is affected upon application of Calcineurin inhibitors or Calmodulin antagonists (Dutz et al., 1993; Takayama and Sitkovsky, 1987). Therefore, it is

currently unclear which molecule is responsible for endocytosis in a calcium-dependent manner. Recently, Yao et al. proposed that Flower, a vesicular membrane protein conserved from worm to human, functions as a calcium channel (Yao et al., 2009) (Figure 2). A Flower mutant displays impaired synaptic vesicle endocytosis and reduced intracellular calcium levels in the neuromuscular junction in *Drosophila*. They proposed a model that upon vesicle fusion, Flower transfers from the vesicle membrane to the plasma membrane to mediate calcium influx (Yao et al., 2009). Flower thus seems to be a potential candidate regulating calcium entry for endocytosis. We investigate its function and potential contribution to the calcium-dependence of endocytosis in primary CTLs from Flower-deficient mice.



Figure 2. Flower protein sequence alignment.

The Flower orthologs with splice variants from *Mus musculus* (m), *Homo sapiens* (h), *Danio rerio* (z) and *Drosophila melanogaster* (d) are aligned. The color code of green, blue and yellow presents Flower antibody binding epitopes used in this study, putative transmembrane domains and exon/intron borders respectively. The marked red sequence is the conserved calcium selectivity filter sequence. The mouse Flower studied in this study is marked in gray.

3.4. SNARE mediated granule exocytosis

Granule fusion is mediated by formation of the SNARE (soluble N-ethylmaleimide-sensitive factor attachment protein (SNAP) receptor) complex (Chen and Scheller, 2001; Jahn et al., 2003). The SNARE complex is formed by four α -helices contributed by synaptobrevin located on the vesicle (v-SNARE), syntaxin and SNAP-25 located at the plasma membrane (t-SNARE). Additionally, synaptotagmin serves as a calcium sensor and regulates SNARE zippering. In CTLs, CG fusion is driven by several SNARE proteins from which Synaptobrevin2 (Syb2) was identified as the v-SNARE on CGs mediating fusion in mouse CTLs (Matti et al., 2013).

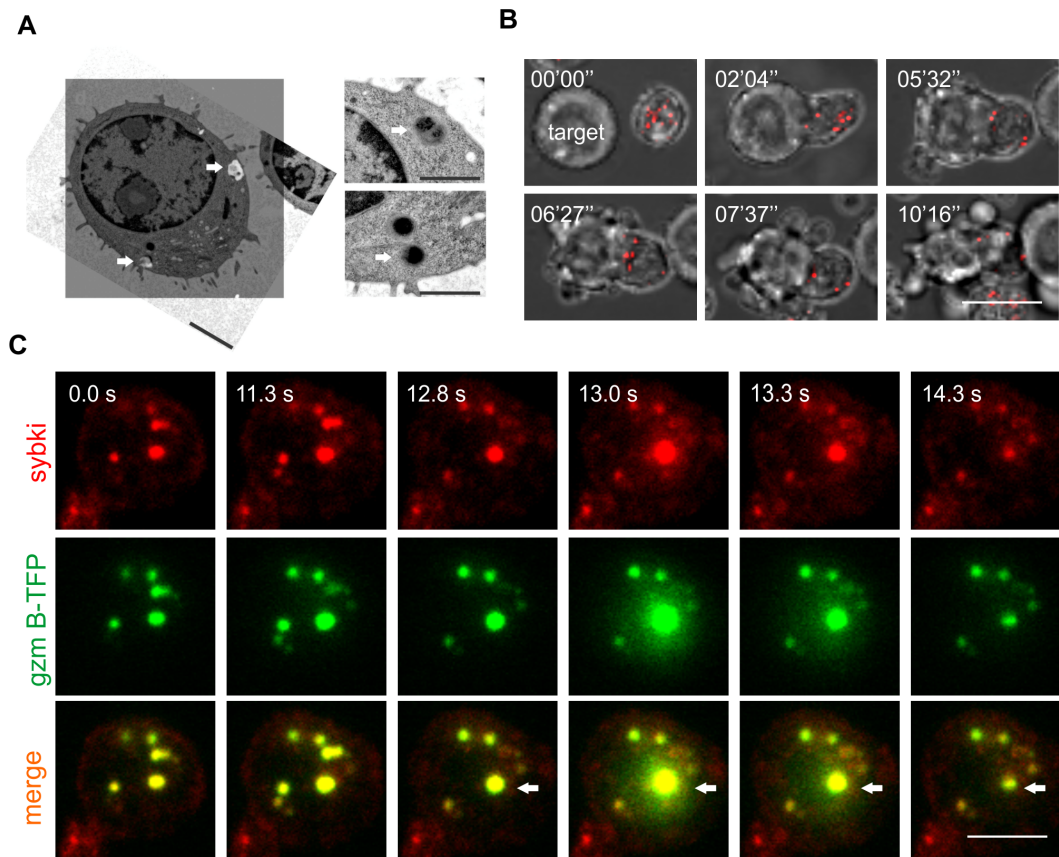


Figure 3. Synaptobrevin2 is a specific marker for fusogenic cytotoxic granules.

(A) Representative CLEM image of a primary mouse CTL obtained from Synaptobrevin2-mRFP knock-in mice. Left, EM image from ultrathin section of 80 nm of a mouse CTL with the corresponding processed SIM-image. SIM image was taken at excitation 561 nm wavelength for mRFP signal from 500 nm thick section. Arrows point to Synaptobrevin2-positive cytotoxic granules. Scale bar: 2 μ m. Right, enlarged areas with the corresponding organelles. Scale bar: 1 μ m. (Figure taken from (Pattu et al., 2013)). (B) Time-lapse snapshots of a Sybki CTL killing a target cell followed by endogenous Syb2-positive CGs (red) polarizing to IS. Scale bar: 10 μ m. (C) TIRF images of CG fusion by a Granzyme B-TFP (green) transfected Sybki (red) CTL. Scale bar: 5 μ m.

We generated Synaptobrevin2-mRFP knock-in (Sybki) mice as a tool to have an endogenous CG marker labeled with red fluorescence to visualize granule trafficking. Correlative fluorescence electron microscopy (CLEM) data show that the Syb2-mRFP positive granules are electron dense granules (Figure 3A) which are characterized most likely containing protease matrix like perforin or granzymes (Peters et al., 1991). Additionally, we find a high degree of co-localization between endogenous Syb2 granules and overexpressed Granzyme B-mTFP. We were also able to observe their fusion by TIRFM upon anti-CD3 coated coverslip activation (Figure 3C). Furthermore, Sybki CTLs polarize their Syb2-mRFP positive granules towards to the target cell upon TCR recognition which sequentially induces target cell apoptotic death (Figure 3B). These data demonstrate that Syb2 is a specific marker for mature CGs and that Syb2-mRFP is ideally suited to investigate CG trafficking by real-time imaging.

3.5. Aim of the study

As described above, we hypothesize CG endocytosis after fusion for sequential rounds of exocytosis in order to achieve efficient serial killing (Figure 4). We use CTLs isolated from Sybki mice to track CG in live cell confocal imaging and to investigate if CG endocytosis exists. If it does, then the following questions would be what is the molecular mechanism in terms of endocytic pathway and extensively if calcium regulates granule endocytosis. Finally, we ask whether endocytic CGs contribute to the efficient killing observed in primary CTLs.

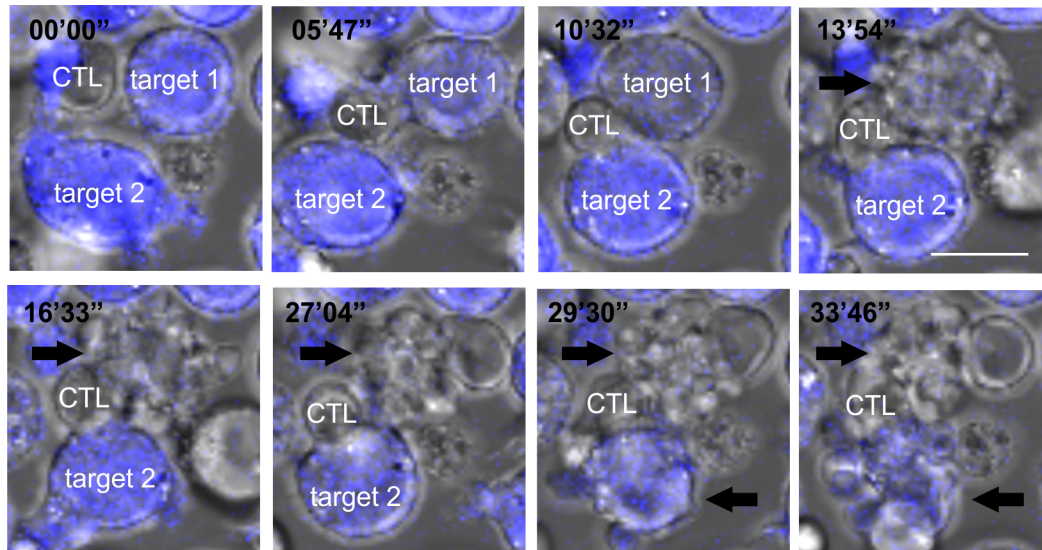


Figure 4. Serial killing by CTL.

Time-lapse images showing the serial killing of two target cells by a CTL. P815 target cells (blue) were loaded with calcein blue as an indicator of cell death. Arrows point to the apoptotic target cells. Scale bar: 10 μ m.

In this study, we show that the CG membrane proteins Syb2 and LAMP1 endocytose upon target cell contact by live cell confocal imaging. CG endocytosis occurs at the IS and is mediated through a Clathrin- and Dynamin-dependent pathway. CALM as a Syb2 specific adaptor protein also is contributing to granule endocytosis. Following refilling of the cytotoxic component Granzyme B into endocytic CGs, endocytic granules polarize to the sequential IS and contribute significantly to the multiple killing of target cells. Moreover, we demonstrate that the four transmembrane protein Flower is located on intracellular vesicles and plays a role in CG endocytosis. Flower-deficiency leads to a defect at the early stage of endocytosis. Re-introducing Flower protein or increase in extracellular calcium can rescue the phenotype. Mutation of tyrosin motifs (Yxx Φ) on Flower results in a relocation of Flower from the vesicle membrane to the plasma membrane. However, the mutant fails to rescue the block of endocytosis, indicating that Flower might be selectively functionalized according to its localization on vesicles or through interaction with other molecules. These data thus identify Flower as an important molecule involved in CG endocytosis in a calcium-dependent or independent-manner.

4. Material and Methods

4.1. Materials

4.1.1. Used commercial kits

kits	company
Dynabeads® FlowComp™ Mouse CD8 Kit	Invitrogen
Alexa Fluor® 488 Monoclonal Antibody Labeling Kit	Invitrogen
EndoFree Plasmid Maxi Kit	Qiagen
Plasmid Midi Kit	Qiagen
Plasmid Mini Kit	Qiagen
QIAquick Gel Extraction Kit	Qiagen
CytoTox 96® Non-Radioactive Cytotoxicity Assay	Promega
Nucleofection kit for mouse T cells	Lonza

4.1.2. Chemicals and reagents

reagents	company
Carbonyl cyanide 3-chlorophenylhydrazone (CCCP)	Sigma
Dynasore	Merck Millipore

4.1.3. Commercial antibodies

antibodies	species	dilution	company
Primary antibody			
Anti-RFP	mouse	WB 1:1000 ICC 1:1000	Genway
Alexa Fluor488 anti-CD107a (LAMP1, clone 1D4B)	mouse	Live imaging 1:50	Biolegend
Alexa Fluor647 anti-CD107a (LAMP1, clone 1D4B)	mouse	Live imaging 1:50	Biolegend
PE-anti-CD107a	mouse	1:500	BD Pharmingen
Anti-CD3e	hamster	Live imaging 1:25	BD Pharmingen
Anti-ZAP70	mouse	ICC 1:100	Merck Millipore
Anti-dynamin	mouse	ICC 1:500	Abcam
Anti-clathrin heavy chain	rabbit	ICC 1:500	Abcam

Anti-clathrin heavy chain (clone X22)	mouse	ICC 1:500	Thermo Scientific
Anti-CALM	goat	WB 1:1000 ICC 1:500	Santa Cruz
Anti-granzyme B	mouse	ICC 1:500	Cell Signaling
Anti-adaptin α (clone 8/Adaptin α)	mouse	ICC 1:500	BD Transduction Laboratories
Anti-HA	rat	ICC 1:1000	Roth
Anti-GAPDH	mouse	WB 1:5000	Sigma
Anti-flower (spleen pre-cleared)	mouse	ICC 1:100 WB 1:1000	Provided from AG Flockerzi
Secondary antibody			
Alexa 488 conjugated anti-rabbit IgG	goat	1:2000	Invitrogen
Alexa 568 conjugated anti-rabbit IgG	goat	1:2000	Invitrogen
Alexa 467 conjugated anti-rabbit IgG	goat	1:2000	Invitrogen
Alexa 405 conjugated anti-mouse IgG	goat	1:2000	Invitrogen
Alexa 488 conjugated anti-mouse IgG	goat	1:2000	Invitrogen
Alexa 647 conjugated anti-goat IgG	donkey	1:2000	Invitrogen
Alexa 633 conjugated anti-mouse IgG	goat	1:2000	Invitrogen
Cy5 conjugated anti-rat IgG	goat	1:1000	Invitrogen
HRP conjugated anti-mouse	goat	1:1000	Life technology
HRP conjugated anti-rabbit	goat	1:10,000	Life technology

4.1.4. Media and solutions

solution	compositions
Culture medium	
Iscove's Modified Dulbecco's Medium (IMDM)	IMDM (GIBCO) +10% FCS +50 μ M 2-Mercaptoethanol +0.5% Pen/Step
RPMI	RPMI (GIBCO) +10% FCS +1% Pen/Step +10mM HEPES

Erythrocyte lysis buffer (pH: 7.3)	155mM NH ₄ Cl 10mM KHCO ₃ 0,13 mM EDTA
Isolation buffer	PBS +0.5% BSA
Extracellular buffer for TIRF measurements (pH: 7.4 and Osmolarity: 300-310 mOsm)	
0 mM calcium buffer	155 mM NaCl 4.5 mM KCl 5 mM HEPES 3 mM MgCl ₂
10 mM calcium buffer	140 mM NaCl 4.5 mM KCl 5 mM HEPES 2 mM MgCl ₂ 10 mM CaCl ₂
Solutions for immunocytochemistry	
Fixation buffer	4% PFA in PBS
Permeablized buffer	0.1% Triton-X100 in PBS
Blocking buffer	0.1% Triton-X100 in PBS+ 2% BSA
Solutions for western blot (pH: 7.4)	
1X TBST	20 mM Tris 0.15 M NaCl 0.05% Tween 20
Lysis buffer	
Lysis buffer	50 mM Tris-Cl 150 mM NaCl 250 µM PMSF 1% Triton-X100 1 mM Deoxycholate 1 mM EDTA 1 mM DTT 1 protease inhibitor tablet (Roth)

4.1.5. Plasmids

For cloning pMax-flower-mTFP construct, pCAGGS-Flower-pHluorin plasmid provided by AG Flockerzi was used as a starting template. Flower was cut out of pCAGGS-Flower-pHluorin plasmid by *EcoRV* (Fermentas). Flower cDNA was then amplified using forward primer: 5'-ATG TAT ACC GGA ATT CGC CGC CAC CAT GAG CGG CTC GGG CGC CGC C-3' and reverse primer: 5'-ATG TAT ATA GTC TAG AAC CGC CGC TTC CGC CGC TCC CAC CCA GTT CCC CCT CGA AAG T-3' by polymerase chain reaction (PCR) and digested with *EcoRI* (Fermentas) and *XbaI* (NEB). Flower cDNA was then ligated into pMax vector. mTFP cDNA was also amplified using forward primer: 5'-ATG TAT ATA GTC TAG AAT GGT GAG CAA GGG CGA GGA G-3' and reverse primer: 5'-ATG TAT ACC GCT CGA GTT ACT TGT ACA GCT CGT CCA T-3' by PCR and digested with *XbaI* (NEB). and *XhoI* (NEB). Lastly, mTFP was ligated into pMax-Flower vector by ligase (Fermentas).

For cloning pMax-Flower mutant-mTFP construct, a Flower-mutant plasmid was purchased from Integrated DNA Technologies. The cloning procedures were described above by using the same restriction enzymes and ligase described above. Both Flower constructs contain a KOZAK sequence (CCG CCG CCA CC) preceding the Flower cDNA and a linker between Flower and mTFP gene.

4.2. Methods

4.2.1. Primary CD8⁺ lymphocyte isolation

C57BL/6 wildtype (WT), homozygous Synaptobrevin2-mRFP knock-in (Sybki), homozygous Flower gene knock-out (Flower KO) and homozygous Flower KO and Syb2-mRFP knock-in cross-breed (Sybki/Flower KO) mice were used for all experiments. The Flower KO mice were generated from AG Flockerzi in Pharmacology department. Spleens from 8-20 week old WT or Sybki or Flower KO mice were taken out and gently pushed through a 70 μ m cell strainer (Corning Life Sciences). The splenocytes were collected in RPMI medium followed by removing erythrocytes using erythrocyte lysis buffer for 30 seconds. After an additional washing step, cells were then isolated using dynabeads FlowComp Mouse CD8 Kit (Invitrogen) as described by the manufacturer. Briefly, the CD8 cells were positively isolated from splenocytes followed by incubating 5×10^7 cells with 25 μ L anti-CD8 antibody for 10 min on ice to select CD8⁺ cells by adding 75 μ L CD8 antibody-coated dynabeads to cells. Lastly, cells were detached from the dynabeads using releasing buffer. CD8⁺ cells were collected and re-suspended in IMDM culture medium.

4.2.2. Activation of naïve to effector cells (CTLs)

The isolated naïve CD8⁺ cells were cultured for 3 days at a density of 1×10^6 cells/mL in IMDM medium at 37°C with 5% CO₂ humidity. Cells were cultured in 2×10^6 cells in 2 mL IMDM medium in a 24-well plate with additional anti-CD3/anti-CD28 activator beads (1:0.8 ratio) to generate effector CTLs. Cells were split after 2 days in culture with additional fresh IMDM medium and 250 U/mL recombinant IL-2 (Life technology). Experiments were performed using day 2 or day 3 cells from this culture.

4.2.3. Electroporation

Effector cells generated as described above were used for electroporation of plasmid DNA. Cells were transfected with different plasmid according to experiment using a nucleofection kit for mouse T cells (Lonza). Briefly, 3×10^6 cells were washed with warm isolation buffer once and re-suspended into 100 μ L nucleofection solution provided with the kit along with 2 μ g of plasmid for each transfection. Cells were then electroporated using electroporation device (Lonza) and cultured in mouse T cell nucleofector medium (Lonza) overnight for experiments.

4.2.4. Anti-RFP antibody labeling with Alexa fluorophore

The coupling of the anti-RFP antibody to different Alexa fluorophores was performed by Antibody Labeling Kits (Life Technologies). Briefly, 100 μ L of anti-RFP antibody (1 mg/mL) was alkalized by mixing with 10 μ L sodium bicarbonate solution (1 M). The alkalized antibody was then added to the Alexa reactive dye (Alexa 488 or Alexa 647 or Alexa 405 with active moiety) provided by the kit and incubated at RT for 1 h with a gentle rotation. The labeled antibodies were then purified by an affinity column provided by the kit. The column should be activated by purification resin provided by the kit before use. Finally, the labeled antibody was eluted from the spin column by centrifugation at 1100 g for 5 min.

4.2.5. Target cell culture

P815 target cells were cultured in RPMI medium (Invitrogen) containing 10% FCS and P/S antibiotics.

4.2.6. Live cell confocal imaging

4.2.6.1. Endocytosis

Effector CTLs generated as described above were used for live imaging experiments. Cells were settled on glass coverslips coated with 0.1 mg/mL poly-ornithine (Sigma). First, CTLs (0.1×10^6 cells) in 80 μ L IMDM were added to the coverslip, followed by P815 cells (0.02×10^6 cells) in 20 μ L IMDM containing 5 μ L anti-CD3 antibodies (1 mg/mL) and 4 μ L of Alexa conjugated anti-LAMP1-488 (0.5 mg/mL) or 4 μ L of anti-RFP488 (~1 mg/mL) antibodies for visualizing LAMP1 or Syb2 endocytosis, respectively.

For the Dynasore experiment shown in Figure 13A, 1×10^6 cells CTLs were pre-treated with 100 μ M Dynasore in serum-free IMDM medium at RT for 10 minutes. Control CTLs were pretreated with 0.1% DMSO and followed the same protocol as Dynasore pretreatment. CTLs were then washed twice in serum-free IMDM medium for live imaging as described above.

For flower experiments shown in Figure 25A and B, CTLs from WT and Flower KO mice generated as described above were transfected with Syb2-mRFP plasmid as a CG marker for live imaging experiments. Target cells were pre-mixed with anti-CD3 and anti-RFP488 and added to the coverslip containing CTLs in culture medium followed the same

concentration of antibodies and cell numbers as described above to visualize CG endocytosis. For observing Flower dynamics in CTLs shown in Figure 29B, Flower KO CTLs were co-transfected with Syb2-mRFP and Flower-pHluorin plasmids to visualize CGs and Flower protein, respectively. Anti-RFP405 antibody was applied additionally in the medium in order to visualize endocytosed CGs.

For the calcium rescue experiment shown in Figure 28, Syb2-mRFP transfected CTLs were imaged with target cells as described above for 30 min and then perfused 10 mM calcium extracellular buffer to the chamber. All live cell imaging experiments were done at 37°C with 5% CO₂ by confocal microscope (Zeiss, LSM 780).

4.2.6.2. Acquisition settings

Considering the size of CGs (~ 300 nm) and the size of CTLs (10 µm), we made 4D images with the best compromise for spatial and temporal resolution by taking 6 images in x, y, and z direction for one time point (t) for the entire recording. In order to image all the CGs of the cell with high-speed acquisition and simultaneously without losing much dynamic information, we set the step size of each z-stack as 1 µm out of the total scanned distance as 5 µm and the acquisition speed of each individual image stack is about 1 s. Thus, we recorded 5 µm thickness of individual cells with 6 z-stack images for 6 s. We collected the data and made serial maximum intensity projection images along time (t).

4.2.6.3. Analysis

The analysis of accumulation of endocytosed CGs at IS was performed by calculating the percentage of total fluorescence of the anti-RFP488 antibody at the IS (% = Fluorescence at the IS/ Fluorescence in the entire cell * 100) over time. The CTL was divided into three equal parts and the IS was defined as one third of the CTL (area) facing the target cell.

4.2.7. Structured illumination microscopy

4.2.7.1. Structured illumination microscopy setup

The SIM setup used was from Zeiss (ELYRA PS.1). Images were acquired using a 63x Plan- Achromat (NA1.4) objective with excitation light of 488, 561 and 647 nm and then processed for SIM to obtain higher resolutions. Z-stacks of 200 nm step size were used to scan cells. Zen 2012 software was used for acquisition and processing of the images for higher resolutions.

4.2.7.2. Dynamin2 mutant experiment

For dynamin2 mutant experiments, CTLs transfected with either control GFP or Dynamin2 K44A-GFP were incubated with cognate target cells for 30 minutes at 37°C in the presence of anti-RFP647 antibody. Cells were then fixed in freshly prepared ice-cold 4% PFA in D-PBS (Invitrogen) washed thrice in PBS and then mounted for imaging. For Dynasore

experiment, CTLs pretreated with or without Dynasore as described before were incubated with P815 cells in the presence of anti-RFP488 antibody in serum-free IMDM medium for 30 minutes at 37°C. Cells were then fixed in freshly prepared ice-cold 4% PFA in D-PBS. After fixation, cells were washed thrice in PBS and permeabilized for 30 minutes in D-PBS containing 0.1% Triton-X 100 (Roth), then blocked for 30 minutes in blocking buffer for immunostaining. Cells were stained with primary anti-CALM, anti-clathrin, anti-granzymeB and the appropriate Alexa conjugated secondary antibodies according to the experiment and then mounted. Cells were imaged by SIM and processed to obtain a high resolution of 100 nm in the x, y direction.

4.2.7.3. Co-localization analysis

For co-localization analysis, Manders' overlap coefficient (Manders et al., 1993) were used for quantification by using JACoP plugin in ImageJ v3.3 (Rasband, WS, USA National Institutes of Health, Bethesda, MD, USA).

4.2.7.4. Dynasore experiments for IS formation and CD3 recycling

For investigating whether Dynasore affects IS formation in CTLs, CTLs were pretreated with Dynasore as described above and incubated with target cells for 10 min with anti-CD3 antibody at 37°C. Cells were then fixed with ice-cold 4% PFA and followed by permeablizing, blocking and stained with anti-ZAP70 antibody as an early IS marker. For further testing whether T-cell receptor recycling is affected by Dynasore, CTLs were pretreated with Dynasore and incubated with target cells for 30 min with presence of Alexa 647 conjugated anti-CD3 antibody in the serum free medium on the glass coverslip. Then cells were fixed and mounted on coverslips for imaging.

4.2.8. Population calcein killing assay

For calcein killing assay, p815 cells were washed with serum free IMDM and loaded with calcein-AM (500 nM, lifetechnology) in serum free IMDM for 15 min at RT. Cells were then washed once and plated into 96-well black plate with clear bottom (BD Falcon). 0.1% Triton-X100 was added to target cell to make maximum target cell lysis. CTLs were added with different ratios to target cells (0.1×10^6 cells/well) for killing measurements at 37°C. The plate was measured with 485/20 nm excitation wavelength and 535/25 nm emission wavelength by GENios Pro plate reader at time zero and after 2 hours. The fluorescence for experimental conditions is adjusted by the parameter γ according to live target cell control fluorescence. γ value should be measured at time zero. $\gamma = \text{Flive} (0) / \text{Fexp} (0)$. The cytotoxicity is calculated according to the loss of calcein fluorescence in target cells. The equation of % target cell lysis = $(\text{Flive} - \gamma \times \text{Fexp}) / (\text{Flive} - \text{Flyse}) \times 100\%$. The abbreviations in the equation stand for only target cell control (live), CTLs with target cells (exp) and maximum target lysis (lyse). Details of calcein killing assay are described in (Kummerow et al., 2014). All experiments were performed in triplicates.

4.2.9. Western blot

4.2.9.1. Lysate preparation

Lysate of whole brain tissue, naive and stimulated CTLs extracted from WT and Flower KO mice were used to detect Flower expression by western blot. For preparing brain lysate, 100 mg of whole brain tissue were dissolved in 150 μ L lysis buffer and were then mechanically sheared using a glass rod in glass homogenizers. After homogenization, lysed tissue were incubated on ice for 1 h. Finally, samples were centrifuged at 13,000 rpm for 10 minutes at 4°C and supernatants were then collected as the lysate for western blot. Lysates stored in aliquots at -80°C. For preparation of cell lysates, 5×10^6 CTLs were washed with ice cold PBS and lysed in freshly made ice-cold 70 μ L lysis buffer. Cells were then homogenized using a 1 mL syringe for five times manually on ice and incubated for 30 min at 4°C with rotation. Cell debris and insoluble materials were pelleted down by high-speed centrifuge at 16,000 g for 10 min. The supernatant is the cell lysate for western blot.

4.2.9.2. Blotting

Lysates were denatured by adding sample buffer containing 1x SDS (Life technologies) with 4% β -mercaptoethanol and boiled at 99°C for 10 min. The lysates then loaded into a denaturing gradient 4-12% Bis-tris gel (NuPAGE, Life technology). For electrophoresis, run the gel at 120 V for 1.5 h then transferred proteins onto a nitrocellulose membrane with 0.2 μ m pore diameter for 2 h at 195 mA. The blot were blocked using 5% non-fat milk in 1x TBST for 2 h at RT and incubated with anti-flower antibody diluted in 5% non-fat milk overnight at 4°C. After blocking, the blot then followed by five times washing with TBST buffer to remove unbound antibody and incubating with HRP conjugated anti-rabbit secondary antibody for 1 h at RT for chemiluminescent detection. Lastly, the blot was developed with Pierce western blot signal enhancer (Thermo scientific) to enhance protein detection. Images were finally acquired by FluorChem E Imaging System (ProteinSimple). For loading control, the blot was stripped with stripping buffer (Thermo scientific) for 11 min at RT and followed by three times washing with TBST and re-incubating with anti-GAPDH primary antibody for 1 h at RT and HRP conjugated anti-mouse secondary antibody. The blot was in the end imaged again to detect GAPDH expression as a loading control.

4.2.9.3. Immunocytochemistry

CTLs were stained with anti-flower antibody (spleen pre-cleared) to detect endogenous Flower expression in WT and Flower KO cells as well as co-staining with anti-HA antibody to test the specificity of flower antibody. Cells were fixed in freshly prepared ice-cold 4% PFA in D-PBS washed thrice in PBS and permeabilized for 1 minute in D-PBS containing 0.1% Triton-X 100 (Roth), then blocked for 30 minutes in blocking buffer contained 5% BSA for immunostaining. Cells were stained with primary anti-flower (1:200), anti-rabbit secondary antibodies (1:1000) and then mounted. Cells were imaged using high-resolution structured illumination microscopy (SIM).

4.2.10. Degranulation assay

For degranulation assay, naïve cells were cultured for 3 days with anti-CD3/anti-CD28 beads in the cell to bead ratio of 1:0.4 to stimulate cells. Stimulated cells (0.2×10^6) were rest for 2 h by removing beads from culture. Cells were then incubated on 10 µg/mL coated anti-CD3 (for stimulated cells) or PBS (for constitutive cells) coated 96-well plate with 0.1 µL anti-CD107a-PE along with 0.15 µL Golgi-stop containing monensin was added to block intracellular protein transport for 3 h at 37°C for degranulation. The control cells were incubated in PBS-coated wells without anti-CD107a-PE and Golgi-stop as a background signal for FACS analysis. Cells were then washed twice with ice-cold PBS containing 0.5% BSA and analyze by Fluorescence-activated cell sorting (FACS, BD FACSAria III). Data were analyzed by using FlowJo software (Celeza-Switzerland). Gates were set based on no fluorescence control cells. Each of the individual experiments was done in triplicate.

4.2.11. Total internal reflection fluorescence microscopy

The TIRFM setup was as described before (Nofal et al., 2007) with the solid-state laser 85 YCA emitting at 561 nm (Melles-Griot). Control Sybki or Dynasore Sybki CTLs (2×10^4 cells) were re-suspended in 30 µL extracellular buffer containing 0 mM Ca^{2+} and allowed to settle for 1 minute on anti-CD3 antibody (30 µg/mL) coated coverslips. Cells were then perfused with extracellular buffer containing 10 mM Ca^{2+} to enhance CG fusion probability. Cells were imaged for 10 min at 561 nm excitation wavelength. The acquisition frequency was 10 Hz and the exposure time was 100 ms. Experiments were carried out at RT. Fusion of lytic granules was analyzed using ImageJ with the plugin Time series Analyzer V2.0. A sudden drop of Syb2-mRFP fluorescence within 300 ms (three acquisition frames) was defined as fusion.

4.2.12. Flower topology experiment

Flower is described as a vesicular transmembrane protein, however, the exact topology was not determined. We therefore used an experimental approach to clarify the topology of Flower by tagging a pH-sensitive protein on different positions of Flower protein. We designed Flower fusion constructs using ratiometric pHluorin fused to the C-terminus of Flower (Flower-pHluorin) or to the loop between the second (S2) and the third (S3) transmembrane segments of Flower (Flower-loop-pHluorin). We also used Syb2-pHluorin as a positive control, because we knew that pHluorin is located in the lumen of the vesicle. Upon acidification, the excitation wavelength of pHluorin at 395 nm decreases with a corresponding increase in the excitation at 475 nm (Figure 5A, upper panel). In the other words, the excitation ratio of fluorescence 395/475 decreases upon pH decreases (Figure 5A, lower panel).

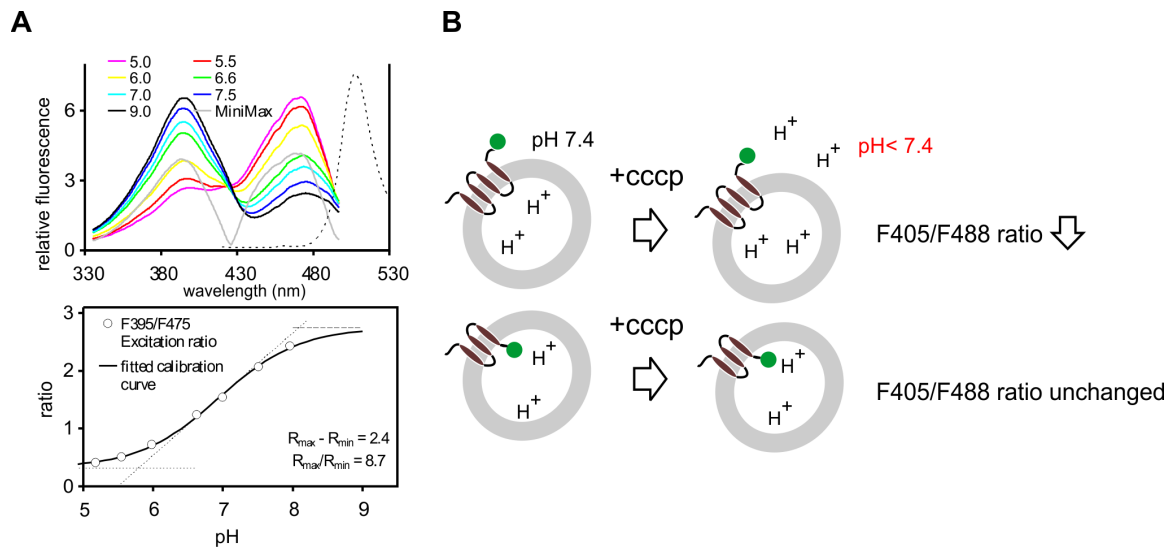


Figure 5. Experimental strategy of investigating the topology of Flower protein.

(A) Excitation spectra of ratiometric pHluorin with peaks at 395 and 475 nm at the indicated pH values. The dotted line shows the emission spectrum with a maximum at 509 nm corresponding to pH 5.5 (upper panel). pH dependence of fluorescence excitation ratio F390/F475 of ratiometric pHluorin. Graph taken from (Schulte et al., 2006). (B) Scheme of the predicted responses of ratiometric pHluorin tagged to Flower upon cytosol acidification by CCCP application.

We transfected these two Flower fusion constructs in CTLs and acidifying cytosol by ionophore CCCP that transports proton across lipid bilayer membranes. CCCP acts to break the proton gradient in the cells. The proton enriched organelles mainly ER and mitochondria release their protons into the cytosol. Therefore, cytosolic pH decrease results in the decrease of pHluorin ratio at the extravascular side (Figure 5B, upper panel). In the other hand, if the pHluorin is in the luminal side, upon cytosol acidification, the inner vesicle environment might not be affected. Therefore, we predicted the ratio of pHluorin will not be changed (Figure 5B, lower panel). For the experiment, Stimulated cells were transfected with flower-pHluorin, flower-loop-pHluorin and syb2-pHluorin individually then treated cells with ionophore, CCCP to acidify cytosol. For CCCP treatment, 0.2×10^6 cells were settled on glass coverslip for 5 min and recorded cells before and after perfusing 50 μ M CCCP in HEPES based buffer containing 2 mM calcium at the excitation of 405 nm and 488 nm at confocal microscope (Zeiss, LSM 780) using 40x objective.

5. Results

5.1. Cytotoxic granule endocytosis in CTLs

5.1.1. LAMP1 endocytosis in CTLs

In order to investigate whether cytotoxic granules (CGs) are endocytosed in CTLs, we first tried to visualize membrane internalization using an antibody labeled with Alexa fluorophore, to the universal cytotoxic granule marker, Lysosomal-associated membrane protein 1 (LAMP1). We applied Alexa 488 labeled anti-LAMP1 antibody (anti-LAMP1-488) to the medium containing CTLs and target cells. Following TCR recognition of MHC I bound to a peptide antigen presented on target cell surface, CTLs release the contents of their CGs via exocytosis. LAMP1 proteins, which reside on the CG membrane, were exposed to the LAMP1-488 antibody following fusion of the CG membrane with the plasma membrane. Binding of the fluorescently labeled antibody to LAMP1 renders LAMP1 fluorescent and allows imaging of LAMP1 endocytosis via this fluorescence (Figure 6).

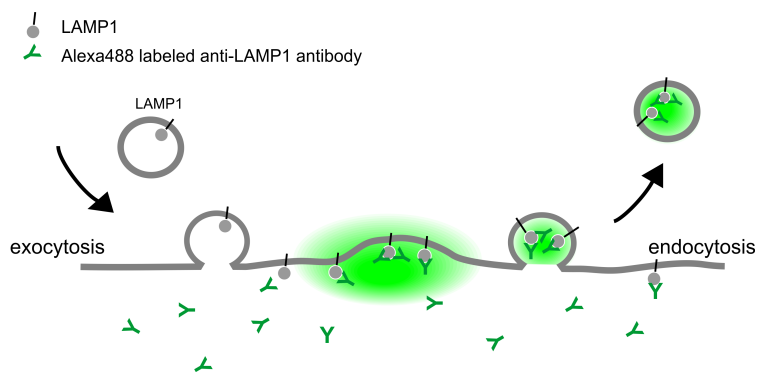


Figure 6. Scheme of LAMP1 endocytosis.

Cartoon of visualizing LAMP1 endocytosis by applying Alexa488 coupled anti-LAMP1 antibody in the medium.

We recorded live cell confocal images of CTLs isolated from Sybki mouse (Sybki CTLs) and target cells in the presence of anti-LAMP1-488 antibody in the medium. Interestingly, we observed endocytosis of LAMP1 in CTLs within a few minutes of contact with a target cell (Figure 8A). LAMP1 endocytosis only occurred in stimulated CTLs that contacted target cells. This indicates LAMP1 endocytosis upon lysosome degranulation occurs specifically in response to the TCR activation. We tested whether endocytosing LAMP1 originated from constitutive exocytosis or an abnormal behavior of Sybki CTLs. Therefore, we also incubated wildtype (WT) CTLs with target cells loaded with cytosolic calcein dye (green) in the presence of anti-LAMP1-647 antibody in the medium. We observed no endocytic LAMP1 events in CTLs that did not contact to target cells (white arrow). In contrast, CTLs that contacted target cells exhibited endocytic LAMP1 vesicles (Figure 7, red arrows). In resting CTLs without anti-CD3 triggering or synapse formation we observed no LAMP1 endocytic

events. This result indicates that LAMP1 endocytosis is specific for triggered degranulation.

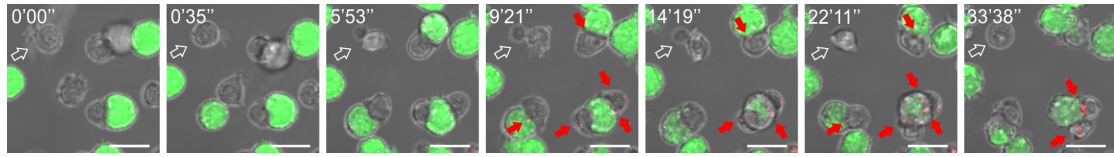


Figure 7. LAMP1 endocytosis occurs only upon target cell contact in CTLs.

Live cell confocal images of WT CTLs in contact with target cells loaded with calcein (green). CTLs were incubated with target cells in the presence of anti-LAMP1 antibody labeled with Alexa647 (red). The red arrows point to the endocytic anti-LAMP1 and the white arrows point to a signal of a CTL without contact to any target cell throughout the recording. Scale bar: 10 μ m.

We took advantage of the endogenous Syb2 labeled with red fluorescence of CTLs from the Sybki mouse to do live imaging of CGs. We expected that fusion of CGs containing both LAMP1 and Syb2, similar amounts of endocytosed LAMP1 and endocytosed Syb2 would be present, and that they might even be in the same endocytosed compartments, i.e. they would be co-localized. As shown in Figure 8C, only a sub-fraction of LAMP1 endocytic vesicles contains Syb2, which is seen as yellow puncta (yellow arrows). Statistical analysis showed that around one fifth of endocytosed LAMP1 vesicles (11.6 ± 1.5) also contain Syb2 (2.7 ± 0.5) (Figure 8B).

These data visualize LAMP1 endocytosis in CTLs by live cell confocal imaging. Additionally, we showed that only a small fraction of LAMP1-containing endocytosed vesicles also contain Syb2. This result led us to the next experiment where we used Syb2 as a specific marker to exclusively study CG endocytosis.

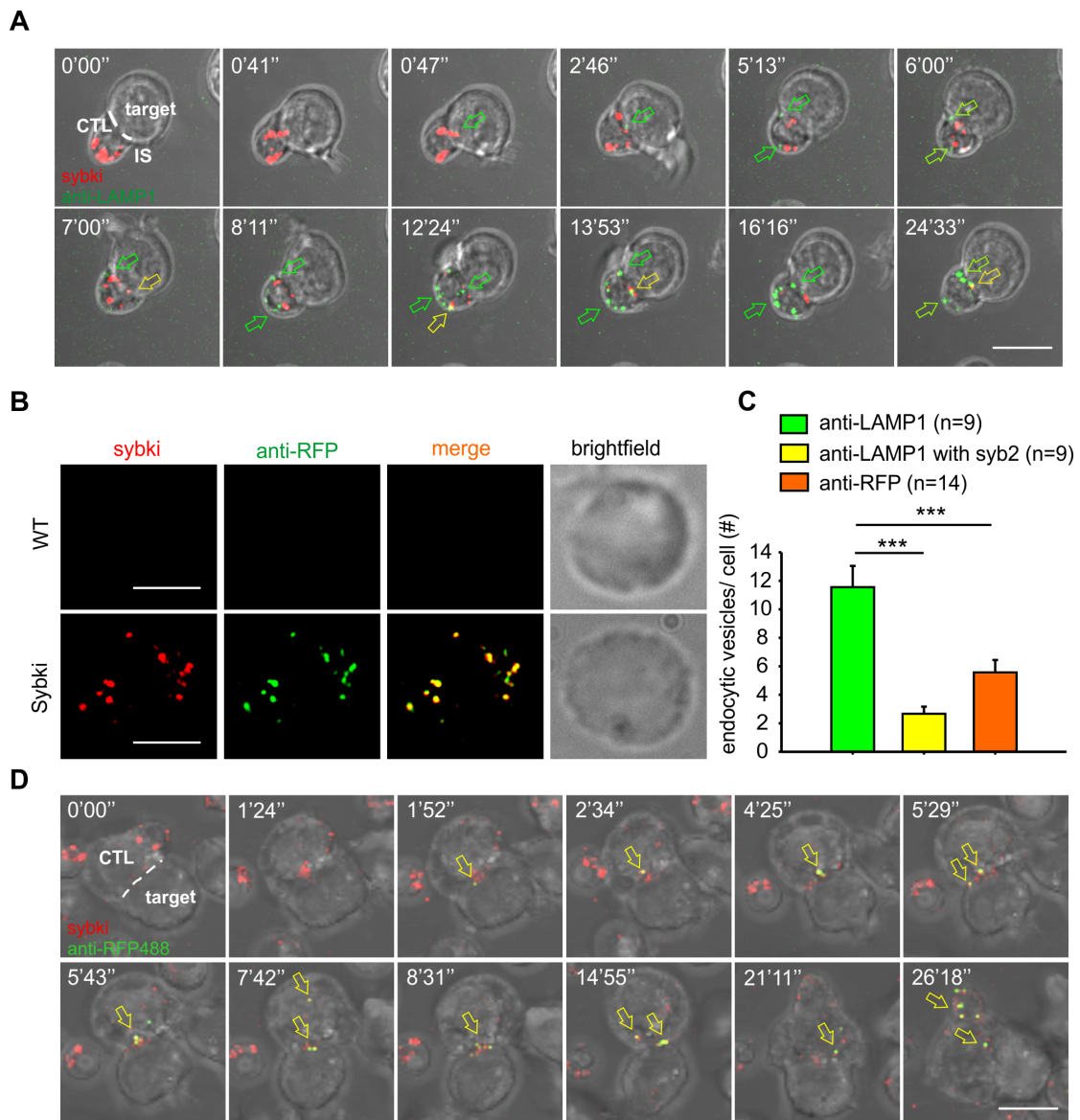


Figure 8. Cytotoxic granule endocytosis in CTLs.

(A) Confocal time-lapse imaging of a Sybki CTL (red) in contact with a target cell in medium containing anti-LAMP1-488 antibodies to visualize endocytosis of LAMP1 (green). Yellow arrows indicate vesicles containing endocytosed LAMP1 and endocytosed Synaptobrevin2. The green arrows indicate vesicles containing only endocytosed LAMP1. The white dotted line indicates the contact zone between CTL and target cell. Scale bar: 10 μ m. (B) SIM image of a WT and a Sybki CTL immunostained with primary anti-RFP antibody (green). Scale bar: 5 μ m. (C) Average number of endocytosed vesicles per cell. Data are represented as mean \pm SEM. Asterisks indicate significance in one-tailed Student's t-test; *** P <0.001. Sybki: Synaptobrevin2-mRFP knock-in, CG: cytotoxic granule. (D) Confocal time-lapse imaging of Sybki CTLs with target cells in medium containing anti-RFP488 antibody to visualize endocytosis of Synaptobrevin2 (green). Yellow arrows indicate endocytosed Synaptobrevin2. White dotted line indicates the contact zone between CTL and target cell. Scale bar: 10 μ m.

5.1.2. Specificity of the anti-RFP antibody

In order to study CG endocytosis, we imaged CGs in CTLs obtained from Sybki mice and tracked their retrieval in CTLs. The CGs from Sybki mice are endogenously

labeled with mRFP fused to Syb2. The mRFP is located in the luminal C-terminal portion of the protein and is thus exposed to the outer surface of the cell following exocytosis. This allowed us to specifically label Syb2-mRFP following granule exocytosis using an antibody against mRFP applied to the medium. Following endocytosis the Syb2 was labeled with mRFP antibody to which an additional fluorophore was added, allowing us to distinguish granules containing endocytosed Syb2 from unfused CGs.

The specificity of the primary anti-RFP antibody was tested by immunocytochemistry comparing Sybki CTLs and control WT CTLs. The Sybki signal showed a perfect co-localization with the anti-RFP antibody in a CTL (Figure 8B, lower panel) while no mRFP signal was detected in WT CTL (Figure 8B, Upper panel). We coupled this specific mRFP-antibody to the Alexa 488 fluorophore (anti-RFP488) for visualization of the endocytosis of Syb2-mRFP.

5.1.3. Cytotoxic granules endocytose at the IS in CTLs

In order to specifically visualize CG endocytosis, we performed live cell imaging as in the LAMP1 endocytosis experiment described above, but applied anti-RFP488 in the medium instead. Following CG exocytosis, the anti-RFP488 antibody (green) binds to Syb2-mRFP (red) and the resulting signal from RFP antibody bound to Syb2-mRFP will appear yellow (Figure 9).

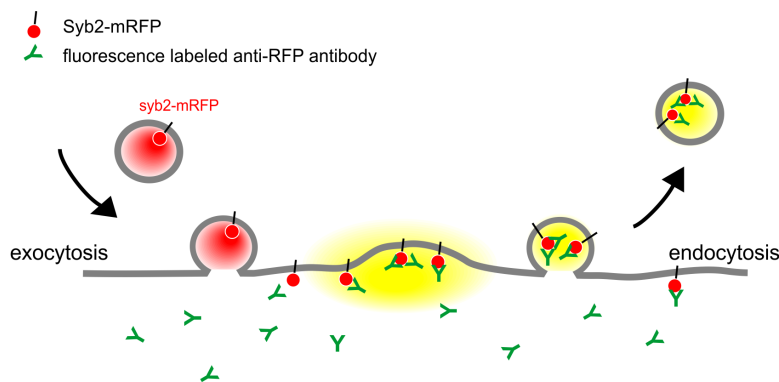


Figure 9. Scheme of cytotoxic granule endocytosis.

Cartoon of visualizing cytotoxic granule endocytosis by applying fluorescently coupled anti-RFP antibody in the medium.

In our live imaging (Figure 8D), we observed that following CTL-target cell contact (time= 0'00''), CGs polarized to the IS (time= 1'24'') and endocytosed CGs appeared within 2 minutes at the IS (time= 1'52'', yellow arrow). The target cells were loaded with the cytosolic dye calcein blue (blue), because loss of this dye is an indicator of cell death. Over time, more endocytosed CGs appeared at the IS and moved away from the IS. We showed that these endocytic events are due to TCR triggering because we observed no anti-RFP488 internalization in a single CTL (Figure 10, white arrows) that did not contact a target cell while in other CTLs endocytic events

occurred upon target cell contact (Figure 10, yellow arrows). This result demonstrates that CG endocytosis occurs in CTLs within minutes after CG polarization to the IS.

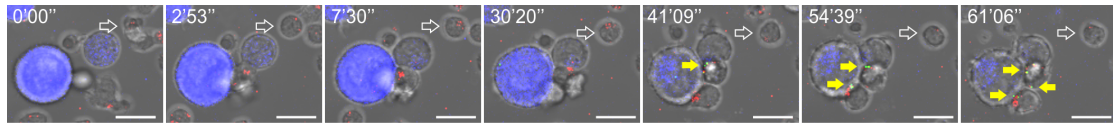


Figure 10. CG endocytosis occurs only upon target cell contact in CTLs.

Live cell confocal images of Sybki CTLs in contact with target cells loaded with calcein blue (blue). CTLs were incubated with target cells in the presence of anti-RFP antibody coupled to Alexa488 (anti-RFP488, green). The yellow arrows point to the endocytic CGs binding anti-RFP488 and the white arrows point to a signal from a CTL without contact to a target cell throughout the recording. Scale bar: 10 μm .

In this study, effector cell and target cell contact were generated by incubating CTLs and P815 target cells with soluble anti-CD3 antibody, which binds to the Fc receptor on P815 cells, cross-links them to CTLs, and thereby stimulates the CTL to induce lysis of target cells. However, this artificial recognition has been criticized as being an unphysiological stimulus for granule endocytosis. Therefore, we instead use CTLs isolated from OT1-Sybki cross-bred mice stimulated with SIINFEKL peptide. The SIINFEKL peptide is the restricted peptide epitope of the ovalbumin protein and is presented on MHC type I complexes to generate a specific cognate recognition with target cells. We incubated CTLs with EL4 target cell pulsed with SIINFEKL in the presence of anti-RFP488 antibody and again visualized the endocytic CGs (yellow) in these CTLs (Figure 11). The obtained result suggests that CG endocytosis also occurs in response to a specific, more physiological trigger.

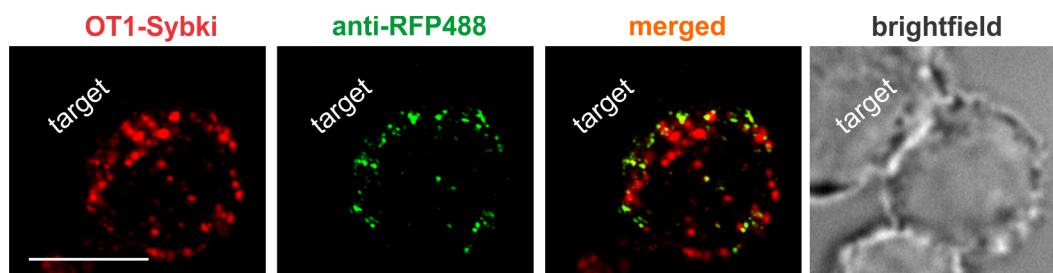


Figure 11. CG endocytosis occurs upon specific antigen recognition.

SIM images of a CTL isolated from OT1-Sybki mouse in contact with a target cell (EL4) pulsed with SIINFEKL peptide. CTLs (red) were incubated with target cells for 30 min in the presence of anti-RFP488 antibody (green) to visualize the endocytic CGs (yellow). Scale bar: 5 μm .

While we observed Syb2 retrieval in CTLs, we further observed that these endocytosed CGs were again polarized to the immune synapse after subsequent CTL contact with another target cell. In Figure 12, a Sybki CTL contacted a target cell (time= 0'00'') and its CGs polarized to the IS within a few minutes (3'34''). The

endocytosed CGs (yellow) then appeared at the IS (19'36''), and were endocytosed. Death of the first target cell occurs, indicated by the loss of blue fluorescence. The CTL then moved to a second target cell (35'10'') and formed a contact with it (44'02''). The CGs again polarized to the contact area and, interestingly, endocytosed CGs also moved to the contact area (44'58''). This live imaging data indicates that the endocytosed CGs are functional in CTLs and might be involved in killing. The data shown in Figure 10 and Figure 12 thus support our hypothesis that endocytosis of CGs occurs and might play a role in the serial killing of target cells by CTLs.

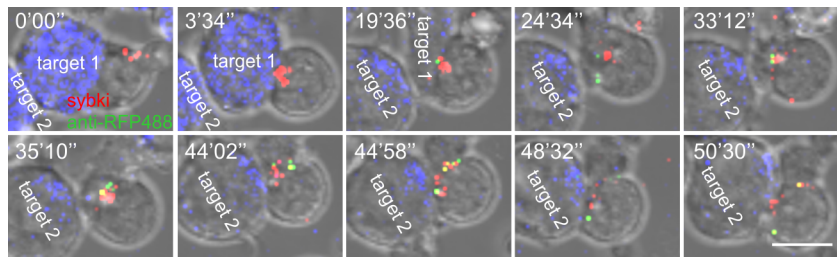


Figure 12. Endocytosed cytotoxic granules are polarized to the sequential immunological synapse.

Live cell confocal images of Sybki CTLs in contact with target cells loaded with calcein blue (blue). CTLs were incubated with target cells in the presence of anti-RFP antibody labeled with Alexa488 (anti-RFP488, green). Scale bar: 10 μ m.

5.2. Cytotoxic granules undergo Clathrin- and Dynamin-mediated endocytosis

5.2.1. Cytotoxic granule endocytosis is Dynamin-dependent

We further investigated the molecular players mediating cytotoxic granule endocytosis. We tested whether endocytosis could be blocked by application of the Dynamin blocker Dynasore. Dynamin induces fission at the last step of Dynamin-mediated endocytosis. We pre-treated CTLs from the Sybki mouse with Dynasore and imaged them in contact with target cells. CG endocytosis was identified as before, using the anti-RFP488 labeling of fused Syb2-mRFP. The endocytic events in Dynasore pre-treated CTLs were blocked at the IS throughout the recording (Figure 13A, lower panel), while endocytic granules appeared normally in the cytoplasm in DMSO-treated control CTLs (Figure 13A, upper panel). We also quantified the block of endocytosis at the IS by Dynasore. For this, we defined one third of the volume of the CTL as the IS area from our 3D maximum intensity projection images and analyzed the accumulation of endocytic events from anti-RFP488 fluorescence signal in this area over time. In control CTLs, the endocytic granules decreased over time ($67 \pm 14.1\%$, $61 \pm 12.2\%$, $58 \pm 9.9\%$, $36 \pm 7.0\%$ and $32 \pm 6.6\%$ at the time point 2.5, 5, 7.5, 10 and 15 minutes, respectively) after first endocytic granule appeared. Within 15 min, the endocytic granules in control cells were evenly distributed in the cytoplasm of the cell. However, in the Dynasore pre-treated CTLs, the endocytic granules remained at the plasma membrane at the IS ($99 \pm 0.6\%$, 100% , $99 \pm 0.1\%$,

99 ± 0.04% and 99 ± 0.02% at time points of 2.5, 5, 7.5, 10 and 15 minutes, respectively, Figure 13B). Dynasore is a widely used blocker to block Dynamin-dependent endocytosis. However, its cytotoxicity and off-target effects have been a concern (McCluskey et al., 2013). For this reason, we added an independent experiment in which we blocked CG endocytosis by using a dominant-negative dynamin2 mutant K44A (DNM2-K44A). In CTLs transfected with the dynamin2 mutant, the Syb2-mRFP-bound mRFP antibody (magenta) remained at the plasma membrane at the IS (Figure 13B, lower panel) whereas in GFP transfected control CTLs, most of the mRFP-positive granules were found in cytoplasm (Figure 13B, upper panel). The over-expressed Dynamin mutant led to a reduction of endocytic events but did not cause a complete block. This is likely due to the presence of endogenous wild type Dynamin in the CTLs. In CTLs expressing mutant Dynamin, 69.4 ± 3.3% of the endocytic events remained at the IS while in control CTLs, 45.9 ± 5.6% of endocytosis granules remained at the plasma membrane after incubating CTLs and target cells for 30 min in the presence of anti-RFP647 (Figure 13D). Since inhibition of the GTPase activity of Dynamin results in an accumulation of coated/uncoated pits that do not pinch off to generate nascent vesicles, we visualized these structures by performing correlative light and electron microscopy (CLEM) experiments in both control and Dynasore-treated CTLs (Figure 13E, F). High-resolution SIM images were acquired from a 100 nm thin section followed by EM. Control cells showed internalization of Syb2-mRFP while in Dynasore-treated CTLs, the anti-RFP488 fluorescence was retained at the IS and correlated with pit-like structures (Chang et al., 2016). Thus, the substantial retention of anti-RFP488/647 fluorescence at the IS in both Dynasore-treated and dynaminK44A-GFP expressing CTLs, as compared to controls as well as the retention of mRFP and its correlation to pit-like structures in the EM images are consistent with a Dynamin-dependence of CG endocytosis (Chang et al., 2016).

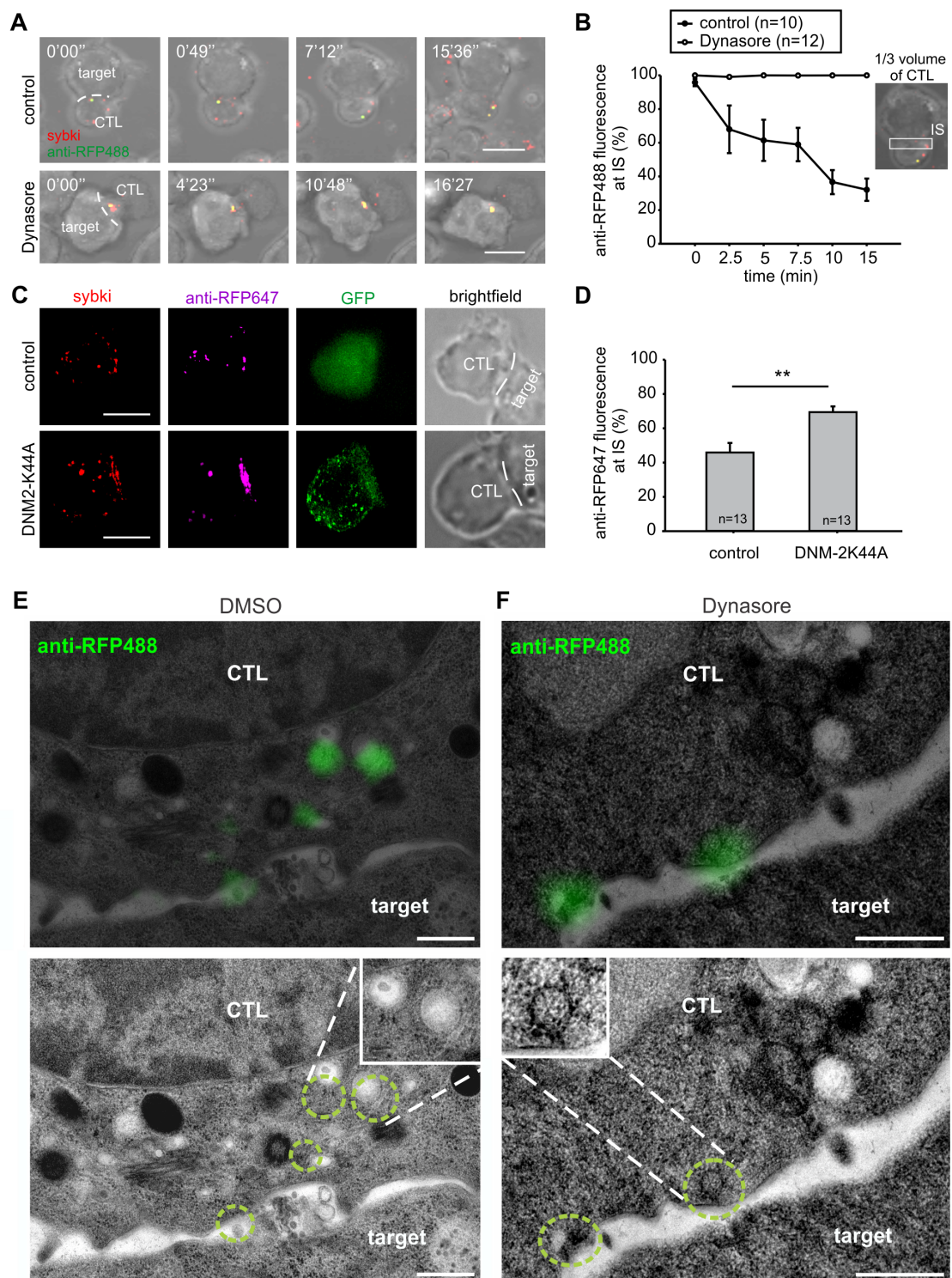


Figure 13. Endocytosis of CG membrane proteins at the IS is Dynamin-dependent.

(A) Confocal time-lapse images of Sybki CTLs (control, upper panel and Dynasore-treated, lower panel) with target cells in medium containing anti-RFP488 antibody to visualize endocytosis of Synaptobrevin2. Scale bar: 10 μ m. (B) Quantification of the percentage of anti-RFP488 fluorescence at the IS in control and Dynasore-treated CTLs over time. Data are represented as mean \pm SEM. (C) SIM images of GFP (control; upper panel) or DNM2-K44A-GFP (mutant Dynamin-K44A, lower panel) expressing CTLs in contact with target cells. CTLs were incubated with target cells for 30 minutes in medium containing anti-RFP647 to visualize

endocytosis of Synaptobrevin2 (magenta). Scale bar: 5 μm . **(D)** Quantification of the percentage of anti-RFP647 fluorescence at the IS in control and DN2-K44A CTLs. **(E)** Upper panel: SIM/TEM overlay of a Sybki CTL in contact with a target cell. Sybki CTLs were incubated with target cells for 35 min in presence of anti-RFP488 antibody (green) in serum-free medium before preparation of the sample for EM. SIM-image and the electron micrograph were acquired from the same resin section (100 nm). Lower panel: Correlated electron micrograph from upper panel. Green circles outline the approximate position of fluorescent spots and their corresponding position in the section. Marked positions (dashed circles) show the corresponding structures underlying the fluorescent spot of the anti-RFP488 signal. Right inset shows the cell structures under the two spots in a higher magnification. **(F)** Upper panel: SIM/TEM overlay of Sybki CTL in contact with target cells pre-treated with Dynasore and pre-incubated with anti-RFP488 antibody (green) as described above. Lower panel: TEM image from upper panel. Marked positions (dashed circles) show the corresponding structures underlying the fluorescent spot of the anti-RFP488 signal. Left inset shows the membrane area under the right spot in a higher magnification. Scale bar: 0.5 μm . Sybki: Synaptobrevin2-mRFP knock-in.

5.2.2. Clathrin and CALM mediate cytotoxic granule endocytosis

Scission of invaginated pits from the plasma membrane is one of the final stages before the formation of nascent vesicles. To investigate what other molecular players might be involved in CG endocytosis, we stopped CG endocytosis by using Dynasore. We fixed Dynasore pre-treated Sybki CTLs in contact with target cells in the presence of anti-RFP488 and immunostained for the endocytic protein, Clathrin, and the Syb2-specific adaptor protein, CALM, using anti-clathrin and anti-CALM antibody respectively, to see whether these proteins are on pits of the endocytosed CGs. We observed a high degree of co-localization of endocytic CGs (anti-RFP488) signal with anti-CALM (0.78 ± 0.05) and with anti-clathrin (0.70 ± 0.04) antibody signal (Figure 14A, B, analyzed by Manders' overlap coefficients). The results confirm that Clathrin and CALM present on the endocytic coated pits for endocytosis. To determine if Clathrin actively participates in CG endocytosis we blocked Clathrin function by using a membrane permeable inhibitor, pitstop2. As controls we used CTLs pre-treated with an inactive pitstop2 analogue (pitstop2-negative). CTLs pre-treated with pitstop2-negative (control) or pitstop2 were incubated with target cells in serum-free IMDM medium containing anti-RFP488 antibodies (Chang et al., 2016). Cells were fixed after 30 minutes of target cell addition, mounted and imaged by SIM (Figure 14C). We quantified the anti-RFP488 fluorescence as described above and found that in control CTLs $35.2 \pm 3.1\%$ of anti-RFP488 remains at the IS after 30 minutes of contact with target cells while in pitstop2-treated CTLs $66.8 \pm 3.4\%$ was retained at the plasma membrane (Figure 14D). The substantial accumulation of anti-RFP488 fluorescence at the IS in pitstop2-treated CTLs indicates that Clathrin is required for CG endocytosis. Next, we tested the functional requirement of CALM using siRNA (Figure 14E, F). CTLs transfected with two different siRNAs against CALM showed a significant accumulation of anti-RFP488 fluorescence at the IS ($77.0 \pm 3.5\%$ and $75.5 \pm 3.8\%$, respectively) compared to CTLs transfected with control siRNA ($51.0 \pm 3.0\%$; Figure 14G, H), clearly showing a role for CALM in CG endocytosis. These results demonstrate that both Clathrin and CALM are involved in the endocytosis of the CG membrane protein Syb2 at the IS (Chang et al., 2016).

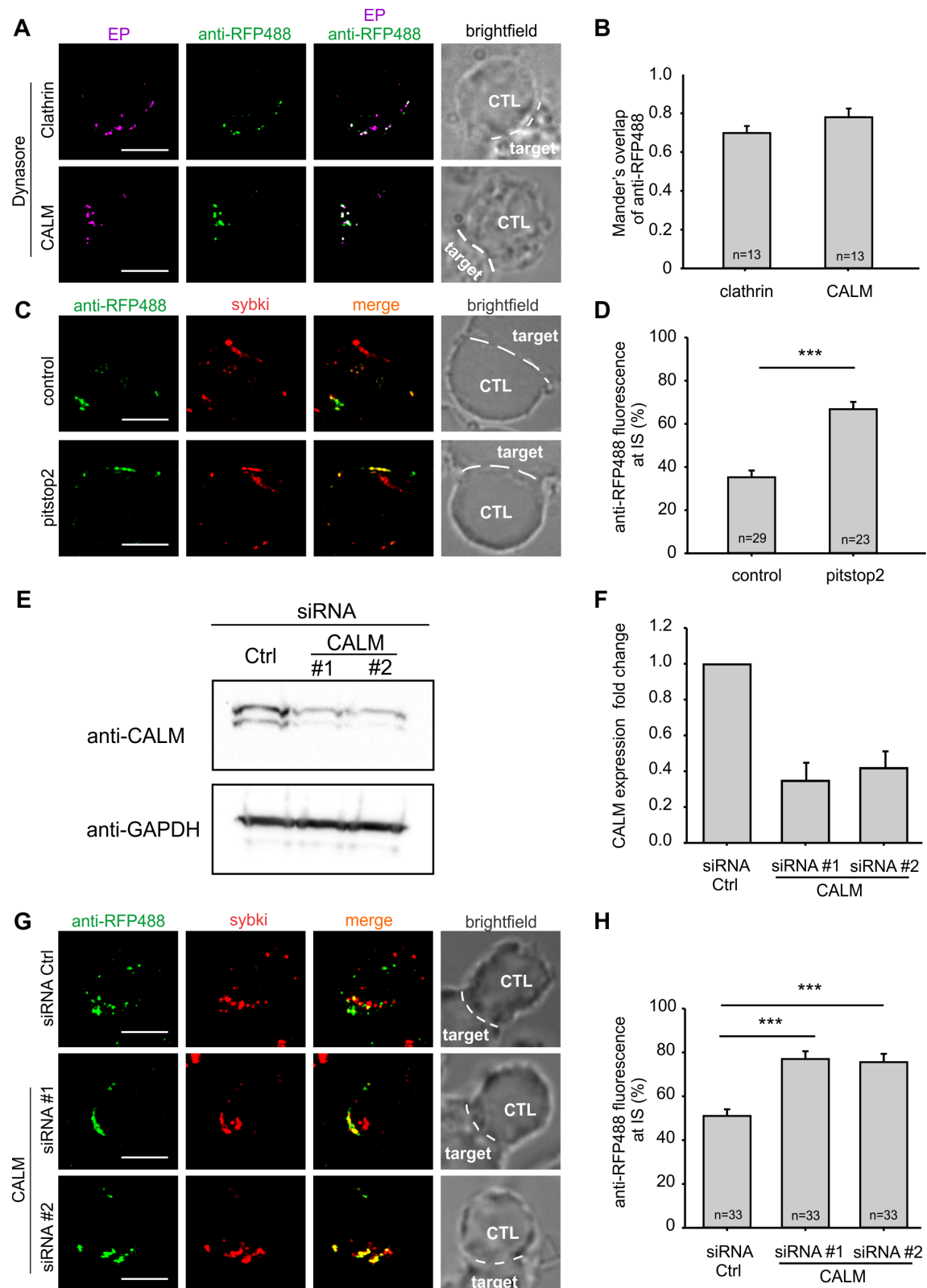


Figure 14. Clathrin and CALM mediate CG endocytosis.

(A) SIM images of Dynasore pre-treated CTLs in contact with target cells for 30 min in medium containing anti-RFP488 antibody (green) and stained with antibodies against endocytic proteins (EP): Clathrin (upper panel; magenta) and CALM (lower panel; magenta). (B) Manders' overlap coefficient of anti-RFP488 antibody with anti-CALM and anti-clathrin. (C) SIM images of Sybki (red) CTLs pre-treated with pitstop2 negative control (upper panel)

or pitstop2 (lower panel) and incubated with target cells for 30 min in serum-free medium containing anti-RFP488 (green). **(D)** Quantification of the percentage of anti-RFP488 fluorescence at the IS. **(E)** Immunoblot of CTLs treated with control siRNA (Ctrl) and two siRNAs specific for CALM: CALM siRNA#1 and #2 with anti-CALM antibody (upper lane) and anti-GAPDH antibody (lower lane). **(F)** Densitometry to quantify the relative expression of CALM in CALM siRNA #1 and #2 treated CTLs normalized to Ctrl siRNA treated CTLs. **(G)** SIM images of Sybki (red) CTLs treated with control siRNA (siRNA Ctrl, upper panel) or two siRNAs specific for down-regulating CALM (CALM#1, middle panel and CALM #2, lower panel) and incubated with target cells for 30 min in medium containing anti-RFP488 antibody (green). **(H)** Quantification of the percentage of anti-RFP488 fluorescence at the IS. Data are represented as mean \pm SEM. White dotted line indicates the contact zone between CTL and target cell. Scale bars: 5 μ m. Sybki: Synaptobrevin2-mRFP knock-in, IS: immune synapse defined for analysis as one third volume of CTL facing target cell.

5.3. Endocytosed cytotoxic granules are re-filled with Granzyme B in CTLs

Having shown that endocytosis of CGs is Clathrin- and Dynamin-mediated, we next examined when these CGs acquire cytotoxicity. We therefore looked at the acquisition of cytotoxic substances by these endocytic granules. We fixed the Sybki CTLs in contact with target cells in medium containing anti-RFP488 antibody to visualize endocytic CGs at 5 min, 15-30 min and 60 min after contact and stained with an anti-granzyme B antibody (anti-gzm B) to see if Granzyme B is acquired and when this happens. The co-localization of endocytic CGs with Granzyme B increased over time (Figure 15B). Granzyme B showed very little co-localization with endocytic CGs (anti-RFP488) in the first 5 min (0.3 ± 0.07) and gradually increased in 15-30 min (0.51 ± 0.04) and reached its maximum within 60 min (0.74 ± 0.05 , Manders' overlap coefficient, Figure 15C) (Chang et al., 2016). Within 60 min, most of the endocytic CGs (60%) co-localized with Granzyme B (Figure 15B, lower panel, white arrows). The unfused granules can clearly be distinguished by lack of anti-RFP488 label (Figure 15B, lower panel, white arrows and yellow arrows respectively). This finding strongly supports our hypothesis that the endocytic CGs are reused for further killing.

The components of CGs are recycled is not unexpected, but to what extent endocytosis is required depends on whether CGs undergo full fusion. If the granules were only partially release their contents in a sort of kiss and run fusion, the recycling of granules and their components would be simplified. We decided to examine whether granules undergo full fusion. We pre-treated CTLs with Dynasore and conjugated them with target cells in the presence of anti-RFP488 antibody. After fixation, we stained with anti-granzyme B antibody to see if Granzyme B still remains in the fused granule carrying anti-RFP488. In the kiss-and-run mode we would expect the co-localization of anti-RFP488 to Granzyme B whereas in the full fusion mode, the invaginated membrane would contain no Granzyme B. We observed no co-localization of endocytic granules (anti-RFP488, green) to Granzyme B (magenta) in CTLs (Figure 15A, value of 0.21 ± 0.06 of Manders' overlap coefficient). These data indicate that CGs undergo a full fusion mode of exocytosis in CTLs.

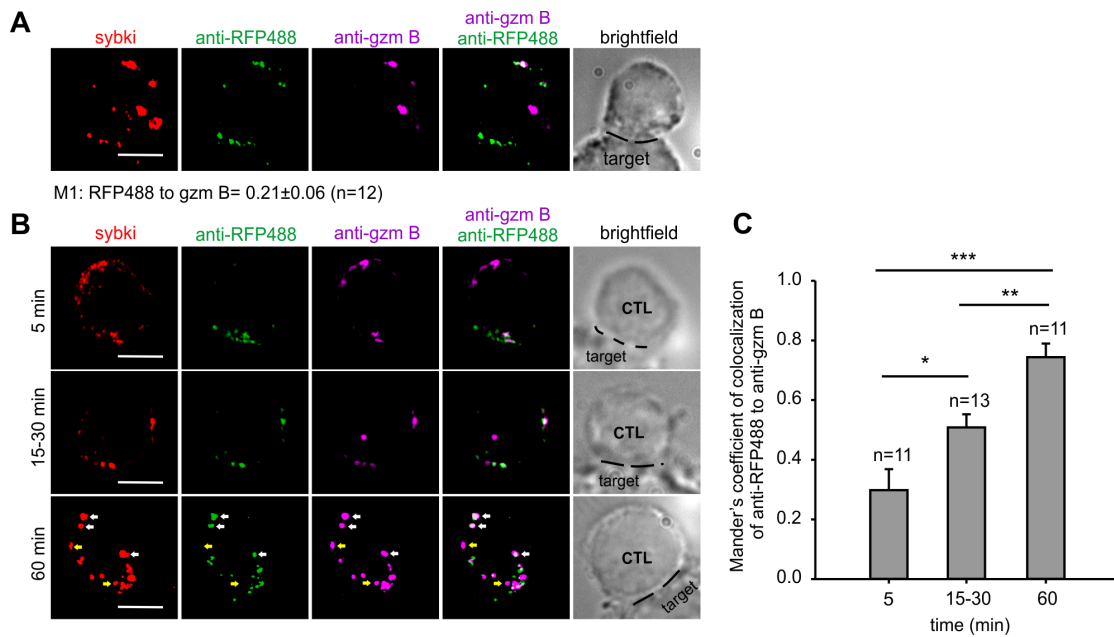


Figure 15. Endocytosed CGs are re-filled with Granzyme B within 60 min.

(A) SIM images of a Dynasore pre-treated Sybki (red) CTL in contact with a target cell in the presence of anti-RFP488 (green) in medium. Cells were then fixed, permeabilized and stained with anti-granzyme B (anti-gzm B) antibody (magenta). The Manders' overlap coefficient of endocytic CGs to Granzyme B is shown below the images. (B) SIM images of Sybki (red) CTLs in contact with target cells in the presence of anti-RFP488 (green) in medium and fixed after 5, 15, 30 and 60 min. Cells were then permeabilized and stained with anti-gzm B antibody (magenta). The black dotted line indicates the contact zone between CTL and target cell. White arrows point to endocytosed Syb2-mRFP488 carrying vesicles and yellow arrows point to the old Syb2-mRFP carrying vesicles. Scale bars: 5 μ m. (C) Quantification of the co-localization of endocytosed CGs (green) to Granzyme B at the indicated times of CTL-target cell conjugation.

Although CG membrane protein Syb2 and LAMP1 endocytose in different granules, both proteins are gradually integrated into the same compartment within 60 min, the time window also observed for refilling with Granzyme B. We incubated CTLs and target cells in the presence of two fluorescently labeled anti-RFP488 and LAMP1-647 antibodies to follow the dynamics of these two proteins in recycling (Figure 16A). The Manders' overlap coefficient of anti-RFP488 to anti-LAMP1 increased to around 0.6 at 60 min (Figure 16B). These data imply again that the proportion of Syb2- and LAMP1-positive vesicles are not identical, however a subpopulation of LAMP1 is sorted into the Syb2-positive compartments. These are probably the mature fusogenic CGs.

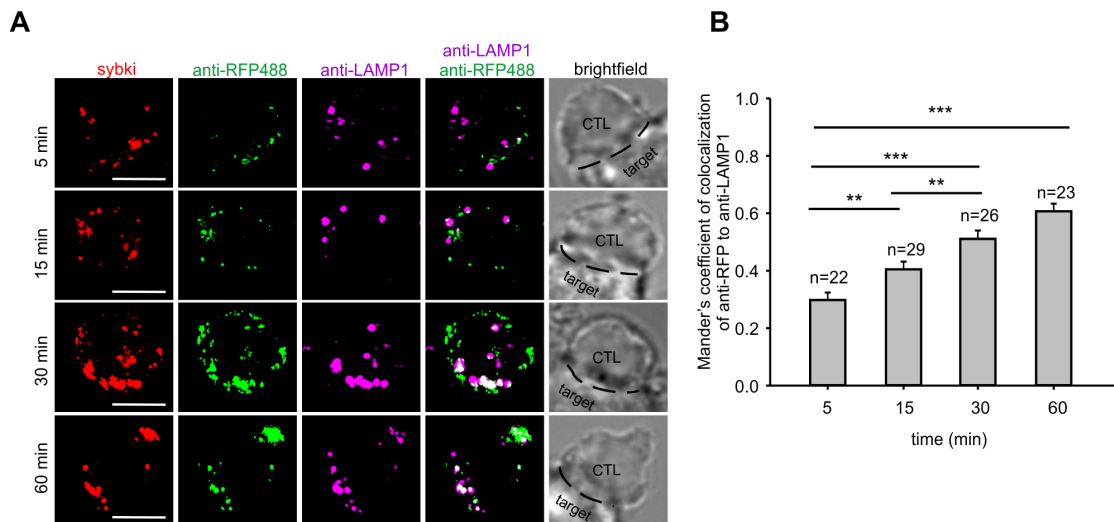


Figure 16. Endocytosed Synaptobrevin2 gradually co-localized with endocytosed LAMP1.

(A) SIM images of endocytosed LAMP1- and RFP-containing vesicles in Sybki CTLs in contact with target cells. CTLs were fixed with target cells after 5, 15, 30 and 60 min of incubation in the presence of anti-LAMP1-647 (magenta) and anti-RFP488 (green) antibodies to mark the endocytic lysosome compartments and cytotoxic granules, respectively. Scale bar: 5 μ m. (B) Quantification of co-localization of endocytic RFP488 to LAMP1 by Manders' overlap coefficient at the indicated time points of CTL-target cell contact.

5.4. Endocytosis of CGs is required for CTL effector function

Our results indicate that endocytic CGs might be functional because first, the endocytic CGs are re-filled with the cytotoxic effector molecule Granzyme B (Figure 15) and second, the endocytic CGs polarize to the synapses formed between the CTL and subsequent target cells (Figure 12). We then investigated the physiological relevance of recycled CGs in the serial killing capacity of CTLs. We prepared target cells that were loaded with the cytosolic dye calcein-AM with an excitation wavelength of either 405 nm (calcein-blue) or 488 nm (calcein-green). We first incubated CTLs with calcein-green loaded target cells (target 1, pink) for 30 minutes in the presence of anti-RFP647 antibody, washed the antibody away and then added target cells loaded with calcein-blue (target 2, blue) (Chang et al., 2016). Cells were incubated for another 20 minutes, then fixed and imaged (Figure 17A, B). Because the anti-RFP647 antibody used to visualize CG endocytosis was washed away before adding target 2, any green fluorescent signal corresponding to endocytosed Synaptobrevin2 in CTLs is due to the result of contact with target 1. The presence of green fluorescence at the CTL:target2 synapse indicates that the CTL was in contact with target 1 previously. Contact was defined as the presence of Syb2-containing granules (non-fused (red) and/or endocytosed (green)) at the CTL:target cell interface (Chang et al., 2016). Only CTL:target2 contacts were analyzed to determine the percentage of contacts with previously endocytosed CGs. Out of 28 CTL:target2 contacts, 16 had both non-fused and endocytosed CGs at the IS, 11 had only endocytosed Syb2 granules at the IS and 1 had only non-fused CGs at the

IS. Therefore, 96.4% of CTL:target 2 synapses contained endocytosed CGs (Chang et al., 2016).

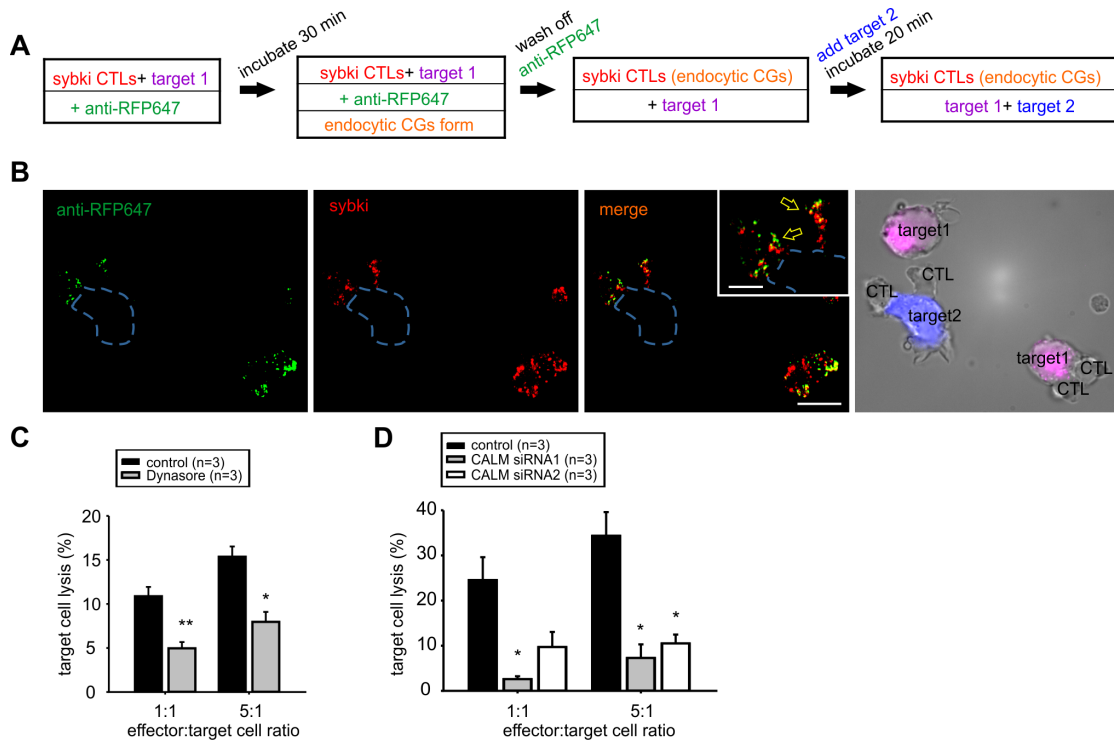


Figure 17. Endocytosis of CGs is required for fulfilling CTL effector function.

(A) Scheme of experimental protocol of imaging sequential contact of Sybki CTLs with two sets of target cells (target 1, pink; target 2, blue). (B) SIM of images of Sybki CTLs depicting sequential contact with target 1 and target 2. Scale bar: 10 μ m, scale bar of inset: 5 μ m. (C) Calcein release-based population killing assay. CTLs were pre-treated with or without Dynasore (Dynasore and control, respectively) and co-cultured with cells at the indicated CTL:target ratios for 2 hours. One representative experiment out of three is shown. Each experiment was performed as triplicates. Data are represented as mean \pm SEM of the triplicate wells of the representative experiment. (D) Calcein release-based population killing assay. CTLs were transfected with CALM siRNA and non-silencing siRNA as a control for killing assay. CTLs were co-cultured with cells at the indicated CTL:target ratios for 4 hours. Three independent experiments are shown. Data are represented as mean \pm SEM. Asterisks indicate significance in one-tailed Student's t-test; * P <0.05. Sybki: Synaptobrevin2-mRFP knock-in.

To confirm the functionality of endocytosed CGs, we incubated control and Dynasore-treated CTLs with target cells in the presence of anti-CD3 antibody at two different effector:target ratios for 2 hours and performed a population-based killing assay measuring the release of the cytosolic dye calcein as described previously (Kummerow et al., 2014; Wang et al., 1993). We found that the killing capacity of Dynasore-treated CTLs was significantly reduced by about 50% in comparison to control CTLs (Figure 17C). In order to provide a second experiment for the physiological relevance of endocytosed CGs, which is independent of the somewhat problematic Dynasore (see Discussion), we down-regulated the expression of the Synaptobrevin2-specific adaptor protein CALM by siRNA (Chang et al., 2016). Our results in Figure 17D show that killing was significantly reduced in CTLs expressing

either of two different CALM-specific siRNAs as compared to non-silencing control CTLs. In three independent experiments with a 1:1 effector:target ratio, a reduction in killing by about 90% in siRNA1 transfected cells (2.5 ± 1.1) and 60% in siRNA2 transfected cells (9.7 ± 5.8) compared to control cells (24.5 ± 5.1). For a higher effector:target ratio of 5:1, a 79% and 60% reduction of killing was obtained in siRNA1 (7.2 ± 5.2) and siRNA2 transfected cells (10.5 ± 3.4), respectively, compared to control cells (34.3 ± 9.1) (Chang et al., 2016). These data show that endocytic CGs contribute to serial killing.

We tested whether Dynasore treatment disrupts IS formation in CTLs. We fixed CTLs in contact with target cells after 10 min and stained for the early IS marker, ZAP70, using a specific ZAP70 antibody. We observed no difference in the ZAP70 signal at the IS in control CTLs and Dynasore pre-treated CTLs (Figure 18B). We also tested whether TCR recycling is affected because receptor internalization has been implicated in modulating receptor signaling. We fixed CTLs in contact with target cells in the presence of Alexa 647 conjugated anti-CD3 in the medium after 30 min to see if external CD3 antibody will be endocytosed into CTLs. As a result, anti-CD3 antibody signal (red) appeared in the cytoplasm in both Dynasore pre-treated CTLs and control CTLs (Figure 18A). These data indicate that IS formation and TCR recycling are not affected by Dynasore pre-treatment. We further investigated if CG exocytosis is affected by Dynamin perturbation. We counted the CG fusion events within 10 min at the TIRF plane of Sybki CTLs with or without Dynasore pre-treatment. Loss of fluorescence of vesicles within 5 frames in TIRFM recording at 10 Hz acquisition frequency were regarded as fusion events (Figure 18C, white arrows). In control CTLs $12.9 \pm 2.9\%$ of CGs fused while in Dynasore pre-treated CTLs, $18.9 \pm 5.1\%$ of CGs fused (Figure 18D). The number of fusion events per cell did not differ in control (1.2 ± 0.3) and Dynasore treated CTLs (1.1 ± 0.3 , Figure 18E). Therefore, we conclude that Dynasore treatment has no immediate effect on CG exocytosis. Data shown in Figure 17 and Figure 18 in combination with the lack of effect of Dynasore on upstream signaling of CG endocytosis clearly show that endocytosed CG membrane proteins contribute significantly to the killing of multiple target cells by CTLs.

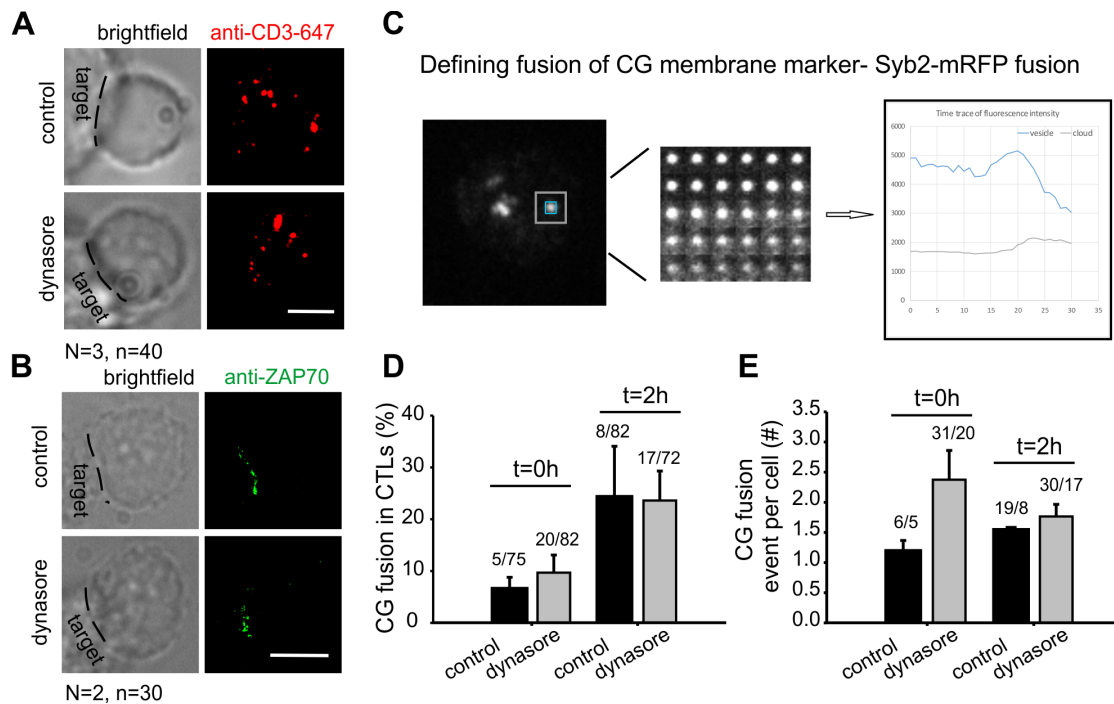


Figure 18. Receptor signaling and IS formation is unchanged upon Dynasore pre-treatment.

(A) SIM images of Sybki CTLs pre-treated with or without Dynasore (Dynasore and control, respectively) in contact with target cells with the recycling anti-CD3-647 (red). (B) SIM images of control CTLs and Dynasore pre-treated CTLs in contact with target cells for 30 min and stained with anti-ZAP70 antibody (green). Black dotted lines in A and B indicate contact zone between CTL and target. Scale bar: 5 μ m. (C) TIRFM snapshot of a Sybki CTL (left); area within the blue box defined as vesicle and area within grey box excluding the blue box defined as cloud for fluorescence intensity measurements over time (right). In the middle is the montage of the 30 images of the vesicle before and after fusion, which were analyzed for fluorescence intensity changes over time. (D) CG fusion analysis in control and Dynasore pre-treated Sybki CTLs. Cells were imaged immediately after pre-treatment (t=0 h) or imaged 2 h after pre-treatment (t=2 h). For the latter condition, cells were incubated in IMDM serum free medium for 1.5 h before imaging. Numbers correspond to cells that showed fusion out of the total number of cells analyzed, e.g.: 5 cells out of 75 cells showed CG fusion in control Sybki at t=0 h. (E) CG fusion analysis of fusion events per cell in the different conditions described in D. Sybki: Synaptobrevin2-mRFP knock-in.

5.5. Calcium dependence of cytotoxic granule endocytosis

CG endocytosis contributes to effector T cell function in target cell killing. Compensatory endocytosis is well studied in neurons where it appears to be calcium-dependent (Marks and McMahon, 1998; Wu et al., 2009). We were curious if CG endocytosis is also calcium-dependent. Calcium entry is required for CTL effector function but it is not clear whether calcium is a trigger for CG release or for endocytosis.

The Flower protein was reported to be involved in synaptic vesicle endocytosis in *drosophila* Yao et al. (2009). Flower contains a sequence similar to a conserved calcium selectivity filter that is found in a number of voltage-gated calcium channels and transient receptor potential channels (TRPV5 and 6). Additionally, Flower

mutants show a defect in synaptic vesicle endocytosis. We have examined Flower function in CTLs and asked whether Flower is involved in CG endocytosis.

5.6. Flower is expressed in mouse CTLs

We first tested the expression of Flower protein in mouse CTLs by Western blot and immunocytochemistry. We extracted whole brain lysate from WT mice as a positive control and from Flower-deficient mice (Flower KO) as a negative control and tested the expression of Flower in CTLs. The Flower protein is detected as a band at 18 kDa. It is expressed in WT brain tissue, in naive CTLs and in stimulated CTLs but could not be detected in brain tissue or CTLs extracted from Flower KO mice (Figure 19A). For immunocytochemistry, we could detect the endogenous signal of Flower in WT CTLs using spleen pre-cleared anti-flower antibody whereas in KO cells, the signal could barely be detected. (Figure 19B, upper panel). Flower shows punctate and plasma membrane staining, indicating that it is localized at the plasma membrane and in vesicular compartments. We also overexpressed a Flower-HA_IRES-GFP construct in WT CTLs to test the specificity of the flower antibody by comparing anti-flower and anti-HA antibody co-staining. We observed an almost perfect co-localization of Flower and HA, indicating that the Flower antibody is specific (Figure 19B, lower panel). These data show that Flower is expressed in mouse CTLs and that the protein can be specifically detected by Flower antibody.

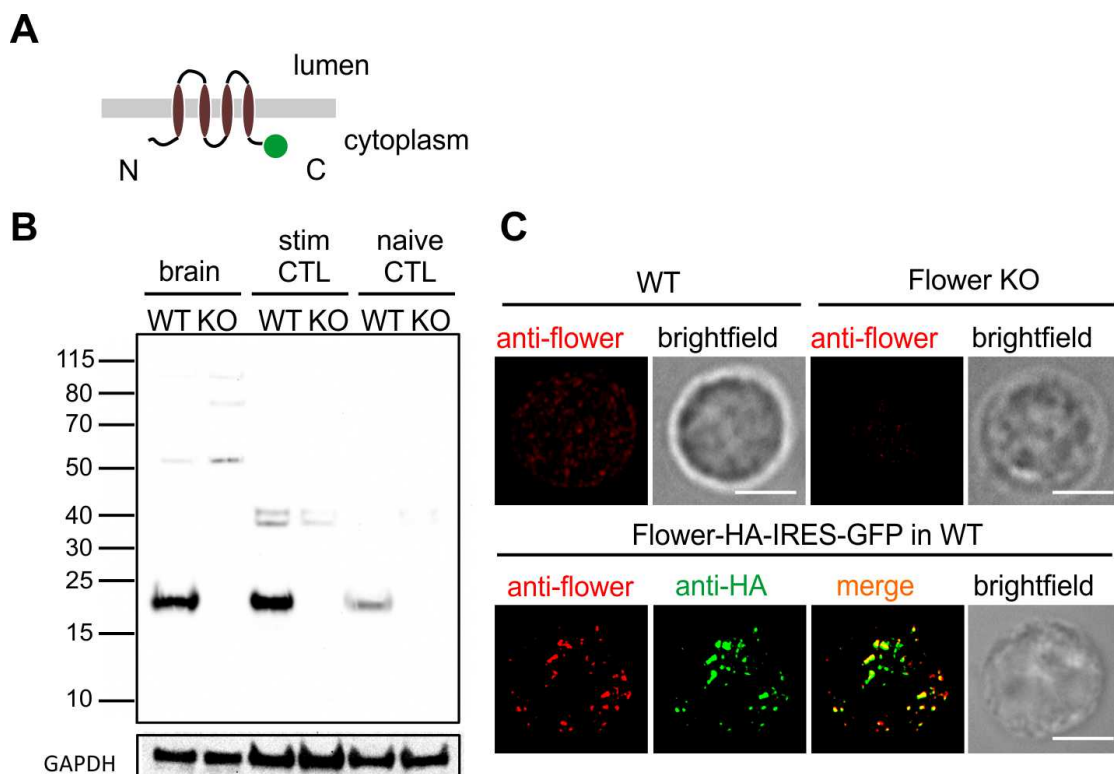


Figure 19. Flower protein is expressed in primary CTLs from mouse.

(A) Cartoon showing the topology of Flower. The green circle indicates the position of the fluorophore used in this study. (B) Western blot analysis of lysates from whole brain, stimulated CTLs and naive CTLs of wild-type (WT) or Flower-deficient (KO) mice using anti-Flower antibody and anti-GAPDH antibody as a loading control. 20 μ g of total lysate was loaded into each lane. Flower protein band is detected only in WT lysates at the expected molecular weight of 18 kDa. (C) Localization of endogenous (upper panel) and over-expressed (lower panel) Flower-HA protein using anti-Flower antibody in WT and Flower KO CTLs. Scale bar: 5 μ m.

5.7. Topology of Flower protein

The topology of Flower is not entirely clear. According to a Kyte-Doolittle hydrophobicity plot, Flower protein possesses three or four transmembrane domains. In order to investigate the topology of Flower, we designed Flower constructs tagged with the ratio-metric dye pHluorin at either the C-terminal (Flower-pHluorin) end or between the second and third transmembrane segment (Flower-loop-pHluorin). The fluorescence of pHluorin is pH-sensitive. Upon acidification, the excitation wavelength of pHluorin at 395 nm decreases with a corresponding increase in the excitation at 475 nm. In other words, the excitation ratio of fluorescence 395/475 decreases upon pH decreases (Figure 5A, see Materials and methods). Therefore, the ratio of pHluorin at these excitation wavelengths will depend on the pH. We also expressed a Syb2-pHluorin as an internal control that the pHluorin is fused at the luminal side of the vesicle. We transfected cells with Flower-pHluorin, Flower-loop-pHluorin and Syb2-pHluorin individually and applied an ionophore, CCCP, in the bath to acidify the cytoplasm. CCCP disrupts the proton gradient within the cell. In this experiment, if Flower contains four transmembrane segments, pHluorin tagged at C-terminal would be cytoplasmic. Upon CCCP application, protons are released from proton-enriched organelles and acidify the cytosol resulting in a decrease of the pHluorin ratio. However, if Flower contains three transmembrane domains, then the C-terminal would be on the luminal side and CCCP application would cause an increase in the ratio. We observed a ratio decrease of pHluorin tagged at C-terminal of Flower after CCCP application (Figure 20, middle). This indicates pHluorin is targeted to the cytoplasm. As an internal control, Syb2-pHluorin shows no change of the ratio indicating pHluorin is localized inside granule (Figure 20, left). We also observed a ratio decrease of pHluorin tagged at the loop of Flower which indicates the loop between the second and the third segment is localized to cytoplasm (Figure 20A, right). Since CCCP is dissolved in DMSO, we also performed a control experiment showing that pHluorin does not change the ratio upon DMSO application (Figure 20A, lower panel). Thus, these data indicate that Flower contains four transmembrane domains.

In order to confirm the topology, we performed a second independent experiment by expressing *drosophila* Flower-mRFP construct in CTLs. It was postulated before that drFlower contains three transmembrane domains (Moreno et al., 2015). We tagged mRFP at the C-terminus of drFlower and applied anti-RFP488 to the medium to see if the antibody can bind directly to mRFP following exocytosis. We observed no anti-RFP488 signal at the plasma membrane in drFlower-mRFP transfected cells (Figure

20B, upper panel). However, when we permeabilized the cells, the transfected cells showed a staining of anti-RFP488 antibody (Figure 20B, lower panel). The results indicate that mRFP is localized to the cytoplasm. Additionally, when we co-expressed drFlower and mFlower in hippocampal neurons, we observed a high degree of co-localization of both proteins in SIM images (Figure 20C), indicating that they are in the same compartment and might have similar function as Flower gene is conserved from worm to human. Again, these results indicate that Flower contains four transmembrane domains.

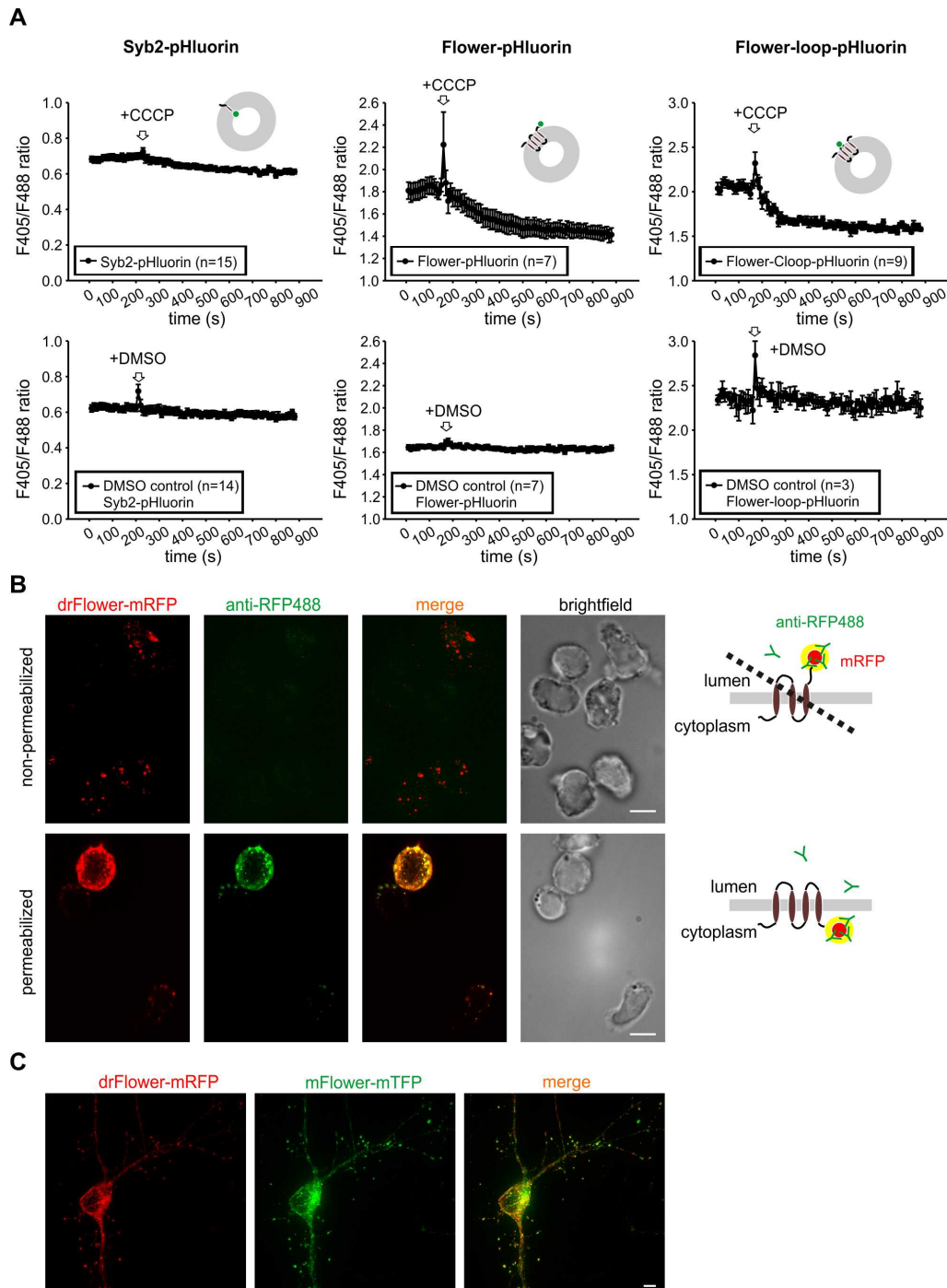


Figure 20. Flower protein contains four transmembrane segments.

(A) CTLs were transfected with Syb2-pHluorin (pHluorin fused to the luminal C-terminus of Synaptobrevin2), Flower-pHluorin (pHluorin fused to the C-terminus of Flower) and Flower-loop-pHluorin (pHluorin fused between the predicted second and third transmembrane segment of Flower), respectively. Cells were then imaged by confocal microscopy before and after applying 50 μ M CCCP to acidify the cytosol. Excitation was at 405 and 488 nm, emission measured at 515 nm. DMSO application was used as control (lower panels). (B) SIM images of drFlower-mRFP transfected CTLs, following fixation, permeabilization with (lower panel) or without (upper panel) 0.1% TritonX-100 and incubation with anti-RFP488 antibody. (C) SIM image of a hippocampal neuron co-transfected with drFlower-mRFP and mFlower-mTFP cDNA.

5.8. Localization of Flower

Flower is a vesicular membrane protein and shows a predominantly punctate staining in CTLs (Figure 19C), indicating that Flower is located on intracellular vesicles. We tried to identify which compartment Flower is localized on. Therefore, we labeled different endosomes by transfecting plasmids of endosome markers into CTLs and stained with anti-flower antibody to test for co-localization of endogenous Flower protein. We used rab5 as an early endosome marker, rab7 as a late endosome marker, rab11 as a recycling endosome marker and Syb2 as a cytotoxic granule marker (Figure 21A). However, we could not observe any co-localization of Flower with any of these compartments by Manders' overlap coefficient analysis (Figure 21B).

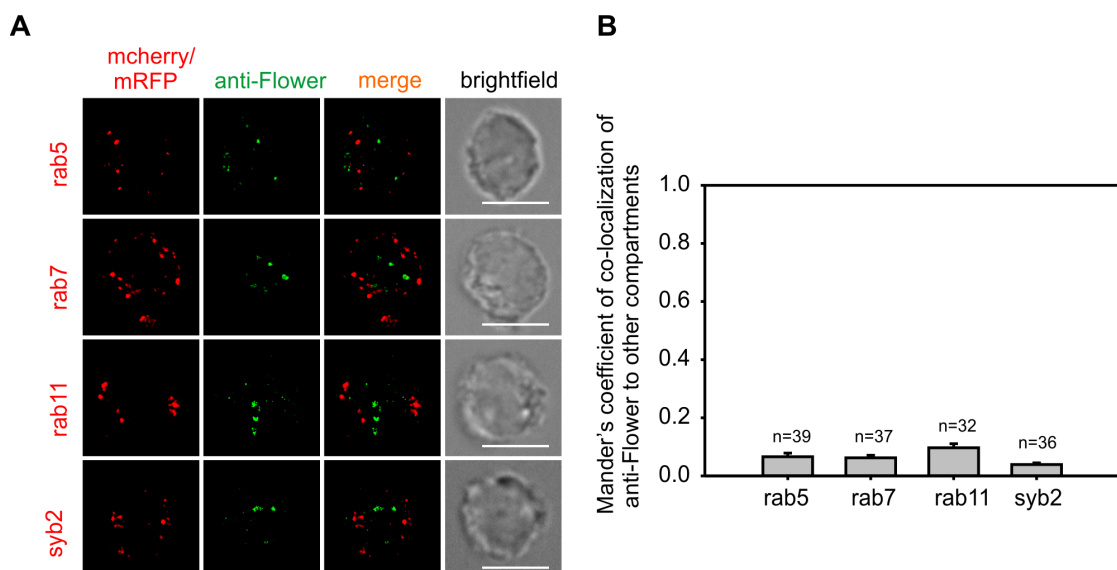


Figure 21. Flower is localized on intracellular vesicles, but not on cytotoxic granules or on endosomal compartments.

(A) SIM images of anti-Flower antibody staining (green) on stimulated WT CTLs transfected with different endosome markers (red, mcherry) or CTLs with endogenously labeled CGs from Sybki mice (Syb2-mRFP, Sybki CTLs). Scale bar: 5 μ m. (B) Manders' overlap coefficient of anti-Flower to rab5-, rab7-, rab11- or syb2-positive compartments.

5.9. Exocytosis is unchanged in Flower-deficient CTLs

We next investigated the effect of Flower on exocytosis by a degranulation assay. Exocytosis of lysosomal contents (degranulation) results in movement of the lysosomal marker LAMP1a to the plasma membrane. Degranulation assays are widely used to evaluate cytotoxicity of CTLs and NK cells based on an increase of LAMP1a (CD107a) on the cell surface (Betts et al., 2003). We compared the degranulation of Flower KO CTLs to WT CTLs by FACS (see Methods). WT CTLs exhibited 53% degranulation while Flower KO CTLs exhibited 56% degranulation upon 10 μ g/mL anti-CD3 stimulation (Figure 22A). Thus neither the stimulated degranulation of the two groups (orange line) nor the constitutive secretion (blue line) was significantly different. We conclude that lysosomal exocytosis does not change in Flower-deficient CTLs.

Since our data pointed out that CGs are not identical to lysosomes (Figure 8 and Figure 16) and very likely that CGs are a subpopulation of lysosomes, we investigated if exocytosis of CGs is affected by the absence of Flower. We transfected a Syb2-mRFP construct in CTLs as a CG marker and monitored individual granule fusion at the immune synapse by TIRF microscopy. The sudden loss of fluorescence within 5 frames was defined as a fusion event (Figure 22B, white arrows). We counted the fusion events in transfected WT CTLs and Flower KO CTLs. In conclusion, we found no statistical difference in the fusion of CGs between WT CTLs ($28.4 \pm 3.4\%$) and Flower KO CTLs ($20.5 \pm 4.9\%$) (Figure 22C). There was also no difference in fusion events per cell (WT; 1.4 ± 0.2 and Flower KO; 1.1 ± 0.1 , Figure 22D). Therefore, we conclude that loss of Flower does not affect either lysosome or CG exocytosis.

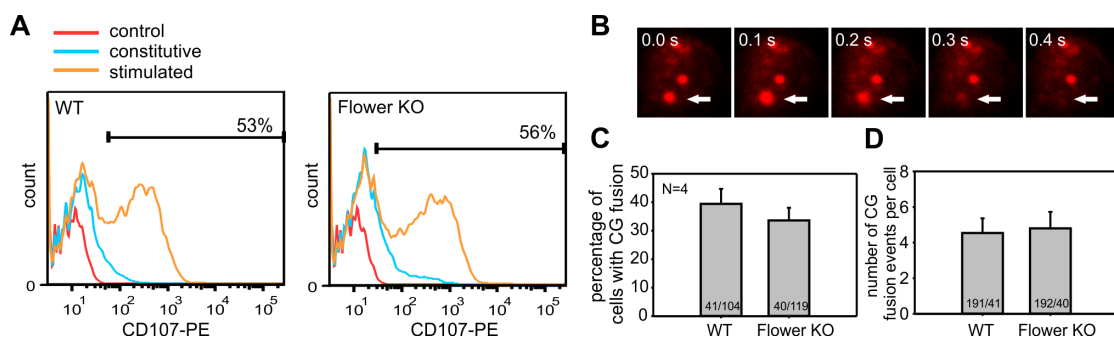


Figure 22. Exocytosis is unchanged in Flower-deficient CTLs.

(A) FACS-based degranulation assay with CTLs derived from WT and Flower-deficient mice using CD107-PE conjugated antibody. Cells were stimulated with 10 μ g/mL anti-CD3 antibody and compared with non-stimulated cells (constitutive). Cells in the absence of CD107-PE antibody served as control. (B) Representative TIRF serial images showing the fusion of a cytotoxic granule (CG). (C, D) CG fusion analysis. CTLs from WT and Flower-deficient mice were transfected with Syb2-mRFP as a CG marker. Cells were plated on anti-CD3 coated coverslips and perfused with 1 mM calcium buffer for TIRF image recording. Percentage of cells that show CG fusion (C) and the number of fusion events per cell (D) are shown.

5.10. Cellular calcium is unchanged in Flower-deficient CTLs

Since Flower has a conserved calcium selectivity filter in its protein sequence, we tested if Flower deficiency affects global calcium in CTLs. We performed Fura-2 measurements to compare WT and KO cell responses after seeding them on anti-CD3 antibody stimulatory coverslips. Cells were loaded with Fura-2 dye and seeded on poly-L-ornithine-coated coverslips as a non-stimulated control. On non-stimulated coverslips, cells showed a slow, low amplitude increase in cytosolic calcium over time in both groups (Figure 23A), whereas cells seeded on anti-CD3 coated coverslips showed a fast cytosolic calcium increase with a higher amplitude. The KO cells tended to show a slight, but not significant delay of calcium increase compared to WT cells (Figure 23B; N=5). In addition, we observed no difference in basic calcium levels (Figure 23C), number of responding cells (Figure 23D), delay (Figure 23E) and amplitude (Figure 23F) of anti-CD3 triggered calcium increase in CTLs derived from WT and Flower KO mice, respectively.

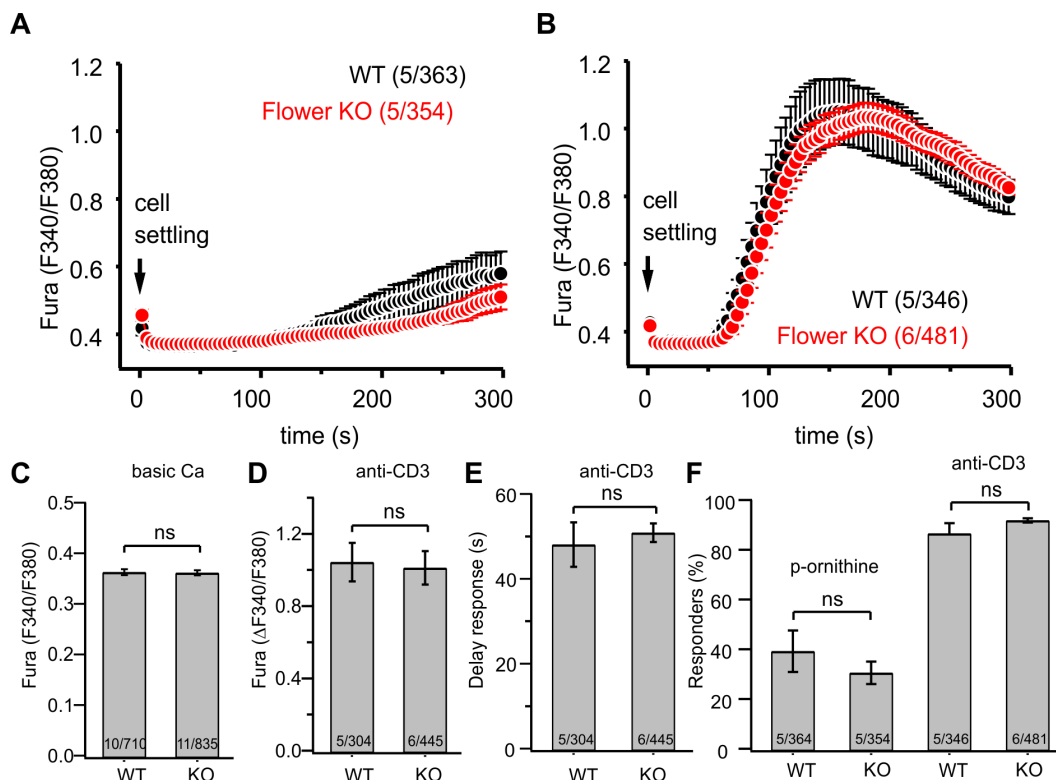


Figure 23. Cellular calcium is unchanged upon CD3 activation in Flower-deficient CTLs.

Ratiometric imaging of cytosolic calcium (Fura F340/F380) in CTLs derived from WT (black) and Flower-deficient (red) mice seeded on control poly-ornithine (A) and anti-CD3 (B) coated coverslips. (C-F) Quantification of data shown in A and B. Basic cytosolic calcium levels (C), percentage of cells responding with an increase of cytosolic calcium while seeded on p-ornithine and anti-CD3-coated coverslips (D), and delay (E) as well as amplitude (F) of the anti-CD3-mediated cytosolic calcium. The number of experiments x with n cells is shown in brackets (x/n).

5.11. Flower-deficiency leads to a block of CG endocytosis

The experiments described above ruled out that Flower-deficiency affects granule exocytosis or basic calcium signaling. We further investigated Flower function in endocytosis. First, we examined if endocytosis of lysosomal compartments is affected while degranulation level is unchanged in the absence of Flower. We incubated CTLs and target cells for 30 min in the presence of anti-LAMP1-647 antibody in the medium and observed an accumulation of anti-LAMP1 antibody at the plasma membrane in the Flower KO cells (Figure 24A, lower panel). The quantitative analysis showed a significant increase of anti-LAMP1 fluorescence signal at the IS in KO cells ($71.8 \pm 4.7\%$) compare to WT cells ($41.2 \pm 6.2\%$) (Figure 24B).

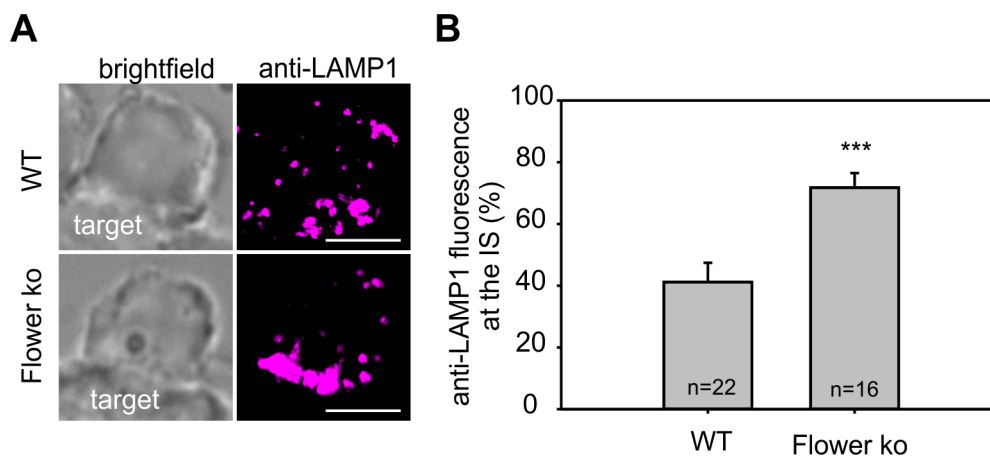


Figure 24. LAMP1 endocytosis is affected in Flower-deficient CTLs.

(A) SIM images of a Sybki CTL and a Flower KO CTL in contact with target cell. CTLs were fixed with target cells after 30 min of incubation in the presence of anti-LAMP1-647 (magenta) antibody. Scale bar: 5 μ m. (B) Quantification of fluorescence signal of endocytic LAMP1 accumulation at the IS (one third area of CTL facing to target cell of MIP image).

Flower-deficiency showed an impaired of LAMP1 endocytosis. We next investigated CG endocytosis by real-time confocal imaging. We transfected Syb2-mRFP plasmid as a CG marker into CTLs and applied anti-RFP488 antibody to the medium to visualize endocytic CGs. Following CGs (red) polarization to the IS, endocytosed anti-RFP488 positive CGs (yellow) appear at the IS in WT (Figure 25A, upper panel, 0'00'') and in Flower KO CTLs (Figure 25A, middle panel, 0'00''). Time 0'00'' is defined as the time the first mRFP antibody-positive puncta appear. We observed a normal CG polarization in Flower KO CTLs by live imaging, that also lead to normal granule exocytosis (Figure 22C). Anti-RFP488 antibody-positive (yellow) puncta appear over time in both WT and Flower KO CTLs, consistent with these observations. However, while the yellow puncta are endocytosed into the cytoplasm within minutes in WT CTLs (Figure 25A, upper panel), they accumulated at the IS without any indication of endocytosis in Flower KO CTLs (Figure 25A, middle panel).

In order to confirm that this defect in endocytosis is caused by the absence of Flower, we over-expressed a Flower-pHluorin construct in Flower KO CTLs to see if the endocytosis defect can be reversed. Since the Flower-pHluorin construct emits at 488 nm (green) we used Alexa 405 (magenta) to fluorescently label the mRFP antibody. After expression of the Flower-pHluorin, the anti-RFP405 antibody-positive puncta (magenta) were internalized and no longer accumulated at the plasma membrane. They were distributed throughout the cytoplasm (magenta) in Flower-pHluorin-Flower-KO cells (Figure 25A, lower panel), indicating that the endocytic defect was reversed by expression of Flower-pHluorin in Flower KO CTLs. We quantified the localization of anti-RFP antibody-positive puncta at the IS (for WT, Flower KO and for Flower-pHluorin rescue) over 15 min. The fluorescence of anti-RFP488 antibody-positive puncta decreased at the IS over time in WT CTLs (mean intensity of $97.3 \pm 1.0\%$, $60.1 \pm 5.8\%$, $61.1 \pm 4.6\%$, $48.9 \pm 4.9\%$, $47.1 \pm 4.8\%$ and $33.3 \pm 3.1\%$ at time points 0, 2.5, 5, 7.5, 10 and 15 minutes, respectively; Figure 25B, closed circle). This result indicates that endocytosis occurs and that endocytosed granules are distributed throughout the cytoplasm within 15 min. However, in Flower KO CTLs, the signal from anti-RFP488 antibody-positive puncta remained constant over time (mean value of $98.9 \pm 0.4\%$, $96.6 \pm 1.5\%$, $95.9 \pm 1.5\%$, $92.3 \pm 4.9\%$, $93.5 \pm 1.5\%$ and $96.3 \pm 1.4\%$ at the time points 0, 2.5, 5, 7.5, 10 and 15 minutes, respectively) indicating that the fused granules are not endocytosed (Figure 25B, open circle). In Flower KO CTLs expressing Flower-pHluorin, the anti-RFP405 antibody-positive puncta dispersed in the cytoplasm as in WT CTLs (mean values of $95.4 \pm 1.9\%$, $71.4 \pm 6.4\%$, $71.3 \pm 6.4\%$, $54.3 \pm 7.3\%$, $52.6 \pm 7.9\%$ and $38.0 \pm 7.5\%$ at time points 0, 2.5, 5, 7.5, 10 and 15 minutes, respectively; Figure 25B, pink triangle).

In order to rule out the possibility that this phenotype is the result of over-expression of Syb2-mRFP, we crossed Sybki mice and Flower KO mice to generate a Flower knock-out/Syb2-mRFP knock-in (Sybki/Flower KO) mouse strain. CTLs from these mice also failed to internalize mRFP antibody-positive puncta when incubated with target cells for 30 min. Sybki CTLs showed normal internalization of anti-RFP antibody (Figure 25C, upper panel) whereas in Sybki/Flower KO CTLs there was an accumulation of mRFP antibody-positive puncta (Figure 25C, lower panel). We also expressed Flower-pHluorin in Sybki/Flower KO CTLs and observed internalization of mRFP antibody-positive puncta in these CTLs. In Figure 25, two KO cells in contact with a target cell are shown. The CTL expressing Flower-pHluorin showed a rescue of endocytosis (anti-RFP647, green) (Figure 25D, upper cell) whereas the untransfected CTL exhibited an accumulation of anti-RFP antibody-positive puncta at the IS (Figure 25D, lower cell). These data support the conclusion that lack of Flower leads to a deficit in endocytosis that can be reversed by the expression of Flower.

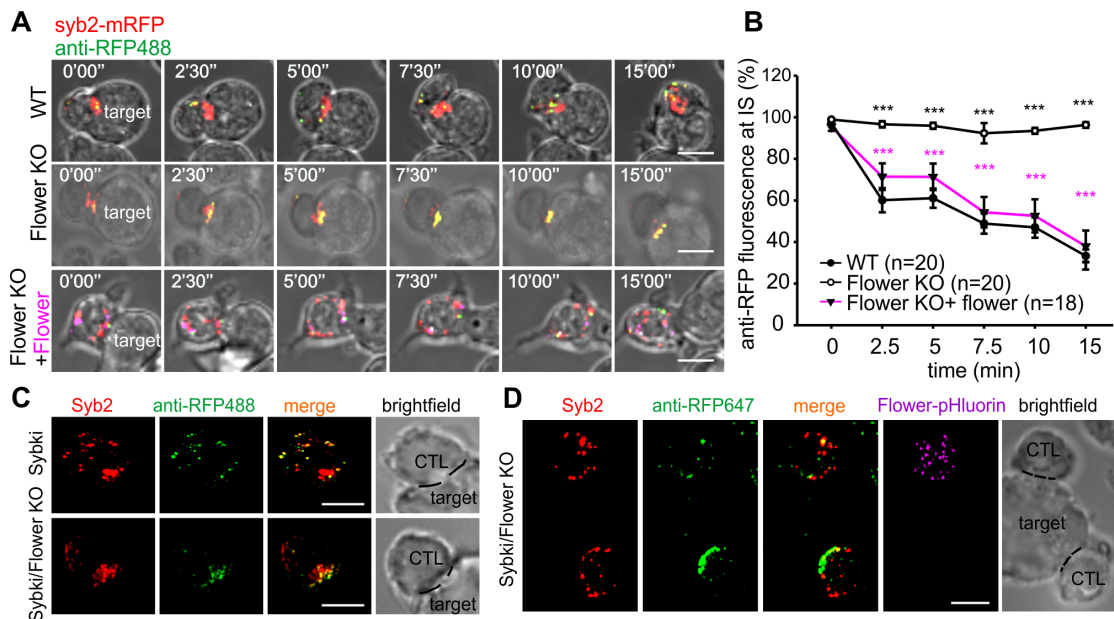


Figure 25. Cytotoxic granule endocytosis is impaired in Flower-deficient CTLs.

(A) Time-lapse snapshots of Syb2-mRFP (red) transfected CTLs conjugated to target cells in the presence of anti-RFP488 antibody (green) in the medium. The endocytosis of CGs (yellow) is shown in WT (upper panel), Flower-deficient (middle panel) and Flower-deficient CTLs over-expressing Flower-pHluorin (magenta) (lower panel). Scale bar: 10 μ m. (B) Quantitative analysis of the accumulation of endocytic CGs at the IS (one third of CTL volume projecting towards the target cell) over time from panel A. Time zero is defined as the appearance of the first endocytic CG at the IS. Data are given as mean \pm SEM; paired t-test, * $p < 0.01$, *** $p < 0.001$. (C) CTLs from synaptobrevin2-mRFP knock-in (Sybki, upper panel) and Sybki/Flower-deficient (Flower KO, lower panel) mice were incubated with target cells (p815) in the presence of Alexa488-conjugated anti-RFP antibody (anti-RFP488) in the medium in order to visualize endocytic granules. Cells were then fixed after 40 min and imaged by SIM. (D) CTLs from Sybki/Flower-deficient (Flower KO, lower panel) mice were transfected with Flower-pHluorin and incubated with target cells (p815) in the presence of Alexa647-conjugated anti-RFP antibody (anti-RFP647) in the medium in order to visualize endocytic granules. Cells were then fixed after 40 min and imaged by SIM. The CTL expressing Flower-pHluorin (upper cell) shows a clear rescue in endocytosis while the un-transfected one (lower cell) does not. Scale bar: 5 μ m.

It is possible that the decreased endocytosis in Flower-deficient CTLs could result from an upstream effect. Therefore, we examined the trafficking in compartments upstream of endocytosis. Recycling endosomes (RE) transport T cell receptors, Syntaxin11 and Munc13-4 to the IS to build the IS (Dudenhofer-Pfeifer et al., 2013; Halimani et al., 2014) for CG secretion. We transfected rab11-mcherry as a RE marker in WT and Flower KO cells and compared the time required for REs to polarize to the IS in CTLs seeded on anti-CD3 coated coverslips in an extracellular medium containing 1 mM calcium. As the rab11-mcherry signal appeared on the plasma membrane as well as on RE, we analyzed the interval between establishment of a footprint (indicating close contact) and appearance of the first RE in the TIRF plane. We observed a delay in the appearance of RE at the IS, although this delay was not statistically significant (49.1 ± 9.0 s ($n=13$) vs 29.6 ± 9.5 s in WT

cells (n=7)) (Figure 25A). We then tested if CG fusion itself is affected by the loss of Flower. We transfected Syb2-mRFP as a CG marker, seeded cells on anti-CD3 stimulatory coverslips and compared the interval between the arrival of the first CGs and the first granule fusion in WT and Flower KO CTLs. It took CGs in Flower-deficient cells much longer to fuse after arrival at the IS (212.9 ± 17.7 s, n=80) than those in WT cells (117.3 ± 12.4 s, n=84) (Figure 25B). This result indicates that Flower-deficiency leads to a delay of granule transport to the IS in CTLs.

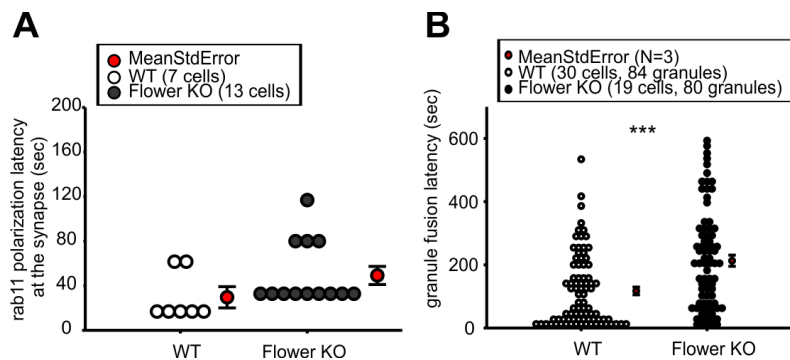


Figure 26. Flower-deficiency leads to a delay of granule transport.

(A) Polarization latency of recycling endosomes (RE). CTLs were transfected with rab11-mcherry as a RE marker and recorded in 1 mM calcium contained extracellular buffer by TIRFM. The polarization latency was analyzed as the interval between the attachment of the cell to the anti-CD3 coated coverslip and the appearance of RE at the TIRF plane. **(B)** Cytotoxic granule fusion latency. CTLs were transfected with Syb2-mRFP as a CG marker. CG fusion events were triggered by anti-CD3 antibody coated glass coverslips. The fusion latency was taken as the interval between the first granule appearance in the TIRF plane and the observed granule fusion event.

5.12. CG endocytosis is blocked in a very early stage in Flower-deficient CTLs

Having established that Flower deficiency leads to a block of CG endocytosis, we further investigated which stage of endocytosis is blocked. For this purpose, we performed CLEM experiments to correlate the fluorescence signal of endocytic events to its ultrastructure by matching SIM and EM images. We incubated Sybki or Sybki/Flower KO CTLs with target cells on sapphire disks for 35 min in the presence of anti-RFP488 antibody to label endocytic events. Afterwards, cells were fixed and sliced into 100 nm thin sections. These sections were then imaged by high resolution SIM and EM. The CLEM data showed again the phenotype of the endocytosis defect (Figure 27A). We defined the area of contact between CTL and target cell as the IS and the rest of the plasma membrane and cytoplasm area as non-IS. We observed an accumulation of anti-RFP488 antibody-positive (green) puncta in Flower KO cells at the IS ($55.2 \pm 6.2\%$, Sybki: 26 cells, 84 endocytic events, Sybki/Flower KO: 25 cells, 104 endocytic events) whereas in Sybki control cells only $30.7 \pm 5.3\%$ of these puncta stayed at the plasma membrane. The non-IS area of KO cells contained $44.8 \pm 6.2\%$ of the puncta whereas in Sybki control cells $69.3 \pm 5.3\%$ of the puncta were

present in the non-IS area (Figure 27D). Correlation of these fluorescent puncta with structure in the EM images showed that at the IS of Flower KO cells (Figure 27C, lower panel), the majority of the puncta were associated with modest invaginations (pits) of the membrane (Figure 27F) which we refer to as endocytic events. We compared the number of these endocytic events at the IS in WT and Flower KO cells. About 31% of the endocytic events occurred at the IS in control cells, while about 70% of the endocytic events were present at the IS in Flower KO cells. In Flower KO cells $40.2 \pm 9.7\%$ ($n=64$) of the pits at the IS were associated with anti-RFP488 antibody-positive puncta, while in WT cells only $9.3 \pm 4.8\%$ ($n=44$) of the pits at the IS were associated with these fluorescent puncta (Figure 27E). The CLEM data thus demonstrate that CG endocytosis is blocked at an early step in the absence of Flower.

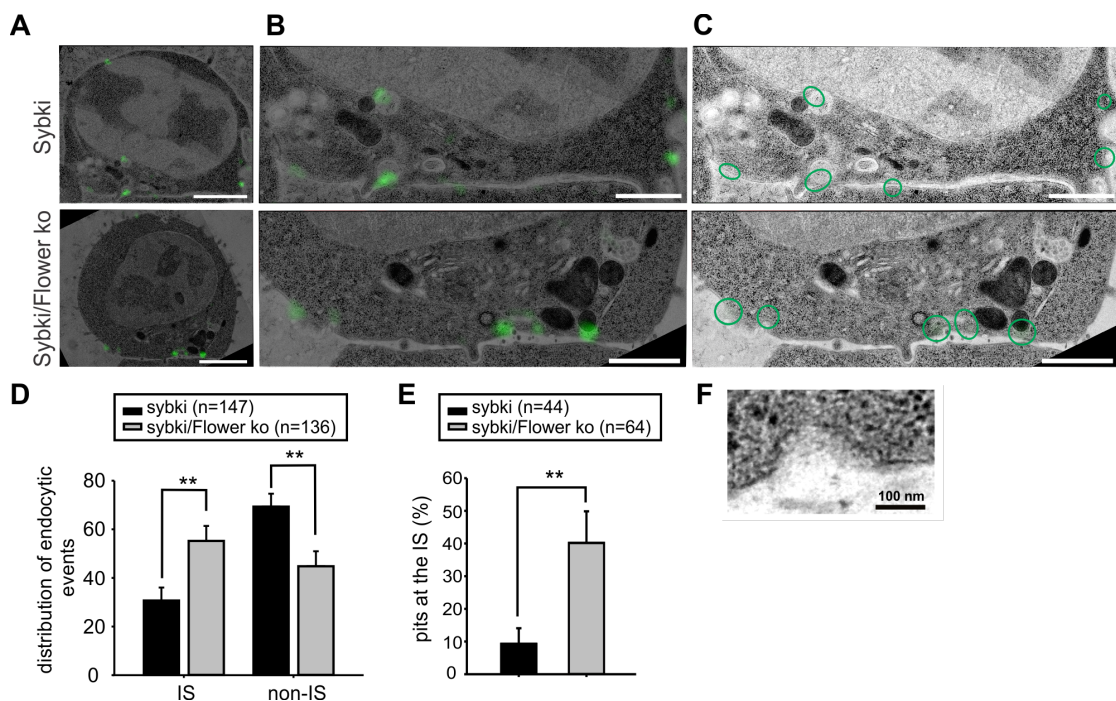


Figure 27. CG endocytosis is blocked in the early stage in Flower-deficient CTLs.

(A) Correlative light and electron microscopy (CLEM) images of Sybki CTL (upper panel) and Sybki/Flower KO CTL (lower panel) in contact with target cell. CTLs were incubated with target cells for 35 min in the presence of anti-RFP488 (green) in the medium to label endocytic CGs. After fixation, the processed fluorescent SIM image was overlaid with the TEM image. Scale bar: 2 μ m. (B) Magnification images from A of CTL and target cell contact region. (C) The TEM images with green open circles mark the endocytic events from SIM images. Scale bar: 1 μ m. (D) Quantitative analysis of endocytic event distribution in Sybki CTLs (control) and Sybki/Flower CTLs from CLEM experiment. We defined the IS as the interface between CTL and target cells at the contact membrane. The non-IS region was considered to be the rest of the CTL including cytoplasm and plasma membrane. 147 endocytic events were analyzed from Sybki CTLs ($n=25$) and 136 endocytic events were analyzed from Sybki/Flower KO CTLs ($n=26$). (E) Quantitative analysis of ultrastructure of endocytic events at the IS corresponding to anti-RFP488 fluorescence puncta. Relative frequency of pits over total events are shown in the graph. 7 pits were observed within 44 endocytic events from Sybki CTLs ($n=25$) and 21 pits were observed within 64 endocytic

events from Sybki/Flower CTLs (n=26). Data are given as mean \pm SEM; Mann–Whitney U test, ** $p < 0.01$.

5.13. High extracellular calcium can rescue the endocytosis defect in Flower-deficient CTLs

Since Flower was proposed to be a calcium channel (Yao et al., 2009), we hypothesized that Flower-containing vesicles can serve as a calcium source or that they fuse with the plasma membrane at the IS where they allow calcium entry from the extracellular space as a stimulus for CG endocytosis. In either case, the failure of endocytosis may be due to a loss of this calcium source. We tested whether the defect in endocytosis due to the loss of Flower could be reversed by increasing the extracellular calcium concentration. Using Syb2-mRFP transfected Flower KO CTLs, we again assayed endocytosis of Syb2 in WT and Flower KO CTLs. We recorded cells in normal medium containing around 1.5 mM calcium in the presence of anti-RFP488 antibody in the medium to label Syb2-mRFP following exocytosis as in the experiment described in Figure 28A. In WT CTLs, the antibody-positive puncta were endocytosed within 7.5 min (Figure 28A, upper panel, 7'30'') from the appearance of the first endocytic granule (0'00''). We then added extracellular buffer containing 10 mM calcium to the chamber and further observed endocytosis of RFP antibody-positive puncta. The accumulated fluorescence at the IS in WT cells decreased from $95.3 \pm 1.5\%$ to $57.4 \pm 5.9\%$ in the 7.5 min after the first observation of exocytosis (Figure 28B, closed circle). After application of the high calcium solution we observed a slower decrease of fluorescence, probably due to increased exocytosis triggered by high calcium (Figure 28A, upper panel, 10'00''). At the time points 8, 9, 10, 11, 13 and 15 minutes the fluorescence was $54.7 \pm 4.8\%$, $54.2 \pm 5.1\%$, $56.8 \pm 5.9\%$, $54.0 \pm 5.1\%$, $48.2 \pm 5.5\%$ and $46.2 \pm 4.8\%$ (Figure 28B, closed circle). We observed more CG exocytosis in CTLs with contact of target cells within 2.5 min of addition of 10 mM calcium. The anti-RFP488 antibody-positive puncta were retrieved into the cytosol. In contrast to WT CTLs, the anti-RFP488 antibody-positive puncta remained at the IS in Flower KO cells in the normal medium (Figure 28A, lower panel, 7'30'') with fluorescence of $97.8 \pm 0.9\%$ to $96.9 \pm 1.4\%$ at the time points 0 and 7.5 min. After 10 mM calcium application, the fluorescence signal in Flower KO CTLs increased at the plasma membrane (Figure 28A, lower panel, 8'00'' to 10'00''), indicating more endocytosis was triggered, and gradually decreased reaching the WT level at 10 min. The fluorescence signal of endocytic events at the IS at the time points 8, 9, 10, 11, 13 and 15 minutes in Flower KO CTLs were $82.4 \pm 5.2\%$, $66.3 \pm 6.6\%$, $57.1 \pm 6.3\%$, $42.0 \pm 6.0\%$, $41.3 \pm 5.5\%$ and $27.4 \pm 5.8\%$, respectively (Figure 28B, open circle). This result clearly shows that high extracellular calcium can reverse the endocytosis defect in Flower KO CTLs.

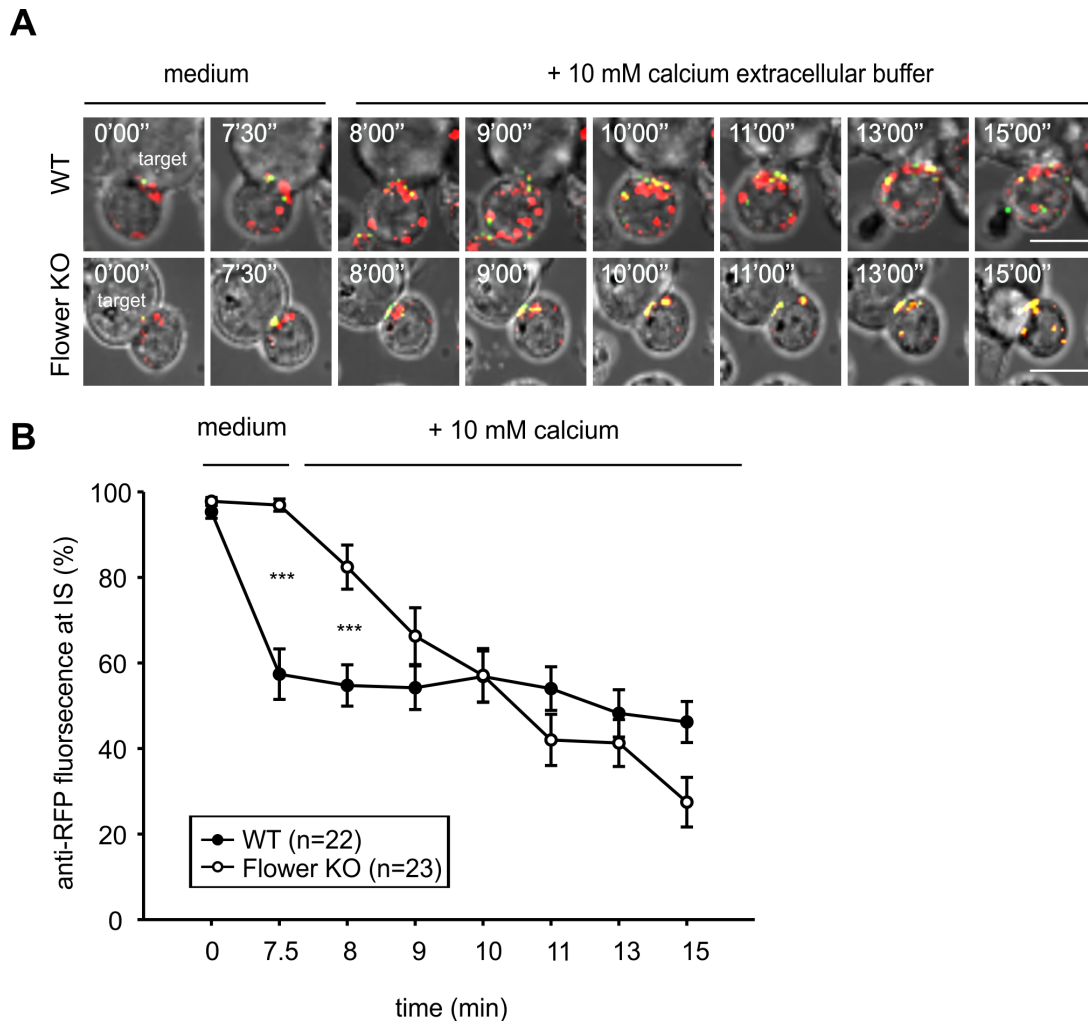


Figure 28. High extracellular calcium can rescue the endocytosis defect in Flower-deficient CTLs.

(A) Time-lapse snapshots of Syb2-mRFP (red) transfected CTLs in contact with target cells before and after application of extracellular buffer containing 10 mM calcium. CTLs were incubated with target cells in the presence of anti-RFP488 antibody (green) in the medium for 30 min and then perfused with 10 mM calcium buffer. Scale bar: 10 μ m. (B) Quantitative analysis of the accumulation of endocytic CGs at the IS (one third of CTL volume projecting towards the target cell) over time from panel A. Time zero is defined as the appearance of the first anti-RFP488 antibody-positive fluorescent puncta at the IS. Data are given as mean \pm SEM; paired t-test, * $p < 0.01$, *** $p < 0.001$.

5.14. Flower vesicles polarize early to the IS and localize in close proximity to fusogenic and endocytic cytotoxic granules

We attempted to determine the distribution of Flower in CTLs. We carried out live imaging to see where and when Flower is present in CTLs. We used Flower KO CTLs transfected with Flower cDNA to visualize Flower protein in a clean genetic background. We located Flower protein using TIRF microscopy to visualize individual granule exocytosis and confocal microscopy to examine endocytosis following target cell contact. First, we co-transfected Gcamp6f-Flower with Granzyme B-mCherry

(Gzm B-mcherry) to examine the localization of Flower-containing vesicles and CGs and whether we could visualize calcium changes upon Granzyme B secretion. In CTLs seeded on anti-CD3 stimulatory coverslips, the Flower-containing vesicles (green, white arrows) polarized to the IS earlier than CGs did (red, Figure 29A). The Flower-containing vesicles arrived at the IS almost immediately after the CTLs contacted the anti-CD3 coating. At the beginning of the recording, as the CTLs begin to attach (time= 0 s), two Flower-containing vesicles (on average) are seen at the IS. More Flower-containing vesicles later arrived at the IS, and after about 35 s the first CGs were observed at the IS (Figure 29C). As Flower vesicles polarized to the IS, they are clearly distinct vesicles from CGs. Interestingly, we observed that the Flower-containing vesicles are co-migrating with the exocytic CGs before they fuse (n=12) (Figure 29A). Concerning the calcium changes reported by Gcamp, it is difficult to interpret from the inappropriate orientation of calcium reporter being at C-terminus of Flower that located in cytoplasm (see discussion).

To test whether Flower is delivered to the plasma membrane to provide calcium for CG endocytosis, we observed how Flower behaves relative to endocytic puncta at the IS. We transfected Syb2-mRFP and Flower-pHluorin constructs in Flower KO CTLs and applied anti-RFP405 antibody in the medium to label endocytic CGs. We observed that Flower-containing vesicles (green), which were smaller than CGs (red), polarize to the IS. Moreover, anti-RFP405 antibody-positive puncta (Figure 29B, magenta arrows) appear to be near to (7'51'' and 9'28'') or even co-localized (17'19'') with Flower-containing vesicles. Although the data were acquired from confocal imaging with a limited resolution, these data, however, support our hypothesis that Flower-containing vesicles are a calcium source for CG endocytosis by its polarization to the IS and its localization near endocytic CGs. We demonstrated Flower vesicles are polarized early to the IS before CGs. Moreover, these vesicles are localized around exocytic and endocytic CGs.

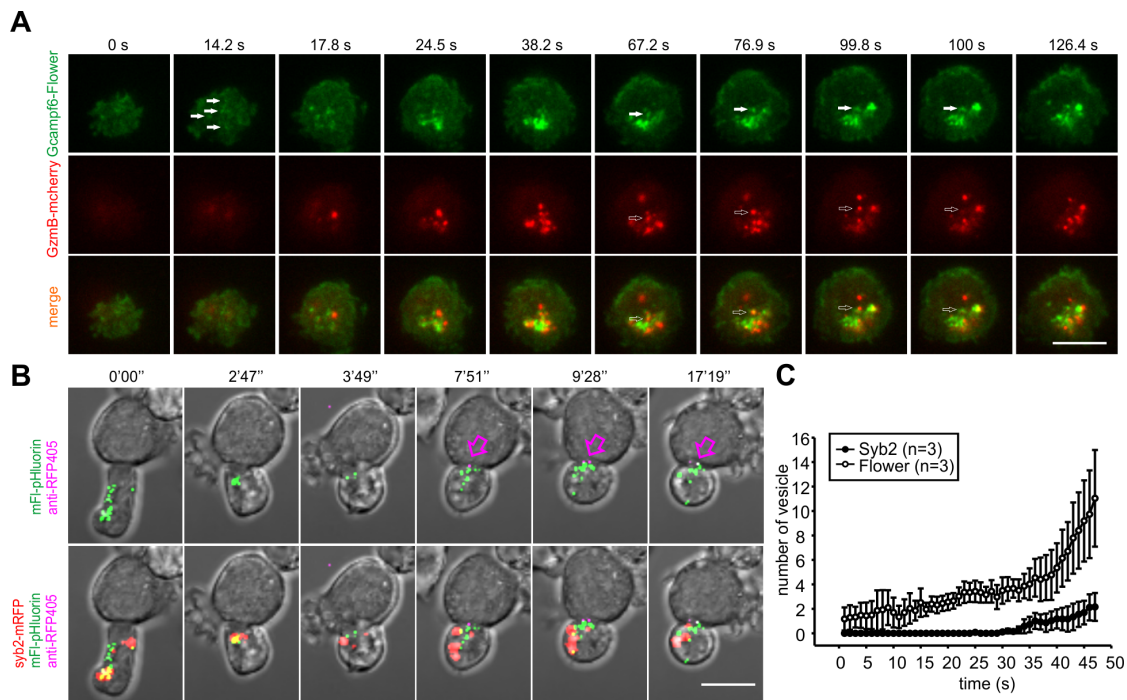


Figure 29. Flower vesicles are polarized to the IS and localized around exocytic and endocytic cytotoxic granules.

(A) Real-time dynamics of Flower-containing vesicles and cytotoxic granules in CTLs monitored by TIRF microscopy. Flower KO CTLs were transfected with Gcamp6f-Flower (green) and Granzyme B-mcherry (red). The white arrows point to the Flower-containing vesicles and the open arrows point to the exocytic CG. Scale bar: 5 μ m. (B) Live cell confocal images of a Flower KO CTL transfected with Flower-pHluorin (green) and Syb2-mRFP (red) conjugates to a target cell with presence of anti-RFP405 antibody (magenta). The arrows point to endocytic CGs. Scale bar: 10 μ m. (C) Quantitative analysis of the number of vesicles arriving at the IS over time.

5.15. Flower mutant can not rescue the endocytosis defect

We next tested whether mutation of the AP2 binding motifs of Flower can shift its localization from vesicles to the plasma membrane with the idea of measuring calcium signal through probably plasma membrane expressed Flower. We tested the mutated Flower protein by a rescue experiment to see if the mutation altered its function. We expressed a Flower mutant with the signal peptide (Yxx Φ) substituted to alanine at the N- and C-termini of the protein sequence. These consensus sequences serve as the specific binding site for adaptor protein 2 (AP2) complex which is the adaptor protein for Clathrin-mediated endocytosis machinery. We substituted these signal moieties (YRWL and YARI) to alanine in order to abolish the ability of AP2 to bind to Flower (Figure 30A). The mutant Flower shifted the expression from vesicles to the plasma membrane (Figure 30B). We compared Flower(wt)-mTFP and Flower(mut)-mTFP to test whether the mutant is able to rescue as efficiently as Flower WT. We incubated CTLs with target cells for 30 min in the presence of anti-RFP647, fixed and observed the granule endocytosis in CTLs. Sybki CTLs showed a normal retrieval of CGs (magenta) whereas in Sybki/Flower KO there was an accumulation of endocytic CGs at the IS as expected (Figure 30C).

The fluorescence signal of endocytic events at the IS in Sybki cells showed a value of $38.42 \pm 3.1\%$ which is comparable to the value in the Flower(wt) rescue group ($39.6 \pm 4.6\%$). In contrast, Sybki/Flower KO showed a value of $81.7 \pm 2.4\%$ and the Flower(mut) showed a value of $71.9 \pm 4.2\%$, indicating that the signal motif mutant of Flower did not reverse the endocytosis deficit of Flower KO CTLs. (Figure 30D).

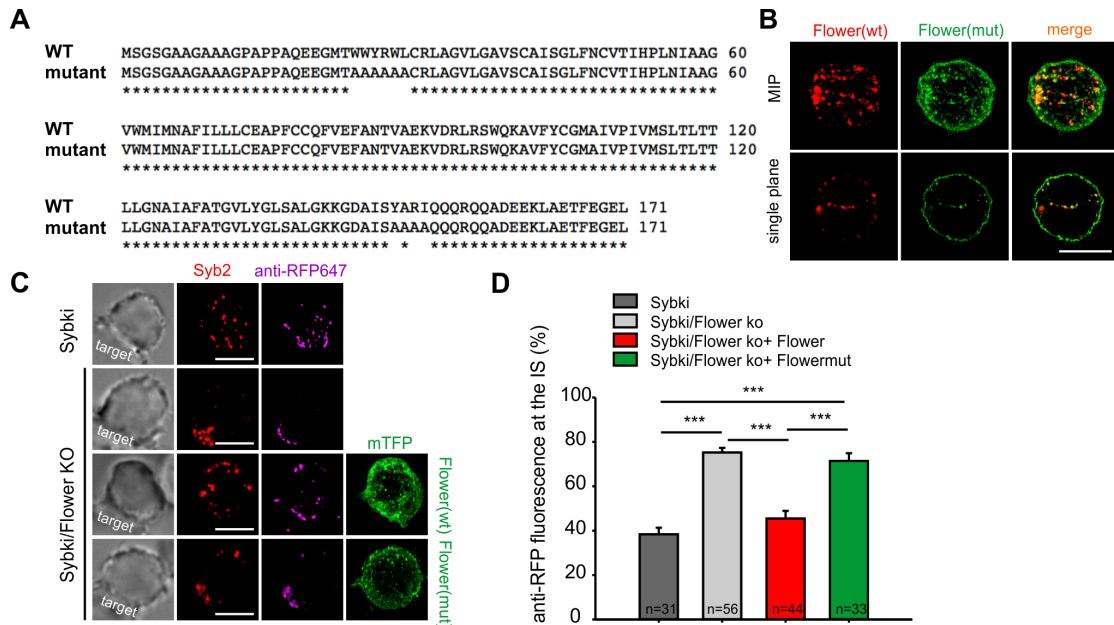


Figure 30. Flower mutant cannot rescue the endocytosis defect.

(A) Alignment of Flower wildtype and mutant protein sequence. (B) SIM images of a CTL cotransfected with wildtype tagRFP-Flower (red) and Flower mutant-mTFP (green) constructs. Scale bar: 5 μ m (C) SIM images of Sybki CTLs (control) and Sybki-Flower KO CTLs in contact with target cells with endocytic anti-RFP647 (magenta). CTLs were incubated with target cells for 30 min in the presence of anti-RFP647 to visualize endocytic cytotoxic granules. Sybki-Flower KO CTLs were transfected with Flower(wt)-mTFP and Flower(mut)-mTFP separately (lower two panel) for rescue experiment. Scale bar: 5 μ m. (D) Quantitative analysis from panel C of endocytic anti-RFP647 fluorescence signal at the IS.

6. Discussion

In the present work, we show that endocytosis of cytotoxic granule (CG) is required for the efficient serial killing of target cells by cytotoxic T lymphocytes. Additionally, we demonstrate that Flower protein is potentially responsible for the calcium-dependence of CG endocytosis. We use Synaptobrevin2 (Syb2) as a specific marker for CGs and take advantage of Syb2-mRFP knock-in mice as a tool to have endogenously labeled CGs for studying granule endocytosis. We visualize the endocytosis of CG membrane proteins LAMP1 and Syb2 in CTLs upon target cell contact by live cell confocal imaging. Syb2 endocytosis occurs at the IS and is dependent on Clathrin and Dynamin. Furthermore, the cytotoxic substance Granzyme B is refilled into the endocytic CGs to guarantee cytotoxicity. The endocytic granules polarize to sequential synapses between different target cells and contribute around 50% to the killing capacity of CTLs. We also identify a potential candidate for the calcium-dependence of CG endocytosis, the vesicular membrane protein Flower. Flower-deficient CTLs show a block of CG endocytosis at the early stage of membrane invagination, but do not affect granule exocytosis. The endocytosis defect can be rescued by reintroducing Flower protein or by increasing the extracellular calcium. Interestingly, Flower-containing vesicles polarize to the IS and localize around exocytic and endocytic granules. Additionally, mutation of Flower by substituting the tyrosin-based signal (YxxΦ) peptides to alanine shifts the localization of the protein from vesicles to the plasma membrane and leads to a failure to rescue the endocytosis defect. Future studies will be needed to identify possible interacting partners and to clarify the exact molecular mechanism of Flower action.

6.1. Cytotoxic granule endocytosis

CTLs are highly efficient killers, being able to kill thousands of target cells. They could reach this efficiency in a number of different ways including fast CG delivery, parallel pathways of CG delivery, sequential killing (i.e. serial) or simultaneous killing (i.e. parallel) (Bertrand et al., 2013; Isaaz et al., 1995; Wiedemann et al., 2006). However, the concept of using endocytosed CGs for multiple rounds of killing has not been discussed as potential scenario in primary T cells. Therefore, we hypothesized that after CG secretion, the membrane proteins of the CG at the plasma membrane could be re-used and re-filled with cytotoxic substances towards a mature cytotoxic granule to ensure serial killing ability. We first visualized endocytosis of the universal CG marker LAMP1 by live cell imaging and found that LAMP1 endocytosis occurs at most parts of the plasma membrane in CTLs upon target cell contact (Figure 8A). Moreover, when we correlate LAMP1 endocytosis in Sybki CTLs, the endocytosed vesicles containing both LAMP1 and Syb2 represent only one fifth of the overall number of LAMP1-containing vesicles (Figure 8C). These results imply that either the proportion of Syb2- and LAMP1-containing granules is not identical or that the

expression level of these two proteins is different. We counted an average of 5.6 ± 0.9 endocytosed Syb2 granules per cell, whereas we observed twice as many endocytic LAMP1-containing granules per cell (11.6 ± 1.5 , $n=9$) during 30 min of live cell recording. The reason for this discrepancy could be conventional lysosome secretion, which responds to the increase of intracellular free calcium upon TCR triggering and results in more LAMP1 endocytosis. The conventional lysosome exocytosis has been suggested to play a role in membrane repair (Andrews, 2000). Alternatively, there are indications that the expression level of LAMP1 and Syb2 is very different. LAMP1 and LAMP2 compose around 50% of the total protein mass found on lysosomal membrane, because they function in providing structural integrity to the organelle (Eskelinen, 2006). In contrast, it was reported that one SNARE complex is enough to trigger vesicle fusion in neuron (van den Bogaart et al., 2010). Since Syb2 is the v-SNARE mediates CG fusion in mouse CTLs (Matti et al., 2013), even a low expression level would be sufficient to mediate productive fusion.

We used Syb2 as a specific marker for CGs to follow CG retrieval. Syb2 is a specific marker for mature, fusogenic CGs due to its function in the final step of CG fusion. Additionally, our CLEM data (Matti et al., 2013) showed that Syb2-positive vesicles have a homogenous size of around 320 nm in diameter with an electron-dense core structure, which is believed constitute the matrix containing Granzyme or Perforin (Peters et al., 1991). CG endocytosis occurs via a Clathrin- and Dynamin-dependent pathway. CG endocytosis can be blocked by the Dynamin blocker Dynasore or by a Dynamin mutant K44A, by the Clathrin inhibitor Pitstop, or by downregulating the Syb2-specific adaptor protein CALM by siRNA. These data demonstrate that Dynamin, Clathrin and CALM are all required for endocytosis of CG membrane proteins (Figure 13A-D, Figure 14C-H). Since CALM is a specific adaptor protein of Syb2 (Koo et al., 2011), the binding of CALM and Syb2 for granule endocytosis indicates that the mRFP signal we track remains fused to Syb2 after endocytosis rather than being cleaved. When inhibiting endocytosis, we observed the accumulation of fluorescently labeled anti-RFP antibody at the IS. This clearly shows that CG endocytosis occurs only at the IS. Regarding reuse of CGs for efficient killing, cells could have different mode of exocytosis, termed full-fusion or kiss-and-run. For full-fusion, the fusion pore is thought to expand until the vesicle collapses and integrates its membrane into the plasma membrane. For kiss-and-run, the fusion pore opens and closes in a relatively short time, which is why part of the vesicle content still remains. In neurons, synaptic vesicles perform both mode of exocytosis. Kiss-and-run is thought to be driven by the need of efficient synaptic transmission (Wightman and Haynes, 2004). In CTLs, we observed only the full fusion of CG exocytosis upon target cells contact under our experimental conditions (Figure 15A). This underlines the reliability of CTL recognition for target cell killing and also supports the fact that CTLs secrete only one to two CGs at the IS in our TIRF measurements, demonstrating that the release of few granules is sufficient to induce target cell death. The endocytic granules re-fill the cytotoxic molecules Granzyme B within 60 min to ensure killing competence (Figure 15B). We tested if these endocytic

granules contribute to killing by incubating CTLs with two batches of target cells labeled with different calcein dye in the presence of anti-RFP647 antibody. We observed that the fused CGs carrying the anti-RFP647 antibody polarized to the sequential synapse with the second batch of target cells within 60 min (Figure 17B), indicating that these endocytic and re-filled granules are functional. Furthermore, blocking CG endocytosis by Dynasore or CALM down-regulation significantly decreased (~ 50%) target cell killing. Although a TCR trigger leads to up-regulation of many proteins including cytotoxic proteins, blocking CG endocytosis still leads to a significant decrease of killing. This suggests that the endocytic granules are probably the faster or the more efficient source for lethal hits.

6.2. Calcium dependence of cytotoxic granule endocytosis

Flower protein is characterized as a synaptic vesicle-associated calcium channel and localizes at periaxial zones upon synaptic vesicle fusion in *drosophila*. One of the remarkable features of Flower is that the second transmembrane domain contains a selectivity filter homologous to that of voltage-gated calcium channels and Transient Receptor Potential channels (TRPV5 and 6). The loss of Flower results in impaired intracellular resting calcium levels and impaired endocytosis at presynaptic terminals (Yao et al., 2009).

The Flower gene is conserved from worm to human. There are five isoforms (mFlowerA, B, C, D, E) in mammals according to the database, and all are expressed in mouse brain. However, only three of them are expressed (mFlowerA, C and E) in mouse CD8 cells (data not shown). Among them, the start codon of mFlowerC does not code for methionine (Figure 2). Therefore, theoretically there are only two Flower proteins expressed in CTLs, mFlowerA (171 aa) and mFlowerE (128 aa). The full-length FlowerA shows a protein size of 18 kDa (Figure 2, grey marked). We generated a polyclonal anti-Flower antibody that recognized two epitopes at the N- and C-terminal of the protein. It is expected to recognize FlowerA, B and E, because they share the identical sequence of the binding epitopes. Since mRNA of FlowerA and E are expressed in CTLs, we expect to find two bands on Western blot. However, we observed only the FlowerA band running at 18 kDa in the WT lysate extracted from mouse brain tissue and isolated CTLs (Figure 19B). Because we did not observe any other band lower than 18 kDa, these data indicate that Flower C might not be expressed at all. It should be noted that the anti-Flower antibody detected several other bands in WT lysates, but all these bands were in the high molecular weight range (above 18 kDa) and were also found in the lysates extracted from Flower KO mice. Therefore, the specific Flower band occurs only at 18 kDa in the denatured gel where the band is not detectable in KO lysates. In this work I focused on full-length FlowerA protein and investigated its function in mouse CTL. We found no change in either lysosome degranulation or the percentage and number of CG exocytosis in Flower KO cells (Figure 22). However, a clear defect of granule endocytosis became apparent in the absence of Flower (Figure 24 and Figure 25).

This phenotype is specifically due to lack of Flower, because the defect can be rescued by re-introducing Flower protein into Flower KO cells. Since exocytosis and endocytosis are tightly coupled, any other upstream process of endocytosis could be the reason results in defect of endocytosis. Therefore, we tested the transport of CGs before exocytosis. Intriguingly, recycling endosome polarization seems to be delayed (Figure 26A) and the CG fusion is significantly delayed (Figure 26B) in the absence of Flower, suggesting that Flower generally influences granule transport. This effect might contribute to the observed defect in granule endocytosis.

Yao et al. report that the loss of Flower leads to an impaired intracellular resting calcium level in presynaptic terminals (Yao et al., 2009). We measured the global intracellular calcium change in CTLs by performing ratiometric Fura-2 experiments. We did not observe differences in basic calcium level and in the calcium influx resulting from anti-CD3 stimulation. However, a slight, but not significant delay of calcium increase (~10 s) upon stimulation in KO cells was observed compared to WT cells (Figure 23). These data are compatible with the assumption that Flower vesicles function as calcium sources, thereby probably forming a transient calcium domain to assist granule transport. In addition to the defect in CG endocytosis, we also observed a defect of LAMP1 endocytosis in Flower-deficient cells (Figure 24). Thus, it appears as if Flower-deficiency leads to a general block of endocytosis, which is also reflected in the distribution of AP2 and Clathrin. Endogenous AP2 and Clathrin tend to accumulate at the plasma membrane in Flower KO cells compared to WT cells upon target cell contact where these two proteins distribute in a more punctate pattern. We observed an accumulation of these two proteins at the plasma membrane in KO cells within 20 min. The enrichment at the IS and on the opposite site of the cell indicates that most of the endocytosis occurs at these two places in CTLs. In contrast to KO cells, AP2 and Clathrin distribute into a punctate pattern in WT CTLs within 20 min. This punctate pattern indicates the undisrupted transport in Clathrin-mediated endocytosis whereas the accumulation might indicate a defect or delay of transport (data not shown). These results suggest that Clathrin-mediated endocytosis is generally delayed in the absence of Flower. One could also envision that a lot more cargo proteins would be affected by dysfunction of this machinery. Future experiments should test whether the endocytosis defect affects a broad range of molecules, whether it occurs in a specific group of proteins or whether endocytosis in other cell types or tissue is affected.

We performed CLEM experiments to correlate the ultrastructure of the blocked endocytic events at the IS to identify the exact step of endocytosis Flower acts on. It is worth to mention that the CLEM data we present here are the same sections imaged by both microscopes in order to acquire the exact ultrastructure from the fluorescence signal. From these thin sections, we found that the fluorescence signal of anti-RFP488 stayed exclusively at the IS in KO cells, verifying the endocytosis defect already observed in confocal microscopy (Figure 27D). The corresponding EM images showed early invaginations at the plasma membrane at the IS (Figure 27F).

Therefore, our CLEM data clearly show that Flower leads to a block at the early stage of granule endocytosis.

Our data also demonstrate that the endocytosis defect is specifically caused by lack of Flower. However, whether the phenotype is due to a lack of calcium supply or not is currently unclear. Yao et al. showed that heterologous expression of Flower allows calcium influx in salivary glands (Yao et al., 2009). The authors expressed WT Flower-HA and Flower(E79Q)-HA mutant in *drosophila* salivary gland cells that normally do not express Flower. They observed an increase of calcium reported by the calcium indicator Fluo 4-AM in Flower-expressing cells compared to the control cells while bathing the cells in extracellular calcium buffer containing 10 μ M calcium. Intriguingly, the calcium increase is diminished significantly in cells expressing the E79Q mutant in which the glutamate in the putative selectivity filter sequence is replaced by glutamine. These data indicate that Flower plays a role in regulating calcium influx and that the glutamate is required in the selectivity filter (Yao et al., 2009). We hypothesize that Flower vesicles provide calcium to trigger granule endocytosis in a spatially and temporally restricted manner. In this hypothesis, supplying other calcium sources would rescue the endocytosis defect in Flower-deficient CTLs. Indeed, raising the extracellular calcium concentration to 10 mM led to a retrieval of the anti-RFP488 antibody from the plasma membrane (Figure 28). Thus, these calcium rescue data support the hypothesis that Flower vesicles might provide calcium required to initiate granule endocytosis (Figure 31). Upon TCR stimulation, Flower-containing vesicles polarize to the IS and localize near the site of endocytic CGs. We think Flower somehow provides calcium at the early stage of endocytosis. An alternative possibility is that Flower interacts with other proteins required for endocytosis probably by interaction via its Yxx Φ motifs. The calcium microdomain temporarily arises near the endocytic sites and the calcium source is either Flower-containing vesicles (Figure 31A) or the extracellular milieu (Figure 31B).

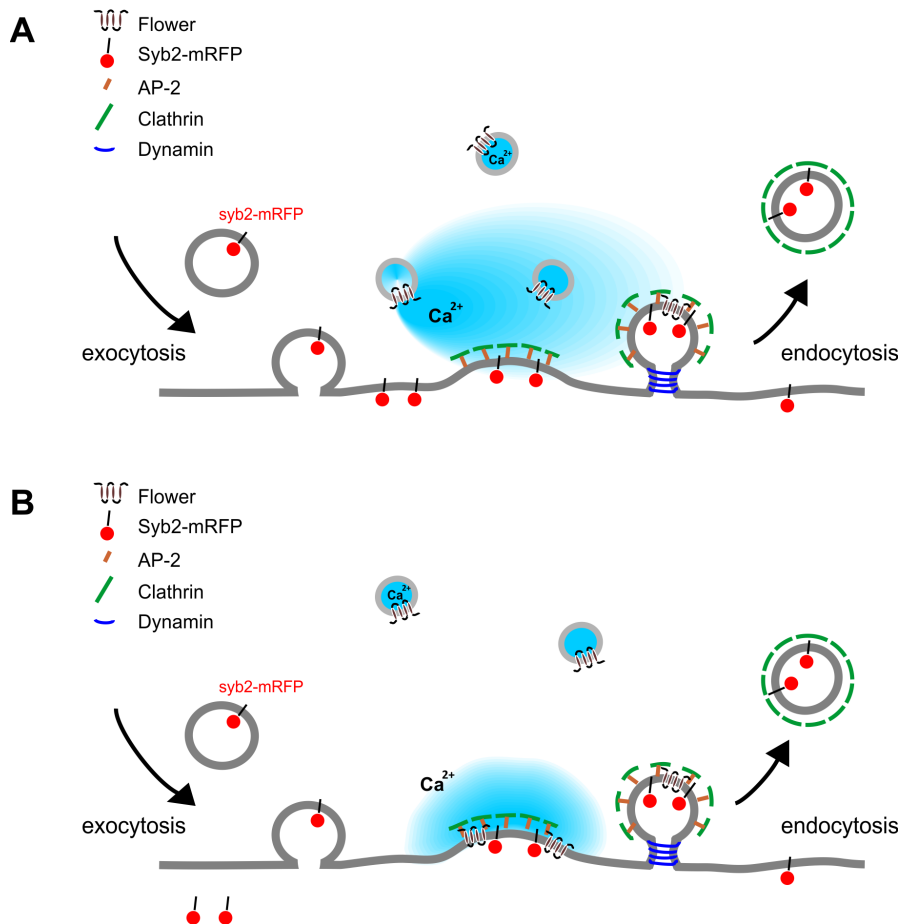


Figure 31. Proposed model of Flower function.

We propose that either Flower-containing vesicles are a calcium source for CG endocytosis (**A**) or that Flower integrates into the plasma membrane and interacts in a potentially calcium-dependent manner with proteins through its YxxΦ motifs (**B**). Sizes of molecules and vesicles are not drawn to scale.

Interestingly, our live cell image data showed that Flower vesicles are localized around the exocytic and endocytic CGs (Figure 29). Our TIRFM data showed that Flower vesicles are polarized very early to the IS, before recycling endosomes and CGs (Figure 29C and data not shown). While the Gcamp6f-Flower construct was generated with the idea of picking up calcium signals from Flower vesicles, we could not precisely correlate the calcium signal to Flower vesicles if there's any. It would be desirable to have the calcium sensor tag on the luminal side of Flower rather than at its C-terminus. However, due to the short space of the luminal part (3 aa in TM1-2 and 1 aa in TM3-4), the tested fusion constructs (Flower(TM1-2)-tagRFPT-Flower, Flower(TM1-2)-Gcamp6f-Flower, Flower(TM1-2)-Gcamp6f-tagRFPT-Flower and Flower(TM1-2)-rpHluorin-Flower) all showed a mislocalization of Flower. Nevertheless, we observed few Flower vesicles (1-2 vesicles) localized closely to the exocytic CGs. These particular Flower vesicles even move along with the exocytic CGs before secretion. Therefore, it seems like that Flower vesicles support CG exocytosis, since Flower-deficiency leads to a defect in granule transport. It is,

however, difficult to interpret the data regarding calcium response due to the intensity of the fluorescence signal from Gcamp6f in TIRF measurements. On one hand, the fluorescence signal increases exponentially by the distance of the fluorophore from the coverslip. On the other hand, the Gcamp6f signal increases upon binding to calcium and decreases in fluorescence not having calcium bound. Therefore, without any calibration, we could only demonstrate that Flower vesicles are around the exocytic CGs (Figure 29A). Concerning the function of Flower vesicles, we observed numerous of them moving at the IS and since only one to two CGs would secrete per cell, one could speculate that the remaining Flower vesicles might work on other exocytic processes. In addition to exocytosis, we also observed that Flower vesicles localize around endocytic CGs (Figure 29B). This raises the possibility that Flower works as a bridge molecule connecting exocytosis and endocytosis. It would be desirable to acquire live imaging continuously in a single cell simultaneously observing exocytosis and endocytosis from the same vesicles. However, currently it is technically impossible to follow live endocytosis events on glass coverslips in TIRFM. Conversely, it is also currently impossible to visualize exocytic events in confocal microscopy at the IS with our current equipment due to limited acquisition speed and resolution. Hopefully, the lipid bilayer surface that provides lipid flexibility for membrane invagination, will allow us to record individual granule exocytosis and endocytosis by TIRFM in the future. It would be informative to know where CG exocytosis and endocytosis occurs and how they couple to each other in CTL.

Recently, Houy et al. demonstrated a potential mechanism of how cells maintain a homeostatic membrane balance through vesicular trafficking in endocrine cells (Houy et al., 2013). They show a potential role of lipids in preserving and sorting secretory granule membranes after exocytosis and thus membrane retrieval retains the specific composition of lipids and even proteins. Thus, granule membranes are maintained together as “microdomains” after exocytosis and are subsequently recaptured without intermixing with the plasma membrane (Houy et al., 2013). The authors followed the internalization of collapsed granule membrane by labeling granule membrane protein, dopamine- β -hydroxylase (DBH), with an immunogold-labeled antibody in cultured chromaffin cells. They found that after full fusion, the DBH remains clustered on plasma membrane with other specific granule markers and is subsequently internalized through vesicular structures composed mainly of granule components by EM and fluorescence microscopy. These recaptured granule membrane is then integrated into an early endosomal compartment, which is Clathrin- and actin-dependent. Therefore, a selective sorting of granule membrane components is facilitated by the physical preservation of granule membrane entity on the plasma membrane after full collapse exocytosis (Ceridono et al., 2011). A similar concept of the ‘inseparable membrane’ mechanism was also demonstrated by Bittner and colleagues (Bittner et al., 2013). The authors demonstrated a nibbling mechanism for Clathrin-mediated retrieval of secretory granule membrane after exocytosis in chromaffin cells. They showed that the fused granule membrane remains a distinct entity and serves as a nucleation site for Clathrin- and Dynamin-

dependent endocytosis. However, the size of chromaffin granules (~ 300 nm) and Clathrin-coated endocytic vesicles (~ 90 nm) makes it unlikely that the Clathrin-mediated endocytosis internalized the entire fused granule membrane (Bittner et al., 2013). Therefore, they proposed that fused granule membrane internalization functions as a bit-by-bit mechanism through Clathrin- and Dynamin-mediated endocytosis. We have observed the similar phenomenon in our TIRF imaging with palmitoylated Gcamp6f (palmpalm-Gcamp6f) to measure calcium signals at the plasma membrane at the sites of Granzyme B secretion. The Gcamp6f composes of a GFP reporter and a calcium sensor Calmodulin. The GFP fluorescence intensity increases upon calcium binding to Calmodulin. The plasma membrane showed a high calcium signal once the cell attached to the anti-CD3 coated glass coverslip and cells change morphologically by spreading out to form a synapse. In response to the CD3 stimulation, CGs polarize to the synapse and secrete Granzyme B at the plasma membrane. In Figure 32, one Granzyme B granule (red) secretion occurs (white arrow, 0.3 s), which leads to a clear disappearance of a piece of membrane signal at the exact spot (green, white open arrows, from 4.2 s). This indicates the collapse of granule membrane integration into plasma membrane. This granule membrane expands a little (12.3 s) in the next few seconds possibly due to the full collapse of the granule and interestingly in company with calcium signal around the hole. Then the fusion pore gradually closes (19.2 s- 64.7s). The closed pore shows a relatively strong signal which indicates a stronger calcium signal around the pore. Alternatively, the increased signal could reflect a higher number of Gcamp molecules. In either scenario, the images clearly show that within 5 min, in which the granule membrane internalization occurs, the signal from Gcamp is completely gone (317.7 s). The second secretion event (white arrow, 93.2 s) also generates a hole at the plasma membrane (93.2 s). These data would support the 'inseparable membrane' mechanism that CG membrane proteins stay in clusters after exocytosis and that endocytosis occurs close to the site of exocytosis. It is worth to mention that the cell is imaged on glass coated coverslip. Since the cell has a very limited flexibility of membrane on coated coverslips that might lead to artifacts, the experiment should be repeated on lipid bilayer coating to have better membrane flow and track the vesicle exo- and endocytosis. Our preliminary data of LAMP1 and Syb2 endocytosis on lipid bilayer coating imaged by TIRFM shows that LAMP1 and Syb2 endocytosis occur at the cSMAC in fixed cells (data not shown) where the granules exocytosis is known to occur in a secretory domain. Therefore, it is possible that exocytosis and endocytosis occur as sequential events at a close neighborhood. This coupled process might indicate Flower indeed localizes around exo- and endocytic granules.

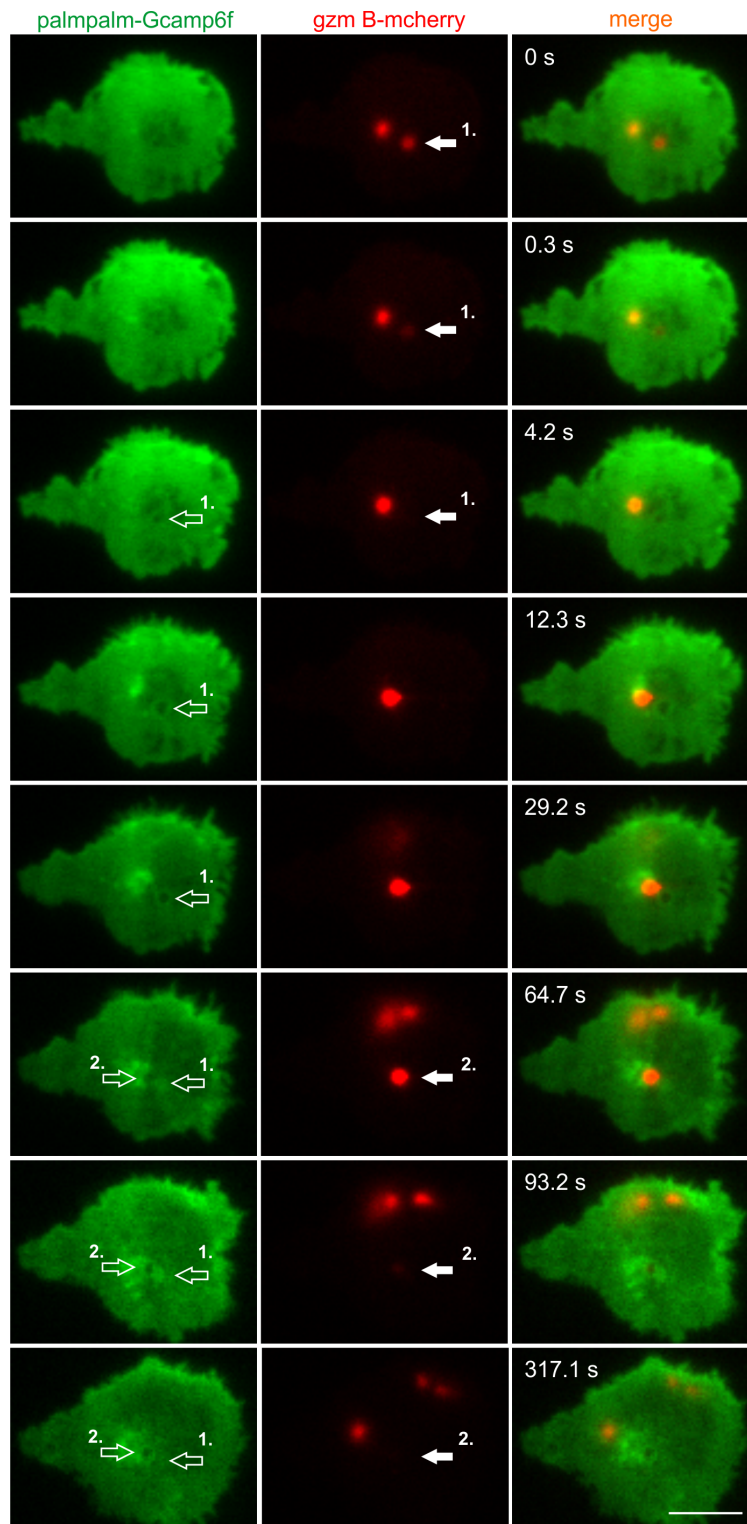


Figure 32. Granule membrane stays in clusters after exocytosis and internalizes distinct from the plasma membrane.

Snapshot images of a CTL with exocytic and endocytic events from real-time TIRF recording. Flower-deficient CTLs transfected with palmpalm-Gcamp6f (green) and Granzyme B-mcherry (red) were seeded on anti-CD3 antibody-coated glass coverslip with extracellular buffer containing 2 mM calcium. Scale bar: 5 μ m.

Flower mutants with substitution of two tyrosine-based signal peptides (YRWL and YARI) to alanine cannot rescue the endocytosis phenotype (Figure 30A, C and D). These tyrosine-based motifs Yxx Φ (where Φ can be F, I, L, M or V) are mostly associated with recruitment of adapter protein AP2 that selects cargo from the plasma membrane for Clathrin-mediated endocytosis (Bonifacino and Traub, 2003; Ohno et al., 1995; Traub, 2003). The mutant shifts the localization of Flower from vesicles to the plasma membrane possibly due to the failed recognition by AP2 (Figure 30B). However, what causes the dysfunction of mutant Flower is not entirely known. One possibility could be the localization, arguing that Flower is only functional if it is localized on vesicles. The other possibility would be that the mutated signal peptides leads to the failed interaction with other proteins involving calcium signaling or phosphorylation. Since AP2 is an essential adaptor protein in Clathrin-mediated endocytosis, it interacts with numerous cargo proteins and links them to Clathrin in order to ensure successful endocytosis. Synaptotagmin is one of the cargo proteins known as a calcium sensor for neurotransmitter release (Brose et al., 1992). Binding of Yxx Φ -based endocytic motifs to AP2 may increase AP2's affinity for Synaptotagmin and thereby facilitate coated pit formation. Haucke and De Camilli demonstrated that AP2 recruitment to Synaptotagmin was stimulated by tyrosine-based endocytic motifs (Haucke and De Camilli, 1999). Additionally, specific protein binding to Yxx Φ motif possibly induces tyrosine phosphorylation. For instance, Kittler and coworkers identified the Yxx Φ -type motif as a specific binding site of γ 2-subunit-containing GABA_A receptors for AP2, which is located in a site for γ 2-subunit tyrosine phosphorylation. They found that blocking GABA_AR-AP2 interactions via this motif increases synaptic responses within minutes. Furthermore, the crystallographic and biochemical studies suggest that phosphorylation of the Yxx Φ motif inhibits AP2 binding which leads to increased surface receptor number (Kittler et al., 2008). Phosphorylation plays an important role in regulation of endocytic coat complexes assembly (Slepnev et al., 1998). Clathrin-mediated endocytosis involves cycles of assembly and disassembly of Clathrin coat molecules and their accessory proteins. Dephosphorylation is shown to promote the assembly of dynamin1, synaptojanin1 and amphiphysin into complexes that also included Clathrin and AP2 in rat brain extract. On the other hand, phosphorylation of dynamin1 and synaptojanin1 inhibits their binding to amphiphysin, whereas phosphorylation of amphiphysin inhibits its binding to AP2 and Clathrin. Therefore, phosphorylation regulates the association and dissociation cycle of the Clathrin-mediated endocytic machinery. Synaptic vesicle endocytosis is triggered by Calcineurin-mediated dephosphorylation of the dephosphin proteins. Calcineurin is activated by calcium influx in nerve terminals and dephosphorylates a group of endocytic proteins called dephosphins (Cousin and Robinson, 2001). Dephosphins are the large GTPase Dynamin I, the adaptor protein AP180 and the accessory proteins amphiphysin I/II, synaptojanin, epsin, esp15 and phosphatidylinositol phosphate kinase type I γ (PIPKI γ) (Clayton et al., 2007). Calcineurin is reported to be universally involved in vesicle endocytosis at neuronal and non-neuronal secretory cells (Wu et al., 2014). Wu et al. demonstrated that

knocking out Calcineurin inhibits all forms of endocytosis regardless of developmental stage in large calyx-type synapses, small conventional cerebellar synapses, and endocrine chromaffin cells. Therefore, the authors suggest that Calcineurin is a key endocytic player in secretory cells (Wu et al., 2014). Another calcium sensor, Calmodulin, is reported to mediate all forms of endocytosis including Clathrin-dependent slow endocytosis, bulk endocytosis, rapid endocytosis and endocytosis overshoot (excess endocytosis) at nerve terminals in rodents (Wu et al., 2009).

Analyzing the Flower protein sequence reveals some potential functional aspects. First, the protein contains a conserved calcium selectivity filter sequence, which makes it a potential molecule in calcium regulation. However, whether it functions by its own or whether it interacts with other proteins remains unclear. Second, the two YxxΦ motifs are essential for the interaction with the μ subunit of AP2, which is involved in Clathrin-mediated endocytosis. As shown in Figure 25, Flower-deficiency leads to a clear phenotype of impaired endocytosis. These data demonstrate that Flower is one of the key molecules involved in endocytosis. However, the mutant Flower with paralyzed YxxΦ motifs cannot rescue the phenotype (Figure 30). Additionally, potential tyrosine phosphorylation of this motif might influence other interactions within the endocytosis machinery, e.g. in regulation of endocytic coat complex assembly (Slepnev et al., 1998). We have immunoprecipitated the AP2 μ subunit from mouse whole brain extract by Flower antibody, which indicates that Flower interacts with AP2 as proposed. Additionally, we have immunoprecipitated a number of kinases from mouse CTL lysate by Flower antibody, which suggests that Flower interacts with these kinases and possibly triggers the phosphorylation (data not shown, preliminary). These data make Flower a potential interactive molecule in the endocytosis machinery. Third, Flower has a potential Calmodulin-binding site at the C-terminus. If Flower interacts with Calmodulin, which is a known calcium sensor for endocytosis (Wu et al., 2009), then the Flower phenotype might be indirectly caused by the interaction with Calmodulin. More experiments will be needed to elucidate the exact molecular mechanism of Flower action on endocytosis.

One final interesting fact is that Flower is localized on vesicles of unknown identity. We were unable to find a marker for Flower vesicles, but could rule out that these vesicles are endosomal compartments or CGs (Figure 21). Since Flower appears to be involved in the calcium dependence of endocytosis, the functional role of these vesicles might be dual, calcium supply and positioning. It is known that while calcium triggers vesicle exocytosis, the positioning of exocytic vesicles near calcium channels may ensure efficient transmitter release upon calcium influx. Young and Neher reported that Synaptotagmin has an essential function in synaptic vesicle positioning for synchronous release in addition to its role as a calcium sensor (Young and Neher, 2009). Since Synaptotagmin is responsible for the exocytosis branch as a positioner, one might speculate that Flower plays a similar role in the endocytosis branch. Our data shown in Figure 29 might support the speculation that Flower vesicles are localized around exocytic and endocytic granules in live cell imaging.

In summary, we show by live cell confocal imaging that CG membrane protein endocytosis exists in primary CTLs from mouse. We further demonstrate that Syb2, the v-SNARE mediating granule fusion at the IS, is a superior marker to LAMP1 to study endocytosis. CG endocytosis occurs at the IS via Clathrin- and Dynamin-mediated pathway. Endocytic granules are re-filled with the cytotoxic substance Granzyme B within 60 min to render them killing-competent. The endocytic granules polarize to newly formed synapses with new target cells and contribute significantly to multiple target cell killing. Furthermore, we investigate the function of a potential calcium channel, Flower, in CTLs. Flower is localized on vesicles with unknown identity. Flower-deficiency leads to a block of CG endocytosis at an early stage while exocytosis is unaffected. The endocytosis defect can be rescued by re-introducing Flower protein or providing high extracellular calcium. Flower vesicles polarize to the IS early and localize around exocytic and endocytic granules. Mutation of AP2-binding sites on Flower result in a failure to rescue the endocytosis defect. Future experiments will be needed to identify binding partners and the molecular mechanism of Flower function in CTLs.

7. Summary

Cytotoxic T lymphocytes (CTLs) efficiently kill antigen-presenting cells to protect our body from infection or tumor cells. We demonstrate here that the sustained supply of the endocytic CGs contribute significantly to the efficient killing, termed multiple target cell killing. We use Synaptobrevin2-mRFP knock-in (Sybki) mice as a tool to endogenously label CGs for live cell imaging. By using Sybki CTLs, we demonstrate that endocytosis of the CG membrane proteins Syb2 and LAMP1 occurs within minutes after target cell contact, albeit in different pathways. CG endocytosis is blocked upon application of specific inhibitors of Dynamin and Clathrin, Dynasore and Pitstop2. Additionally, expression of a dominant-negative mutant, Dynamin2-K44A, resulted in a block of CG endocytosis, suggesting that Syb2 endocytosis is mediated through a Clathrin- and Dynamin-dependent pathway. Down-regulation of the Syb2-specific adaptor protein CALM by siRNA inhibits endocytosis as well, identifying CALM as another protein involved in CG endocytosis. The cytotoxic substance Granzyme B is re-filled into the endocytic granules within 60 min to maintain cytotoxicity. Block of CG endocytosis by Dynasore or CALM down-regulation reduces the amount of target cell lysis in population killing assays by 50%, demonstrating the significant contribution of endocytic CG to multiple target cell killing. In addition, we identify the Flower protein as an important molecule initiating granule endocytosis in a probably calcium-dependent manner. We generated Flower-deficient mice (Flower KO) and found that Flower-deficiency leads to a complete block of CG endocytosis in CTLs. Re-introducing Flower or increasing the extracellular calcium concentration can rescue the endocytosis defect in Flower KO cells. CLEM experiments demonstrate that Flower acts at an early stage of endocytosis. Flower vesicles polarize to the IS before arrival of recycling endosomes and CGs and localize around exocytic and endocytic granules, suggesting Flower might play a role to connect exo- and endocytosis. A Flower mutant with defective tyrosin motifs (YxxΦ) is localized at the plasma membrane rather than on vesicles, but fails to rescue the phenotype. These data suggest that Flower either functions while being localized on vesicles or through the interaction with endocytic proteins like AP2 while being localized on the plasma membrane.

8. Outlook

In this study, we address the original hypothesis of whether CG endocytosis exists and if they contribute to physiological importance of multiple target cell killing. By visualizing CG endocytosis in live cell imaging, we further decipher the endocytic pathway and demonstrate the significant contribution of endocytic CGs to multiple target cell killing. Although synaptic vesicles endocytosis is well characterized in neuronal cells, CG endocytosis has not been investigated at all in CTLs. Now that the formal proof of the importance of CG endocytosis has been accomplished, it will be interesting to further investigate the molecular details of how endocytosis is initiated, what molecules are involved and how it is regulated. In order to visualize granule endocytosis at the synapse, lipid bilayer coating will be necessary, improving membrane flexibility and allowing the application of external antibody to label endocytic vesicles. Additionally, lipid bilayer TIRF live imaging would probably help to decipher the molecular detail in a more physiological content. Finally, it would also be interesting to visualize CG endocytosis *in vivo* to test the contribution of endocytic CGs in multiple killing in a real physiological environment.

The vesicular membrane protein Flower was shown to function as a calcium channel to regulate synaptic endocytosis at the *drosophila* neuromuscular junction (Yao et al., 2009). However, Xue et al. later questioned this proposal, being unable to detect calcium currents at the plasma membrane at a mammalian nerve terminal. We observe a defect of CG endocytosis in Flower-deficient CTLs and confirm that the phenotype is specifically due to the lack of Flower. Intriguingly, increase of extracellular calcium can rescue the endocytosis defect indicating calcium supply, somehow compensating the absence of Flower. Furthermore, a Flower mutant with defective tyrosin signal motifs (WWYRWL and YARI) redistributes from intracellular vesicles to the plasma membrane and fails to rescue the block of endocytosis. This result indicates either Flower is functions on vesicle or active Flower requires interaction with other molecules via tyrosin motifs. Besides it's binding to AP2 through the tyrosin motif (YxxΦ), the adjacent WWY motif is also reported as a binding site on myosin to proteins involve in endosomal trafficking or Clathrin-mediated endocytosis such as TOM1, Dab2 and LTK2. Generating more specific mutants will lead to a broader insight of how Flower might function via these binding motifs. Also, unbiased biochemical methods are needed to identify potential interacting partners of Flower, such as yeast two-hybrid screens and co-immunoprecipitation experiments.

9. References

- Andrews, N.W. (2000). Regulated secretion of conventional lysosomes. *Trends in cell biology* 10, 316-321.
- Batters, C., Brack, D., Ellrich, H., Averbek, B., and Veigel, C. (2016). Calcium can mobilize and activate myosin-VI. *Proceedings of the National Academy of Sciences of the United States of America* 113, E1162-1169.
- Bertrand, F., Muller, S., Roh, K.H., Laurent, C., Dupre, L., and Valitutti, S. (2013). An initial and rapid step of lytic granule secretion precedes microtubule organizing center polarization at the cytotoxic T lymphocyte/target cell synapse. *Proceedings of the National Academy of Sciences of the United States of America* 110, 6073-6078.
- Betts, M.R., Brenchley, J.M., Price, D.A., De Rosa, S.C., Douek, D.C., Roederer, M., and Koup, R.A. (2003). Sensitive and viable identification of antigen-specific CD8⁺ T cells by a flow cytometric assay for degranulation. *Journal of immunological methods* 281, 65-78.
- Bittner, M.A., Aikman, R.L., and Holz, R.W. (2013). A nibbling mechanism for clathrin-mediated retrieval of secretory granule membrane after exocytosis. *The Journal of biological chemistry* 288, 9177-9188.
- Bonifacino, J.S., and Traub, L.M. (2003). Signals for sorting of transmembrane proteins to endosomes and lysosomes. *Annual review of biochemistry* 72, 395-447.
- Brose, N., Petrenko, A.G., Sudhof, T.C., and Jahn, R. (1992). Synaptotagmin: a calcium sensor on the synaptic vesicle surface. *Science* 256, 1021-1025.
- Ceridono, M., Ory, S., Momboisse, F., Chasserot-Golaz, S., Houy, S., Calco, V., Haeberle, A.M., Demais, V., Bailly, Y., Bader, M.F., and Gasman, S. (2011). Selective recapture of secretory granule components after full collapse exocytosis in neuroendocrine chromaffin cells. *Traffic* 12, 72-88.
- Chang, H.F., Bzeih, H., Schirra, C., Chitirala, P., Halimani, M., Cordat, E., Krause, E., Rettig, J., and Pattu, V. (2016). Endocytosis of Cytotoxic Granules Is Essential for Multiple Killing of Target Cells by T Lymphocytes. *Journal of immunology* 197, 2473-2484.
- Chen, Y.A., and Scheller, R.H. (2001). SNARE-mediated membrane fusion. *Nature reviews. Molecular cell biology* 2, 98-106.
- Clayton, E.L., Evans, G.J., and Cousin, M.A. (2007). Activity-dependent control of bulk endocytosis by protein dephosphorylation in central nerve terminals. *The Journal of physiology* 585, 687-691.
- Cousin, M.A., and Robinson, P.J. (2001). The dephosphins: dephosphorylation by calcineurin triggers synaptic vesicle endocytosis. *Trends in neurosciences* 24, 659-665.
- Dudenhofer-Pfeifer, M., Schirra, C., Pattu, V., Halimani, M., Maier-Peuschel, M., Marshall, M.R., Matti, U., Becherer, U., Dirks, J., Jung, M., *et al.* (2013). Different Munc13 isoforms function as priming factors in lytic granule release from murine cytotoxic T lymphocytes. *Traffic* 14, 798-809.
- Dutz, J.P., Fruman, D.A., Burakoff, S.J., and Bierer, B.E. (1993). A role for calcineurin in degranulation of murine cytotoxic T lymphocytes. *Journal of immunology* 150, 2591-2598.
- Eskelinen, E.L. (2006). Roles of LAMP-1 and LAMP-2 in lysosome biogenesis and autophagy. *Molecular aspects of medicine* 27, 495-502.
- Esser, M.T., Haverstick, D.M., Fuller, C.L., Gullo, C.A., and Braciale, V.L. (1998). Ca²⁺ signaling modulates cytolytic T lymphocyte effector functions. *The Journal of experimental medicine* 187, 1057-1067.
- Faroudi, M., Utzny, C., Salio, M., Cerundolo, V., Guiraud, M., Muller, S., and Valitutti, S. (2003). Lytic versus stimulatory synapse in cytotoxic T lymphocyte/target cell interaction: manifestation of a dual activation threshold. *Proc Natl Acad Sci U S A* 100, 14145-14150.

- Feldmann, J., Callebaut, I., Raposo, G., Certain, S., Bacq, D., Dumont, C., Lambert, N., Ouachee-Chardin, M., Chedeville, G., Tamary, H., *et al.* (2003). Munc13-4 is essential for cytolytic granules fusion and is mutated in a form of familial hemophagocytic lymphohistiocytosis (FHL3). *Cell* *115*, 461-473.
- Grakoui, A., Bromley, S.K., Sumen, C., Davis, M.M., Shaw, A.S., Allen, P.M., and Dustin, M.L. (1999). The immunological synapse: a molecular machine controlling T cell activation. *Science* *285*, 221-227.
- Griffiths, G.M., Tsun, A., and Stinchcombe, J.C. (2010). The immunological synapse: a focal point for endocytosis and exocytosis. *The Journal of cell biology* *189*, 399-406.
- Halimani, M., Pattu, V., Marshall, M.R., Chang, H.F., Matti, U., Jung, M., Becherer, U., Krause, E., Hoth, M., Schwarz, E.C., and Rettig, J. (2014). Syntaxin11 serves as a t-SNARE for the fusion of lytic granules in human cytotoxic T lymphocytes. *European journal of immunology* *44*, 573-584.
- Haucke, V., and De Camilli, P. (1999). AP-2 recruitment to synaptotagmin stimulated by tyrosine-based endocytic motifs. *Science* *285*, 1268-1271.
- Houy, S., Croise, P., Gubar, O., Chasserot-Golaz, S., Tryoen-Toth, P., Bailly, Y., Ory, S., Bader, M.F., and Gasman, S. (2013). Exocytosis and endocytosis in neuroendocrine cells: inseparable membranes! *Frontiers in endocrinology* *4*, 135.
- Isaaz, S., Baetz, K., Olsen, K., Podack, E., and Griffiths, G.M. (1995). Serial killing by cytotoxic T lymphocytes: T cell receptor triggers degranulation, re-filling of the lytic granules and secretion of lytic proteins via a non-granule pathway. *European journal of immunology* *25*, 1071-1079.
- Jahn, R., Lang, T., and Sudhof, T.C. (2003). Membrane fusion. *Cell* *112*, 519-533.
- Kittler, J.T., Chen, G., Kukhtina, V., Vahedi-Faridi, A., Gu, Z., Tretter, V., Smith, K.R., McAinsh, K., Arancibia-Carcamo, I.L., Saenger, W., *et al.* (2008). Regulation of synaptic inhibition by phospho-dependent binding of the AP2 complex to a YECL motif in the GABAA receptor gamma2 subunit. *Proceedings of the National Academy of Sciences of the United States of America* *105*, 3616-3621.
- Koo, S.J., Markovic, S., Puchkov, D., Mahrenholz, C.C., Beceren-Braun, F., Maritzen, T., Dornedde, J., Volkmer, R., Oschkinat, H., and Haucke, V. (2011). SNARE motif-mediated sorting of synaptobrevin by the endocytic adaptors clathrin assembly lymphoid myeloid leukemia (CALM) and AP180 at synapses. *Proceedings of the National Academy of Sciences of the United States of America* *108*, 13540-13545.
- Kummerow, C., Schwarz, E.C., Bufe, B., Zufall, F., Hoth, M., and Qu, B. (2014). A simple, economic, time-resolved killing assay. *European journal of immunology* *44*, 1870-1872.
- Lancki, D.W., Weiss, A., and Fitch, F.W. (1987). Requirements for triggering of lysis by cytolytic T lymphocyte clones. *Journal of immunology* *138*, 3646-3653.
- Lopez, J.A., Jenkins, M.R., Rudd-Schmidt, J.A., Brennan, A.J., Danne, J.C., Mannering, S.I., Trapani, J.A., and Voskoboinik, I. (2013). Rapid and unidirectional perforin pore delivery at the cytotoxic immune synapse. *Journal of immunology* *191*, 2328-2334.
- Lyubchenko, T.A., Wurth, G.A., and Zweifach, A. (2001). Role of calcium influx in cytotoxic T lymphocyte lytic granule exocytosis during target cell killing. *Immunity* *15*, 847-859.
- MacLennan, I.C., Gotch, F.M., and Golstein, P. (1980). Limited specific T-cell mediated cytolysis in the absence of extracellular Ca²⁺. *Immunology* *39*, 109-117.
- Manders, E.M.M., Verbeek, F.J., and Aten, J.A. (1993). Measurement of Colocalization of Objects in Dual-Color Confocal Images. *J Microsc-Oxford* *169*, 375-382.
- Marks, B., and McMahon, H.T. (1998). Calcium triggers calcineurin-dependent synaptic vesicle recycling in mammalian nerve terminals. *Current biology : CB* *8*, 740-749.
- Matti, U., Pattu, V., Halimani, M., Schirra, C., Krause, E., Liu, Y., Weins, L., Chang, H.F., Guzman, R., Olausson, J., *et al.* (2013). Synaptobrevin2 is the v-SNARE

- required for cytotoxic T-lymphocyte lytic granule fusion. *Nature communications* 4, 1439.
- McCluskey, A., Daniel, J.A., Hadzic, G., Chau, N., Clayton, E.L., Mariana, A., Whiting, A., Gorgani, N.N., Lloyd, J., Quan, A., *et al.* (2013). Building a better dynasore: the dyngo compounds potentially inhibit dynamin and endocytosis. *Traffic* 14, 1272-1289.
- Menager, M.M., Menasche, G., Romao, M., Knapnougel, P., Ho, C.H., Garfa, M., Raposo, G., Feldmann, J., Fischer, A., and de Saint Basile, G. (2007). Secretory cytotoxic granule maturation and exocytosis require the effector protein hMunc13-4. *Nature immunology* 8, 257-267.
- Monks, C.R., Freiberg, B.A., Kupfer, H., Sciaky, N., and Kupfer, A. (1998). Three-dimensional segregation of supramolecular activation clusters in T cells. *Nature* 395, 82-86.
- Moreno, E., Fernandez-Marrero, Y., Meyer, P., and Rhiner, C. (2015). Brain regeneration in *Drosophila* involves comparison of neuronal fitness. *Current biology : CB* 25, 955-963.
- Nofal, S., Becherer, U., Hof, D., Matti, U., and Rettig, J. (2007). Primed vesicles can be distinguished from docked vesicles by analyzing their mobility. *The Journal of neuroscience : the official journal of the Society for Neuroscience* 27, 1386-1395.
- O'Keefe, J.P., and Gajewski, T.F. (2005). Cutting edge: cytotoxic granule polarization and cytolysis can occur without central supramolecular activation cluster formation in CD8+ effector T cells. *J Immunol* 175, 5581-5585.
- Ohno, H., Stewart, J., Fournier, M.C., Bosshart, H., Rhee, I., Miyatake, S., Saito, T., Gallusser, A., Kirchhausen, T., and Bonifacino, J.S. (1995). Interaction of tyrosine-based sorting signals with clathrin-associated proteins. *Science* 269, 1872-1875.
- Pattu, V., Halimani, M., Ming, M., Schirra, C., Hahn, U., Bzeih, H., Chang, H.F., Weins, L., Krause, E., and Rettig, J. (2013). In the crosshairs: investigating lytic granules by high-resolution microscopy and electrophysiology. *Frontiers in immunology* 4, 411.
- Peters, P.J., Borst, J., Oorschot, V., Fukuda, M., Krahenbuhl, O., Tschopp, J., Slot, J.W., and Geuze, H.J. (1991). Cytotoxic T lymphocyte granules are secretory lysosomes, containing both perforin and granzymes. *The Journal of experimental medicine* 173, 1099-1109.
- Prakriya, M., Feske, S., Gwack, Y., Srikanth, S., Rao, A., and Hogan, P.G. (2006). Orai1 is an essential pore subunit of the CRAC channel. *Nature* 443, 230-233.
- Purbhoo, M.A., Irvine, D.J., Huppa, J.B., and Davis, M.M. (2004). T cell killing does not require the formation of a stable mature immunological synapse. *Nature immunology* 5, 524-530.
- Schulte, A., Lorenzen, I., Bottcher, M., and Plieth, C. (2006). A novel fluorescent pH probe for expression in plants. *Plant methods* 2, 7.
- Slepnev, V.I., Ochoa, G.C., Butler, M.H., Grabs, D., and De Camilli, P. (1998). Role of phosphorylation in regulation of the assembly of endocytic coat complexes. *Science* 281, 821-824.
- Stinchcombe, J.C., Bossi, G., Booth, S., and Griffiths, G.M. (2001). The immunological synapse of CTL contains a secretory domain and membrane bridges. *Immunity* 15, 751-761.
- Takayama, H., and Sitkovsky, M.V. (1987). Antigen receptor-regulated exocytosis in cytotoxic T lymphocytes. *The Journal of experimental medicine* 166, 725-743.
- Traub, L.M. (2003). Sorting it out: AP-2 and alternate clathrin adaptors in endocytic cargo selection. *The Journal of cell biology* 163, 203-208.
- Trenn, G., Taffs, R., Hohman, R., Kincaid, R., Shevach, E.M., and Sitkovsky, M. (1989). Biochemical characterization of the inhibitory effect of CsA on cytolytic T lymphocyte effector functions. *Journal of immunology* 142, 3796-3802.
- van den Bogaart, G., Holt, M.G., Bunt, G., Riedel, D., Wouters, F.S., and Jahn, R. (2010). One SNARE complex is sufficient for membrane fusion. *Nature structural & molecular biology* 17, 358-364.

- Vig, M., Peinelt, C., Beck, A., Koomoa, D.L., Rabah, D., Koblan-Huberson, M., Kraft, S., Turner, H., Fleig, A., Penner, R., and Kinet, J.P. (2006). CRACM1 is a plasma membrane protein essential for store-operated Ca²⁺ entry. *Science* *312*, 1220-1223.
- Voskoboinik, I., Dunstone, M.A., Baran, K., Whisstock, J.C., and Trapani, J.A. (2010). Perforin: structure, function, and role in human immunopathology. *Immunological reviews* *235*, 35-54.
- Wada, F., Nakata, A., Tatsu, Y., Ooashi, N., Fukuda, T., Nabetani, T., and Kamiguchi, H. (2016). Myosin Va and Endoplasmic Reticulum Calcium Channel Complex Regulates Membrane Export during Axon Guidance. *Cell reports* *15*, 1329-1344.
- Wang, X.M., Terasaki, P.I., Rankin, G.W., Jr., Chia, D., Zhong, H.P., and Hardy, S. (1993). A new microcellular cytotoxicity test based on calcein AM release. *Human immunology* *37*, 264-270.
- Weidinger, C., Shaw, P.J., and Feske, S. (2013). STIM1 and STIM2-mediated Ca²⁺ influx regulates antitumour immunity by CD8(+) T cells. *EMBO molecular medicine* *5*, 1311-1321.
- Wiedemann, A., Depoil, D., Faroudi, M., and Valitutti, S. (2006). Cytotoxic T lymphocytes kill multiple targets simultaneously via spatiotemporal uncoupling of lytic and stimulatory synapses. *Proceedings of the National Academy of Sciences of the United States of America* *103*, 10985-10990.
- Wightman, R.M., and Haynes, C.L. (2004). Synaptic vesicles really do kiss and run. *Nature neuroscience* *7*, 321-322.
- Wu, X.S., McNeil, B.D., Xu, J., Fan, J., Xue, L., Melicoff, E., Adachi, R., Bai, L., and Wu, L.G. (2009). Ca²⁺ and calmodulin initiate all forms of endocytosis during depolarization at a nerve terminal. *Nature neuroscience* *12*, 1003-1010.
- Wu, X.S., Zhang, Z., Zhao, W.D., Wang, D., Luo, F., and Wu, L.G. (2014). Calcineurin is universally involved in vesicle endocytosis at neuronal and nonneuronal secretory cells. *Cell reports* *7*, 982-988.
- Yao, C.K., Lin, Y.Q., Ly, C.V., Ohyama, T., Haueter, C.M., Moiseenkova-Bell, V.Y., Wensel, T.G., and Bellen, H.J. (2009). A synaptic vesicle-associated Ca²⁺ channel promotes endocytosis and couples exocytosis to endocytosis. *Cell* *138*, 947-960.
- Young, S.M., Jr., and Neher, E. (2009). Synaptotagmin has an essential function in synaptic vesicle positioning for synchronous release in addition to its role as a calcium sensor. *Neuron* *63*, 482-496.
- Zweifach, A., and Lewis, R.S. (1993). Mitogen-regulated Ca²⁺ current of T lymphocytes is activated by depletion of intracellular Ca²⁺ stores. *Proceedings of the National Academy of Sciences of the United States of America* *90*, 6295-6299.